







Faculteit Bio-ingenieurswetenschappen

Academiejaar 2014 – 2015

## DBD discharge treatment of chlorinated hydrocarbons

Dries Davister

Promotor: Prof.dr.Ir. Stijn van Hulle

Tutor: dr. Anton Nikiforov

Masterthesis voorgedragen tot het behalen van de graad van  
Master in de industriële wetenschappen: Chemie



## Copyright

The author, promotor and tutor give permission to make this master dissertation available for consultations and to copy parts of this master dissertation for personal use. In case of any other use, the limitations of the copyright have to be respected, in particular with regard to the obligation to state expressly the source when quoting results from this master dissertation.

## Auteursrecht

De auteur, de promotoren en de tutor geven de toelating deze masterproef voor consultatie beschikbaar te stellen en delen ervan te kopiëren voor persoonlijk gebruik. Elk ander gebruik valt onder de beperkingen van het auteursrecht, in het bijzonder met de verplichting uitdrukkelijk de bron te vermelden bij het aanhalen van resultaten uit deze masterproef.

Kortrijk, June 2015

Dries Davister,

Prof.dr.Ir. Stijn Van Hulle,

dr. Anton Nikiforov,

A handwritten signature in black ink, appearing to read 'Anton Nikiforov', written in a cursive style. The signature is positioned below the printed name 'dr. Anton Nikiforov'.

## Preface

---

Dear reader,

Here I proudly present to you, my master's thesis. After 10 months of hard work, here is finally the finished version. I want to thank you, for taking the time to read through this work. Here, I will reflect the knowledge and abilities I have acquired over the past 4 years as a chemical engineering student.

While working on this thesis, I came in contact with a whole new aspect, called plasma technology. Working in the lab taught me a lot about the current research in applied physics. That is why I want to thank Prof. dr. ir. Stijn Van Hulle for giving me this opportunity to do something different than what we are used to in the lab at Campus Kortrijk. I would also like to thank my tutor, Anton Nikiforov, for providing the knowledge that led me through the research. He obviously knows a lot about plasma treatment and spectroscopy and was always the person to go to if there were any problems.

I also like to thank ir. Patrick Vanreas for giving a lot of great tips on writing in English and for helping me out in the lab. He also provided me a lot of basic knowledge about physics and the plasma world. In the beginning at the Technicum in Ghent, an internship from Shanghai, named Sue Di, helped me a lot with the experiments. Therefore, I also like to thank him for helping and keeping me company for the first 2 months.

Back in Kortrijk I had a lot of help of Yannick Verheust. He helped me out with developing a GC-MS method for the micropollutants. Besides that, he also provided a lot of knowledge about composing a decent extraction method. I could also count on the advice of dr. Wim Audenaert about the do's and don'ts when it comes to degradation of micropollutants. Michael Chys, gave me some insight as well when it comes to ozone monitoring, for which I am very grateful. Besides Yannick, I could also count on the help of Justine De Ketele for giving great advice when it comes to GC-MS analysis.

Finally, I would like to thank whoever supported me on this journey. Especially my parents, because without them, I would not be able to pull this off financially.

## Contents

---

Preface .....	II
List of symbols and abbreviations .....	VII
Summary: DBD Discharge treatment of chlorinated hydrocarbons .....	VIII
Samenvatting: DBD ontlading voor de behandeling van gechloreerde koolwaterstoffen ....	X
List of tables .....	XIII
List of figures.....	XIV
Introduction.....	1
I. literature study .....	2
1 Micropollutants.....	3
1.1 Pesticides .....	4
1.2 Chlorinated hydrocarbons .....	4
1.2.1 Use of chlorinated cyclic hydro carbonates.....	5
1.2.2 Properties and behavior .....	6
1.2.3 Hazard analysis .....	7
2 Micropollutant removal techniques .....	9
2.1 Activated carbon.....	9
2.2 Advanced oxidation processes.....	9
2.3 Nano filtration.....	9
2.4 Coagulation/flocculation .....	9
3 Plasma Technology .....	11
3.1 Plasma parameters.....	11
3.1.1 Density.....	11
3.1.2 Temperature.....	11
3.1.3 Debye Length.....	12
3.2 Discharge types .....	12

3.3	Non-thermal plasma .....	13
3.4	Dielectric barrier discharge.....	14
3.5	Plasma chemistry .....	14
3.5.1	Hydrogen Peroxide .....	15
3.5.2	Ozone .....	16
3.5.3	Nitric acid .....	16
3.5.4	Other active species.....	17
II.	Experimental setup, methods and materials .....	18
4	Materials and experimental setup.....	19
4.1	List of chemical products .....	19
4.2	Measuring instruments and devices .....	19
4.2.1	Oscilloscope and probes.....	19
4.2.2	Ozone monitor .....	20
4.2.3	UV-VIS spectrometer .....	20
4.2.4	GC-MS.....	20
4.3	Experimental setup: the reactor .....	20
4.3.1	Design.....	20
4.3.2	Specifications .....	22
4.3.3	Design motives.....	24
5	Analysis techniques.....	25
5.1	Power measurements.....	25
5.2	Ozone measurements.....	26
5.2.1	Ozone in water.....	26
5.2.2	Ozone in air .....	29
5.3	Hydrogen peroxide measurements .....	30
5.3.1	Method.....	30
5.3.2	Calculation .....	31



5.4	Analysis of methylene blue.....	32
5.5	GC-MS calibration and preparation.....	33
5.5.1	Optimizing the method.....	33
5.5.2	Calibration .....	36
5.5.3	Extraction .....	37
5.6	Statistical analysis.....	40
III.	Experimental results .....	41
6	Parameters and active species .....	42
6.1	Parameters.....	42
6.1.1	Conductivity and pH .....	42
6.1.2	Relation between pH, conductivity and power .....	44
6.1.3	Voltage and duty cycle.....	45
6.2	Active species.....	46
6.2.1	Hydrogen peroxide and ozone comparison.....	46
6.2.2	Gas phase.....	49
6.2.3	Activated carbon cloth .....	51
6.3	Conclusion.....	52
7	Methylene blue.....	53
7.1	Spectrum .....	53
7.2	Kinetics .....	54
7.2.1	Order determination .....	54
7.2.2	Reaction rate constants.....	56
7.2.3	Influence of ozone.....	56
7.3	Influence of voltage waveform .....	57
7.3.1	Effect of voltage.....	57
7.3.2	Effect of duty cycle.....	58
7.3.3	Power efficiency .....	58

7.4	Single pass.....	62
7.5	Conclusion.....	63
8	Micropollutants.....	64
8.1	Kinetics .....	64
8.1.1	Order determination .....	64
8.1.2	Reaction rate constant.....	65
8.2	Influence of voltage waveform .....	66
8.2.1	Effect of voltage.....	66
8.2.2	Effect of duty cycle.....	66
8.2.3	Power efficiency .....	67
8.3	Influence of active cloth .....	68
8.4	Single pass.....	69
8.5	Conclusion.....	70
9	Overall conclusion.....	71
10	Ideas for further research .....	72
	References .....	73
	Annex A: Calibration curves in Ethyl acetate.....	1
	Annex B: Calibration curves after extraction with dichloromethane .....	2

## List of symbols and abbreviations

---

### Chemicals

PeCB	Pentachlorobenzene
$\alpha$ -HCH	Alpha hexachlorocyclohexane
O <sub>3</sub>	Ozone
H <sub>2</sub> O <sub>2</sub>	Hydrogen peroxide
N <sub>x</sub> O <sub>y</sub>	Nitrogen species
N <sub>2</sub>	Nitrogen gas
HCB	Hexachlorobenzene
PCB	Polychlorinated biphenyl's
OH°	Hydroxyl radicals
HO <sub>2</sub> °	hydroperoxyl radicals
O°	Oxygen radicals
ONOOH	Peroxynitrite

### Symbols

C <sub>0</sub>	Initial concentration
V <sub>0</sub>	Initial Volume
K	Reaction rate constant
P	Power
P <sub>0</sub>	Initial power, without added pulse (duty cycle)
DC	Duty cycle
GC-MS	Gas chromatograph mass spectrometer
MP	Micropollutants
VMM	Flemish Environmental Agency
HS	Hazardous substances
ACF	Activated carbon fibers
MWCO	Molecular weight cut-off
AOPs	Advanced Oxidation Processes
N <sub>e</sub>	Electron density
ROS	Reactive oxygen species
RNS	Reactive nitrogen species
HV	High voltage
T <sub>on</sub>	Time that power is turned on
T <sub>off</sub>	Time that power is turned off
$\epsilon$	Molar absorptivity
b	Path length
IS	Internal standard
SIM	Single ion monitoring
r <sup>2</sup>	Determination coefficient
SPE	Solid phase extraction
LLE	Liquid-liquid extraction
G	Conductivity
AC	Activated carbon
MB	Methylene blue
DBD	Dielectric barrier discharge
G <sub>50</sub>	Amount of component in grams, removed per kWh to get a 50% reduction
EEO	Electric energy per order
HRT	Hydraulic retention time
t <sub>1/2</sub>	Half life

## Summary: DBD Discharge treatment of chlorinated hydrocarbons

### I. Introduction

Because of the use of pesticides, surfactants, pharmaceuticals and cosmetics, water gets contaminated with pollutants at a very low concentration ( $\mu\text{g/l}$  to  $\text{ng/l}$ ). These pollutants are called micropollutants and can have a negative impact on the environment. The pollutants end up in the wastewater and are hard to remove. A wide variety of techniques have been proposed to eliminate these compounds. Especially Advanced Oxidation Processes (AOPs), a technique that uses the high oxidation potential of OH radicals to degrade micropollutants, have a good removal performance. However, these techniques are expensive so an alternative such as plasma treatment is opted. In this thesis, DBD discharge will be used to remove a model compound such as methylene blue. Also, removal of pesticides such as pentachlorobenzene (PeCB) and alpha hexachlorocyclohexane ( $\alpha\text{-HCH}$ ) will be investigated.

### II. Reactor

The setup is a combination of a plasma reactor and an ozonation chamber. Where the ozonation chamber also acts like a reservoir (Figure 1). So water is pumped through the plasma reactor, back into the reservoir. This way, water transfer is a closed system. Gas phase on the other hand goes first through the plasma reactor and takes up active species. The same gas goes then through the ozonation chamber and leaves the system via the exhaust. The plasma itself is induced with a periodically interrupted power input, power can be varied using the duty cycle and by changing the voltage. The plasma reactor consists of

an activated carbon cloth to guide water through the plasma.

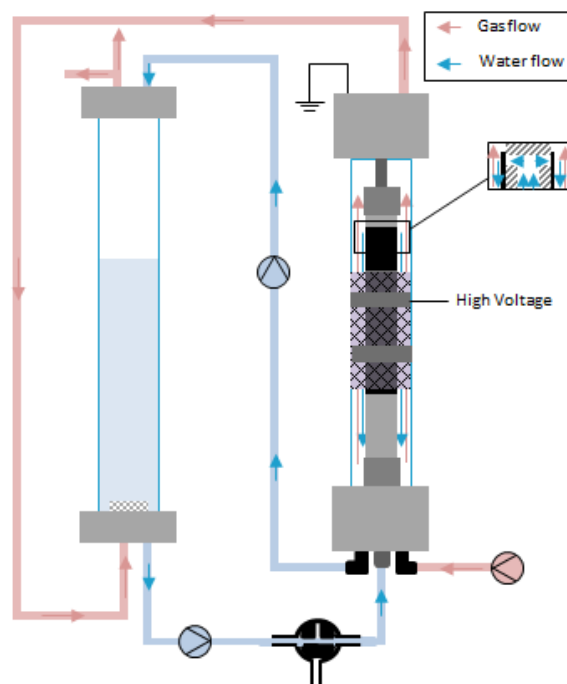
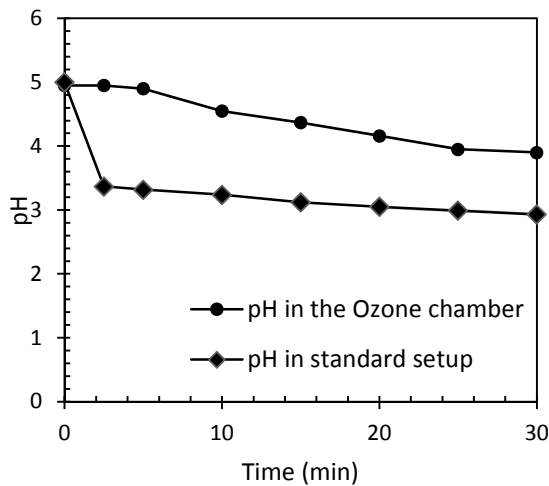


Figure 1: Overview of the complete setup

### III. Results

Plasma in contact with water, introduces a lot of active species into that water. Most of them have a short lifespan and are immeasurable with the available techniques. On the other hand long living active species such as  $\text{O}_3$  and  $\text{H}_2\text{O}_2$  can be measured and were found to be highly influenced by the power settings. The gas going through the system is dry air. Air contains about 80%  $\text{N}_2$ . This means in contact with plasma, a lot of nitrogen species such as  $\text{N}_x\text{O}_y$  and  $\text{HNO}_3$  will be introduced into the water. This can have a large influence on the performance of other active species. To give an idea of those nitrogen species, pH was measured. Configuration of the complete setup allows the plasma reactor and ozonation chamber to be used separately. When pH is measured in the ozone chamber if only the gas is coupled to the plasma chamber, pH is more constant, compared to the complete setup (Figure 2) because less  $\text{HNO}_3$  is produced.



**Figure 2:** pH in different configurations of the setup

Also a model compound is used to investigate the degradation behavior of the reactor. This model compound is methylene blue. It was found that degradation is a first order reaction. Because of the versatility of the reactor, the process of ozonation and direct plasma contact can be separated. So water can be treated with either reactor or the combination of both. When methylene blue was treated with all 3 configurations, the one with the ozone bubbling had the highest removal rate.

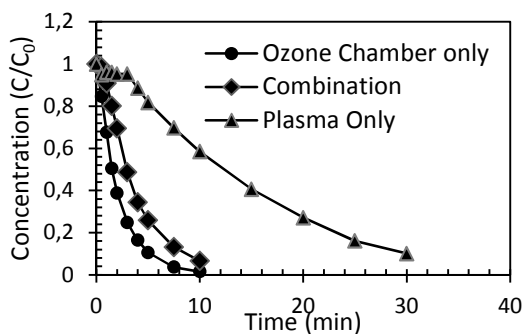


**Figure 3:** Degradation of methylene blue for different configurations

Different reactor configurations were compared using the energy efficiency,  $G_{50}$  (g/kWh) defined by Eq. 1. With  $C_0$  the initial concentration in mg/l,  $V_0$  the total volume in

liter,  $k$  the reaction rate constant in  $\text{min}^{-1}$  and  $P$  the power in watt.

$$G_{50} = \frac{30 \cdot C_0 \cdot V_0 \cdot k}{P \cdot \ln 2} \quad \text{Eq.1}$$

It was found that the highest efficiency (4.07 g/kWh) was achieved when using the lowest duty cycle setting. Compared to 5 similar reactors, this one also had the most efficiency.

After checking degradation of methylene blue, micropollutant removal was investigated. PeCB ( $C_0 = 155 \mu\text{g/l}$ ) and  $\alpha$ -HCH ( $C_0 = 308 \mu\text{g/l}$ ) were measured using GC-MS with liquid-liquid extraction. For these pollutants, 4 parameters were examined: the influence of the active carbon cloth, duty cycle and voltage were changed and a single pass experiment was conducted. The adsorption of the active carbon cloth was almost as high as the actual removal. This is not necessarily a bad thing, because the addition of plasma assures the removal of the components. The change of voltage had little to no influence on the degradation rate. However, a higher duty cycle (0.35) increased the removal significantly. Also a single pass experiment was used to check how the reactor operates in a continuous flow configuration. It was found that for both micropollutants the placement of the ozone reactor before the plasma reactor gave a higher removal of 7 to 12% for  $\alpha$ -HCH and PeCB respectively (with a hydraulic retention time (HRT) of 5.22 min).

#### IV. Conclusion

This reactor is clearly a competitor for current AOPs, because a lot of different active species can be combined. However, the energy consumption of this reactor is too high to operate in current wastewater treatment plants.

## Samenvatting: DBD ontleding voor de behandeling van gechloreerde koolwaterstoffen

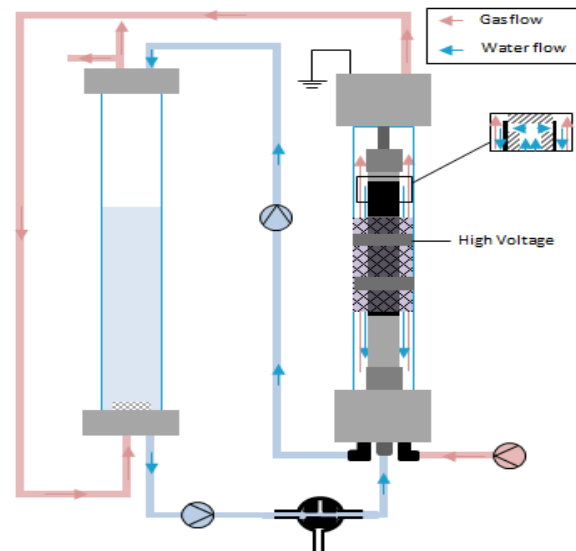
### I. Inleiding

Het gebruik van pesticiden, oppervlakte actieve stoffen, geneesmiddelen en cosmetica zorgt ervoor dat het water verontreinigd wordt met polluenten met een lage concentratie (mg/l tot  $\mu\text{g/l}$ ). Dit soort polluenten worden micropolluenten genoemd en kunnen een negatieve impact hebben op het milieu. Deze polluenten komen uiteindelijk terecht in het afvalwater en zijn daar dan ook moeilijk uit te verwijderen. Er worden daarom vele technieken voorgesteld om deze micropolluenten toch te verwijderen. Vooral geavanceerde oxidatie processen (AOPs), een techniek die gebruik maakt van sterk oxiderende hydroxyl radicalen, heeft bewezen een goede verwijdering te brengen. Het grote nadeel is echter dat deze technieken duur zijn, vandaar dat plasmabehandeling een goed alternatief zou kunnen zijn. In deze thesis zal er gebruik gemaakt worden van een Dielectric barrier discharge (DBD) ontleding voor de verwijdering van een model component zoals methyleenblauw. Daarnaast zal ook de verwijdering van pesticiden zoals pentachlorobenzeen (PeCB) en alfa hexachlorocyclohexaan ( $\alpha\text{-HCH}$ ) worden nagegaan.

### II. De reactor

De opstelling is een combinatie van een plasmareactor met een ozonisatiekamer (Figuur 1). Hierbij zal de ozonisatiekamer ook fungeren als een reservoir. Vandaar zal het water worden verpompt naar de plasma reactor en dan terug naar het reservoir. Op die manier kan de waterfase gezien worden als een gesloten systeem. Het gas daarentegen zal eerst door de plasmareactor gaan en actieve bestanddelen opnemen. Vervolgens zal dit gas door de ozonisatiekamer worden

geborreld en zal uiteindelijk het systeem verlaten langs de uitlaat. Het plasma zelf wordt gerealiseerd door het vermogen periodisch aan en uit te zetten. Hierdoor kan het vermogen worden gevarieerd door de spanning te wijzigen alsook door de tijd dat het signaal aan staat te variëren (z.g. duty cycle).

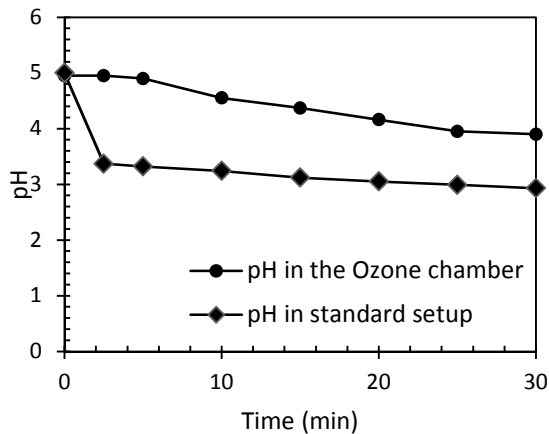


**Figuur 1:** Overzicht van de complete opstelling

### III. Resultaten

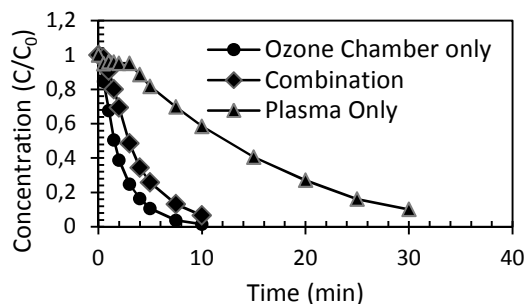
Plasma in contact met water, zorgt ervoor dat een verscheidenheid aan actieve bestanddelen in het water terecht komen. Hiervan heeft een groot deel slechts een korte levensduur en zijn haast onmeetbaar met de beschikbare technieken. Daarnaast zullen componenten zoals  $\text{O}_3$  en  $\text{H}_2\text{O}_2$  een langere levensduur hebben en dus wel meetbaar zijn. Deze laatste 2 worden sterk beïnvloed door de experimentele instellingen. Het gas dat door het systeem wordt gestuurd is droge lucht. Lucht bevat ongeveer 80%  $\text{N}_2$ . Dit betekent dat in contact met plasma, veel stikstof componenten zoals  $\text{N}_x\text{O}_y$  en  $\text{HNO}_3$  in het water zullen worden overgedragen. Deze stikstof componenten kunnen worden benaderd door gebruik te maken van de pH. Omdat het systeem makkelijk om te bouwen is kunnen de plasmareactor en de

ozonisatiekamer apart worden gebruikt. Wanneer pH dan gemeten wordt in de ozonisatiekamer en indien alleen het gas van de plasmakamer binnen kan, is de pH veel constanter in vergelijking met de standaardopstelling (Figuur 2).



**Figuur 2:** pH in verschillende uitvoeringen

Er werd een modelcomponent (methyleenblauw) gebruikt om degradaties te onderzoeken. Deze component wordt gemeten aan de hand van een UV-VIS signaal. Deze degradatie volgt een eerste order reactie. Hierbij werd de ozonisatiekamer en de plasmakamer als aparte reactor gebruikt. Wanneer methyleenblauw met de 3 configuraties werd behandeld bleek de ozonisatiekamer als aparte reactor de beste verwijdering te brengen.



**Figuur 3:** Degradatie van methyleen blauw voor verschillende opstellingen

Verschillende reactoren kunnen worden vergeleken door te werken met energie efficiëntie of  $G_{50}$  (vgl. 1) in g/kWh. Waarbij  $C_0$  de initiële concentratie uitgedrukt wordt

in mg/l,  $V_0$  het volume in liter,  $k$  de reactie snelheids-constante in  $\text{min}^{-1}$  en  $P$  het vermogen in watt.

$$G_{50} = \frac{30 \cdot C_0 \cdot V_0 \cdot k}{P \cdot \ln 2}$$

vgl.1

De hoogste efficiëntie (4.07 g/kWh) werd bereikt bij de laagste duty cycle instelling. In vergelijking met 5 andere gelijkaardige reactoren uit de literatuur, bleek deze het meest efficiënt te zijn.

Na het onderzoek van de model component (methyleenblauw), werd de verwijdering van micropolluenten onderzocht. PeCB ( $C_0 = 155 \mu\text{g/l}$ ) en  $\alpha$ -HCH ( $C_0 = 308 \mu\text{g/l}$ ) werden opgemeten met een GC-MS en een vloeistof-vloeistof extractie. Bij deze micropolluenten werden 4 verschillende parameters onderzocht, de invloed van actief koolstof doek, de duty cycle, de spanningsinstelling en ook een single pass experiment werd uitgevoerd. De verwijdering door adsorptie aan de actieve kooldoek was bijna even groot als de verwijdering in combinatie met het plasma. Dit toont niet meteen een slechte werking aan, omdat het toevoegen van het plasma de effectieve verwijdering garandeert. Het veranderen van de spanning had weinig invloed op de verwijdering van beide componenten. Daarentegen had een hogere duty cycle (0.35) een significant grotere invloed op de verwijdering. Ten laatste werd een single pass experiment uitgevoerd om het effect van de verwijdering te zien bij een continue doorstroming. Hierbij werd gevonden dat de verwijdering 7 tot 12% beter was, voor PeCB en  $\alpha$ -HCH respectievelijk, wanneer de ozonreactor eerst werd geplaatst. De hydraulische verblijftijd (HRT) van dit experiment bedroeg 5.22 min.

#### IV. Besluit

Deze reactor kan zeker worden aanzien als een concurrent voor de huidige AOPs, omdat vele actieve bestanddelen kunnen worden gecombineerd. Dit kan aan de hand van een minimale kost van elektriciteit en lucht. Toch is de energieconsumptie te hoog voor huidige waterzuiveringsinstallaties.



## List of tables

---

Table 1-1: Occurrence of $\alpha$ -HCH, PeCB and HCB in Flanders (VMM 2013) .....	4
Table 1-2: Overview of physical properties of $\alpha$ -HCH, PeCB and HCB.....	6
Table 1-3: Environmental quality standards for different types of waters (all units are in $\mu\text{g/l}$ ). (VLAREM II 2014). .....	8
Table 2-1: Overview of 4 different techniques for micropollutant removal (Luo et al. 2014, Thuy et al. 2008, Van der Bruggen et al. 2001).....	10
Table 3-1: Type of industrial plasmas (Chang 2009).....	13
Table 4-1: List of all used chemicals throughout this thesis.....	19
Table 4-2: Technical details about the power supply .....	23
Table 4-3: Requirements for an energy efficient plasma source based on (Muhammad Arif Malik 2010).....	24
Table 5-1: Overview of the different concentrations using the UV method.....	28
Table 5-2: Concentration of the necessary compounds to make 100 ml of the metavanadate solution.....	30
Table 5-3: Constant parameters of GC-MS.....	33
Table 5-4: Overview of the progress of the optimization of the oven program .....	34
Table 5-5: Overview of the retention time and mass/charge ratios for the pollutants and the internal standard .....	35
Table 5-6: Different determination coefficients for different calibrations.....	37
Table 5-7: Full procedure for solid phase extraction .....	38
Table 5-8: Overview of different recoveries for 3 types of SPE cartridges .....	39
Table 6-1: Comparison between calculated and actual conductivity .....	43
Table 6-2: Influence of initial pH and conductivity on pH and conductivity after 30 minutes .....	44
Table 6-3: Visual representation of excitation of active species for different voltage and duty cycle settings.....	45
Table 6-4: Power efficiency of $\text{H}_2\text{O}_2$ and $\text{O}_3$ .....	47
Table 7-1: Overview of determination coefficients ( $r^2$ ) for different reaction orders and initial concentrations.....	54
Table 7-2: Overview of decolorization and first order reaction rate constants of methylene blue for different parameters.....	56
Table 7-3: $G_{50}$ for different power settings (voltage and duty cycle) .....	59
Table 7-4: Comparison of efficiency between different reactors using $G_{50}$ for MB degradation .....	60
Table 7-5: EEO for different power settings (power and duty cycle).....	60
Table 7-6: Comparison of efficiency between different AOPs using EEO .....	61
Table 7-7: Overview on the effect of scavengers on the $G_{50}$ and EEO on methylene blue decolorization (Initial concentration MB of $7.5 \text{ mg/l}$ ).....	61
Table 8-1: Overview of determination coefficients ( $r^2$ ) to determine reaction order of PeCB and $\alpha$ -HCH. Unless mentioned otherwise, initial concentrations for PeCB and $\alpha$ -HCH are respectively $155 \text{ }\mu\text{g/l}$ and $308 \text{ }\mu\text{g/l}$ . .....	65
Table 8-2: Overview of reaction rate constants, half-life and percentage degraded after 30 minutes of runtime for PeCB and $\alpha$ -HCH <sup>(1)</sup> measured at 15 minutes) .....	65
Table 8-3: Overview of energy efficiency ( $G_{50}$ and EEO) for PeCB and $\alpha$ -HCH.....	68

## List of figures

Figure 1-1: Pathway of different types of micropollutants in the environment (Nikolaou et al. 2007) .....	3
Figure 1-2: Representation of the 4 first stereoisomers, namely the 2 $\alpha$ -HCH enantiomers, $\beta$ -HCH and $\gamma$ -HCH (Willett et al. 1998). .....	6
Figure 3-1: The four states of matter (solid, liquid, gas and plasma).....	11
Figure 3-2: Current-voltage characteristic (Plasma Universe 2014) .....	12
Figure 3-3: Illustration of electron chain reaction in Townsend discharge (Saltechtips 2014) .....	12
Figure 3-4: Schematic representation of OH radical formation by plasma (Locke and Shih 2011) .....	15
Figure 3-5: Formation path of nitric acid (Brisset et al. 2011).....	16
Figure 3-6: Complete overview of all reactions occurring in and around water (Bruggeman and Leys 2009) .....	17
Figure 4-1: Schematic overview of the reactor. 1 Mass flow controller; 2 PR 4000 controller; 3 TGP 110 pulse generator; 4 High voltage power generator; 5 custom peristaltic pump; 6 Roth cyclo II peristaltic pump; 7 Tektronic TDS 210 oscilloscope; 8 M450 ozone monitor and 9 T- shaped 3 way ball valve.....	21
Figure 4-2: Schematic of the setup for single pass experiments.....	22
Figure 4-3: Activated carbon cloth (Zorflex).....	23
Figure 5-1: Voltage and current signal with noise during $T_{on}$ (measured with oscilloscope) .....	25
Figure 5-2: Illustration of duty cycle (0.15) with $T_{on}$ and $T_{off}$ respectively 4.5 and 25.5 ms .....	26
Figure 5-3: Reaction of Indigo trisulfonic acid with ozone and corresponding molar absorptivity $\epsilon_{600}$ at 600 nm.....	27
Figure 5-4: Indigo absorbance spectrum after adding a certain amount of ozone (ml)....	27
Figure 5-5: Calibration curve of the indigo method, absorbance at 600 nm in function of concentration of ozone. On x-axis the ozone concentration and on the y-axis the absorbance of the indigo solution without ozone minus the absorbance with ozone.....	29
Figure 5-6: Spectrum of vanadate solution after addition of $H_2O_2$ diluted samples (presented as dilution ratios of $H_2O_2$ ) .....	30
Figure 5-7: Calibration curve of $H_2O_2$ metavanadate method .....	31
Figure 5-8: Spectrum of methylene blue, for different concentrations .....	32
Figure 5-9: Calibration curve MB, 660 nm.....	32
Figure 5-10: Calibration curve MB, 290 nm.....	32
Figure 5-11: Retention time for all standards, represented in the chromatogram. On the x-axis time (min) is presented and on the y-axis the signal intensity.....	34
Figure 5-12: Mass spectrum of Pentachlorobenzene. On the x-axis mass charge ratio is presented and on the y-axis the signal intensity.....	35
Figure 5-13: Overlay of all points of the calibration curve. On the x-axis time (min) is presented and on the y-axis the Abundance. ....	36
Figure 5-14: Calibration curves of alpha hexachlorocyclohexane, pentachlorobenzene and hexachlorobenzene.....	37
Figure 5-15: Percentage retrieved after sequential extraction steps .....	40
Figure 6-1: pH and conductivity in function of time (standard settings: Power 49.7 W and DC 0.15).....	42
Figure 6-2: Comparison between pH in standard setup and pH in ozone chamber.....	43

Figure 6-3: Conductivity in function of power for different voltage (DC: 0.15) and duty cycle settings .....	44
Figure 6-4: pH in function of power for different voltage (DC: 0.15) and duty cycle settings .....	45
Figure 6-5: Plasma spectrum with designation of different active species .....	46
Figure 6-6: Concentration of ozone in function of time, for different voltage settings .....	47
Figure 6-7: Concentration of hydrogen peroxide in function of time, for different voltage settings .....	47
Figure 6-8: Concentration of H <sub>2</sub> O <sub>2</sub> for different duty cycles .....	48
Figure 6-9: Concentration of ozone in gas phase for different duty cycles .....	49
Figure 6-10: Concentration of aqueous ozone in function of gaseous ozone .....	50
Figure 6-11: Concentration of ozone in water, with and without gas bubbling .....	50
Figure 6-12: Concentration of hydrogen peroxide in water, with and without gas bubbling .....	50
Figure 6-13: Effect of the addition of active carbon cloth on hydrogen peroxide concentration .....	51
Figure 6-14: Effect of the addition of active carbon cloth on ozone concentration .....	52
Figure 7-1: Full spectrum of methylene blue degradation for different stages in the process .....	53
Figure 7-2: Methylene blue degradation in function of time for different initial concentrations .....	54
Figure 7-3: Visual representation of the graphical method (first order reaction) with an initial concentration of 7.5 mg/l .....	55
Figure 7-4: Determination of actual order .....	55
Figure 7-5: Influence of plasma (plasma chamber), ozone bubbling (ozone chamber) and combination of both on MB degradation .....	57
Figure 7-6: Concentration of methylene blue in function of time for different voltage settings .....	57
Figure 7-7: Concentration of methylene blue in function of time for different duty cycle .....	58
Figure 7-8: Cost per volume (m <sup>3</sup> ) versus energy efficiency. ....	59
Figure 7-9: Decolorization of methylene blue in function of time for a continuous flow configuration, with an initial concentration of 7.5 mg/l .....	62
Figure 8-1: Degradation of PeCB (C <sub>0</sub> : 155 µg/l) and α-HCH (C <sub>0</sub> : 308 µg/l) for standard settings (49.7 W and DC: 0.15) .....	64
Figure 8-2: Degradation of pentachlorobenzene over time for different voltages .....	66
Figure 8-3: Degradation of alpha hexachlorocyclohexane over time for different voltages .....	66
Figure 8-4: Degradation of pentachlorobenzene over time for different duty cycles .....	67
Figure 8-5: Degradation of alpha hexachlorocyclohexane over time for different duty cycles .....	67
Figure 8-6: Influence on the removal of PeCB when plasma is turned off .....	68
Figure 8-7: Influence on the removal of α-HCH when plasma is turned off .....	69
Figure 8-8: Degradation of pentachlorobenzene in function of time for a steady state configuration .....	69
Figure 8-9: Degradation of pentachlorobenzene in function of time for a steady state configuration .....	70

## Introduction

---

The removal of organic components that come in small concentrations ( $\mu\text{g/l}$ ) have been studied for many years. These components are called micropollutants and have the potential to be harmful for many species, including humans (Andreozzi et al. 2003). These micropollutants percolate through farmlands (pesticides) and are excreted by humans (hormones, drugs, etc. ) and eventually end up in waste water and sometimes drinking water (when no appropriate treatment is foreseen). It is up to waste water treatment facilities to remove them completely or reduce them to harmless concentrations.

Advanced oxidation (AOPs) is a well-studied approach to remove these components. These AOPs rely on the production of reactive species to degrade the organics pollutants. Reactive species such as hydrogen peroxide are produced in situ by a large number of different combination reactions. Also processes such as ozonation and radiation (UV) help to break down the unwanted components in waste water (Esplugas et al. 2007). The only downside is the high production cost of reaction products. That is why optimization is necessary in order to reduce these costs.

A good way to combine several of these AOPs and produce a wide variety of reaction products is the use of plasma discharge in contact with the waste water. Although very promising, this technique is still in its early stages of development. That is why this thesis focusses on the potential of plasma technology to produce active species such as ozone and hydrogen peroxide. As an example, the removal of chlorinated cyclic hydrocarbons is investigated. Prior to that, a model compound such as methylene blue is used to give an estimate of removal patterns.

---

# *I. literature study*

---

## 1 Micropollutants

Micropollutants (MP) are pollutants that can be found in wastewater at very low concentrations ( $\mu\text{g/l}$  to  $\text{ng/l}$ ). These pollutants can vary from pesticides, pharmaceutical compounds, surfactants and cosmetics, to hormones that are excreted by humans. These compounds can all have negative impact on the environment.

Micropollutants constitute a major problem since these components are not, or only partially, removed by current wastewater treatment facilities. They form a threat for aquatic life (Andreozzi et al. 2003), because most of the micropollutants have endocrine disrupting effects. A well-known effect is feminization of fish. Also, aquatic life is more susceptible to chronic effects due to constant interaction with contaminated water (Yu et al. 2011).

The major source of micropollutants in water are wastewater treatment plants, as illustrated in Figure 1-1 (Nikolaou et al. 2007). Pollutants such as pharmaceuticals and their metabolites are mostly excreted and washed away with the wastewater. Pesticides on the other hand percolate through the soil into the groundwater.

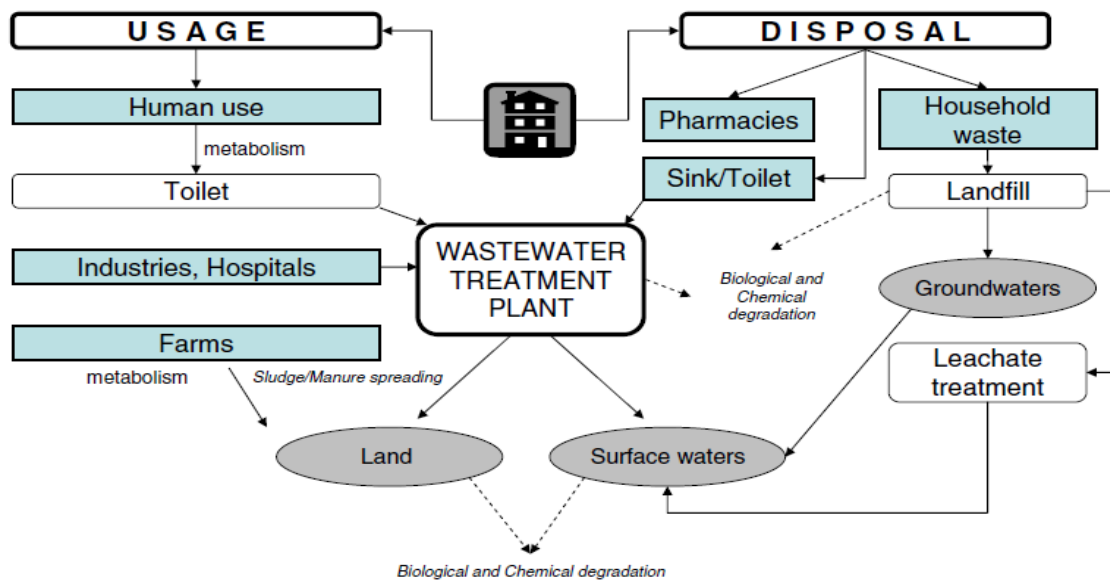


**Figure 1-1:** Pathway of different types of micropollutants in the environment (Nikolaou et al. 2007)

There is a large number of different micropollutants and this chapter will give a better understanding of the negative effects of pesticides on the environment, especially chlorinated hydrocarbons. Also, an overview of their properties will be given to understand how these products are released into and interact with the environment.

## 1.1 Pesticides

---

Nearly 20 years have passed since the Flemish Environmental Agency (VMM) systematically started monitoring pesticides in surface waters. The number of different pesticides, measured at 116 different places, rose to around 100 in 2013. These numbers are for Flanders alone. Measures are necessary to meet the monitoring obligations of the European legislation (VMM 2013).

The package of the pesticides to be monitored contains among others atrazine, isoproturon and simazine, etc. For all these compounds European and Flemish standards are available. Nevertheless, relatively new compounds that replace the banned pesticides are also carefully monitored. Following compounds and degradation products are found in almost 90% of the monitoring sites: diuron, terbutylazine, 2-hydroxy-atrazine, linuron and carbendazim.

Because of the diversity of micropollutants, this thesis will only focus on pesticides, namely chlorinated cyclic hydrocarbons such as pentachlorobenzene (PeCB), hexachlorobenzene (HCB) and alpha-hexachlorocyclohexane ( $\alpha$  – HCH). These components are described as priority hazardous substances by Flemish regulations for environmental licenses (VLAREM II 2014).

## 1.2 Chlorinated hydrocarbons

---

In Flanders, compounds such as pentachlorobenzene (PeCB), hexachlorobenzene (HCB) and alpha-hexachlorocyclohexane ( $\alpha$  – HCH) are uncommon and do not exceed the European standards. This can be shown with the data obtained by the Flemish Environmental Agency (VMM) in Table 1-1 (VMM 2013). Nonetheless these compounds accumulate on places such as Antarctica and the Southern Ocean, far away from their original source. They can travel such great distances due to long range atmospheric transport and disposition (Cristóbal Galbán-Malagón et al. 2013).

**Table 1-1:** Occurrence of  $\alpha$ -HCH, PeCB and HCB in Flanders (VMM 2013)

	2012		2013	
	Number of tested sites	Percentage of sites with exceedance	Number of tested sites	Percentage of sites with exceedance
Alpha-hexachlorocyclohexane	102	0	100	5
Pentachlorobenzene	5	0	33	0
Hexachlorobenzene	9	0	39	0

### 1.2.1 Use of chlorinated cyclic hydro carbonates

---

As mentioned before, all of these compounds are pesticides or by-products of other pesticides. Although all 3 components are banned for agricultural use in Europe, they can still be used in other industries and find their way into the environment (EFSA 2006).

Between 1948 and 1997, it was estimated that usage of technical HCH was approximately 10 billion kilo worldwide (Li 1999). This product was first synthesized by Michael Faraday in 1825. It was only until 1942 that the insecticidal properties of the  $\gamma$ -isomer were discovered (Metcalf 1955). HCH is available in 2 main different compositions, first being technical HCH and secondly being lindane. The 2 vary from the proportion of isomers:

- Technical HCH:  $\alpha$ : 55-80%,  $\beta$ : 5-14%,  $\gamma$ : 8-15%,  $\delta$ : 2-16% and  $\epsilon$ : 3-5%
- Lindane:  $\gamma$ : > 90%

The use of HCH has drastically increased agricultural gaining protection of livestock and reduced the threat of diseases (Woodwell et al. 1975).

Pentachlorobenzene is a substance that is used to make another chemical, namely pentachloronitrobenzene. The latter was used as a fungicide. Therefore, when pentachloronitrobenzene was used, pentachlorobenzene could enter the environment as byproduct (EPA 1987).

Pentachlorobenzene was also used in Canada in dielectric fluids, in combination with polychlorinated biphenyl's (PCB's) (CEPA 2007). When PCB's where banned in the 1980's, the amount of PeCB declined drastically.

As with previous compounds, hexachlorobenzene has no commercial use anymore (EPA 2000). It was however used as pesticide until it got banned in 1965. Other uses for this pollutant were in productions of rubber, aluminum, and dyes and in wood preservation. The only way hexachlorobenzene is produced nowadays is through formation of byproducts when synthesizing other chemicals.



## 1.2.2 Properties and behavior

Knowing physical properties of these compounds gives a better view on their behavior in the environment. This data is also important when developing an analysis method (see Chapter 4: Methods). An overview of properties can be found in Table 1-2.

Alpha-hexachlorocyclohexane is a stereoisomer of hexachlorocyclohexane and is the major component in technical hexachlorocyclohexane. All isomers differ in axial equatorial substitution pattern of chlorine around the ring, as illustrated in Figure 1-2. In this figure,  $\alpha$ -HCH has 2 representations, because this isomer can exist as two enantiomers. This means that two stereoisomers are mirror images of each other. Because the molecules pentachlorobenzene and hexachlorobenzene are planar molecules, no stereoisomers can exist (Willett et al. 1998).

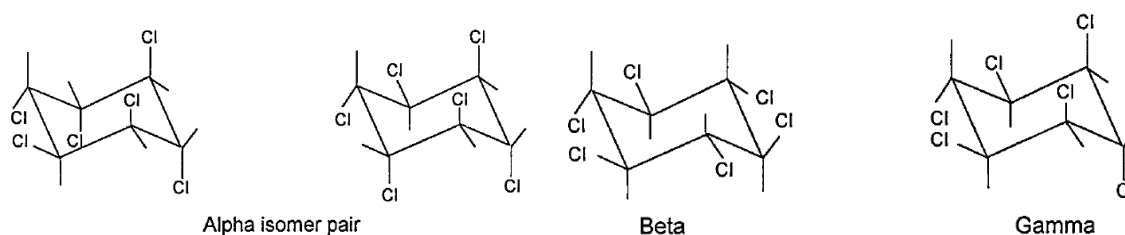


**Figure 1-2:** Representation of the 4 first stereoisomers, namely the 2  $\alpha$ -HCH enantiomers,  $\beta$ -HCH and  $\gamma$ -HCH (Willett et al. 1998).

**Table 1-2:** Overview of physical properties of  $\alpha$ -HCH, PeCB and HCB.

	Alpha Hexachlorocyclohexane	Pentachlorobenzene	Hexachlorobenzene
Chemical formula	$C_6H_6Cl_6$	$C_6HCl_5$	$C_6Cl_6$
Structural formula			
Molar mass (g/mol)	290.83	250.34	284.80
Density (g/ml)	1.87	1.80	2.04
Melting point (°C)	159 – 160	86	231
Boiling point (°C)	288	275 - 277	323 - 326
Vapor Pressure (mPa)	5.99	222.9	1.45
Solubility in water (mg/l)	10.0 (20 °C) (ATSDR 2005)	0.65 (20 °C) (GSI 2013)	0.035 (EPA 2014)

At room temperature, these 3 components are white or colorless solids. They are odorless and can be found as small crystals or powder. PeCB, HCB and  $\alpha$ -HCH are, despite their high boiling point, considered to be volatile compounds, due to their high vapor pressure.

Nonvolatile pesticides such as glyphosate and benomyl have vapor pressure of about 0.002 and 0.005 mPa respectively (Ecobichon 1998). In comparison with, for example, ethanol they are far from volatile (vapor pressure: 5.95 kPa).

Half-life of pentachlorobenzene is estimated to be 45 to 467 days, while half-life of hexachlorobenzene is up to 2 years. For  $\alpha$ -HCH this is 115 days. Because all of these compounds have an atmospheric half-life of more than 2 days, they meet the POP (persistent organic pollutants) criterion. Thus, these micropollutants are capable of undergoing long-range atmospheric transport (Van de Plassche et al. 2002).

Semi-volatile pesticides such as HCH and HCB are mainly produced in the northern hemisphere. Nonetheless, they are also found in the Antarctic region. This phenomena can be explained by the efficiency of long-range atmospheric transport due to their volatile properties (Cristóbal J Galbán-Malagón et al. 2013).

### 1.2.3 Hazard analysis

---

Because of their persistence, these pesticides have tendency to accumulate over a long period of time. For instance,  $\beta$  – HCH is the most toxicologically significant due to the fact that it accumulates easily in mammalian tissues. Also, this isomer has a half-time of 7.2 years in blood, in comparison to only 1 day of accumulation for  $\gamma$ -HCH (Li 1999).

HCH itself affects the central nervous system, it will inhibit neurotransmission and stimulation related to neurotransmitter release (Willett et al. 1998). For  $\alpha$ -HCH, its inhibition effects are 15 – 30 times less potent than those of  $\gamma$ -HCH (Vale et al. 1998). However, long term oral intake of  $\alpha$ -HCH by laboratory rats resulted in liver cancer. Therefore, HCH and all its isomers are determined to be reasonably anticipated to cause cancer in humans by The Department of Health and Human Services (ATSDR 2005). The US environmental Protection Agency (EPA) however declared technical HCH and  $\alpha$ -HCH as only probable human carcinogenic (ATSDR 2005).

PeCB has been tested on mice and rats for acute toxicity. For oral exposure, the LD50 was about 250 mg/kg bodyweight. Whereas for dermal exposure, no toxic effect where seen at a dose of 2500 mg/kg bodyweight. Most recorded effects of oral intake of PeCB are liver and kidney malfunctions (EPA 1987, (Linder et al. 1980) and Van de Plassche et al. 2002).

A study on rats showed that HCB distorted the distribution of certain enzymes in the liver at a dose of 32 mg of HCB/day/kg bodyweight. Also female rats where more sensitive than males to the toxic effects of HCB (Kuiper-Goodman et al. 1977). Neurological, teratogenic, liver, and immune system effects have been reported in the offspring of animals orally exposed to hexachlorobenzene while they were pregnant. Although human data on the carcinogenic effects of HCB are scarce, HCB tends to induce tumors of liver and kidney in several animal species. EPA has classified this compound as probable carcinogenic (EPA 2014).

In summary, all of these pesticides are considered priority hazardous substances. Therefore, measures have been taken for cessation or phasing out of discharges, emissions and losses of  $\alpha$ -HCH, PeCB and HCB. In Table 1-3, the environmental quality standards for different types of water can be found. When concentration exceeds the Classification criterion for hazardous substances (HS), water is considered as industrial wastewater containing hazardous substances. In and around west of Europe concentrations for  $\alpha$ -HCH lie around 0.5 ng/l. For HCB these values are about 0,15 ng/l and for PeCB, 0.30 ng/l (Bergqvist et al. 1998).

**Table 1-3:** Environmental quality standards for different types of waters (all units are in  $\mu\text{g/l}$ ). (VLAREM II 2014).

	Rivers and lakes		Transitional waters		Classification criterion HS
	Average	Maximum	Average	Maximum	
HCH	0.02	0.04	0.002	0.02	0.02
PeCB	0.007	Does not apply	0.0007	Does not apply	0.007
HCB	0.01	0.05	0.01	0.05	0.01

## 2 Micropollutant removal techniques

---

Micropollutant removal can be induced with a variety of techniques. This chapter will give an overview of 4 commonly used methods to remove persistent pollutants. Table 2-1 will provide a summary of effectiveness and drawbacks of these techniques. These techniques are not capable of removing all micropollutants so development of new methods to remove these pollutants is necessary. Plasma treatment might be a good alternative.

### 2.1 Activated carbon

---

Because of physical and chemical adsorbent characteristics of activated carbon, removal of organic micropollutants is possible (Quinlivan et al. 2005). Because of adsorption, activated carbon can eliminate nonpolar components. In order to get higher selectivity activated carbon fibers (ACF) can be used, which have a higher adsorption rate and selectivity than granular activated carbon (Li et al. 2011).

### 2.2 Advanced oxidation processes

---

Advanced oxidation processes are a group of oxidative processes that uses hydroxyl radicals to degrade micropollutants. Hydroxyl radicals break down a variety of organic compounds with low selectivity (Esplugas et al. 2007). These radicals can be produced in many different ways (Echigo et al. 1996):

- Fenton process ( $\text{Fe}^{2+}$  and hydrogen peroxide)
- Ozone, hydrogen peroxide, UV and combinations

### 2.3 Nano filtration

---

Traditionally, nanofiltration is used for water softening, but also can be used to remove organic pollutants. The removal by nanofiltration is characterized by the molecular size of the components. A parameter that shows the rejection of 90% of the compounds with a higher molecular weight is called molecular weight cut-off (MWCO). MWCO for most nanofiltrations is around 200 till 500 g/mol, which is also about the molar mass of most micropollutants (Verliefde et al. 2007).

### 2.4 Coagulation/flocculation

---

Coagulation – flocculation is a technique in conventional drinking water treatment facilities that removes colloidal particles. Using aluminium- or iron-based salts, coagulation is induced by reducing repulsive interactions between particles (Thuy et al. 2008). This allows particles to accumulate in order to remove them by filtration or sedimentation. Micropollutants can be adsorbed in the particles in the water, allowing them to be removed more easily (Adams et al. 2002, Ballard and MacKay 2005).

**Table 2-1:** Overview of 4 different techniques for micropollutant removal (Luo et al. 2014, Thuy et al. 2008, Van der Bruggen et al. 2001)

Technique	Removal efficiency					Micropollutant related factors	Disadvantages	Residues
	Pharmaceuticals	Personal care products	Steroid hormones	Pesticides	Industrial chemicals			
Active carbon	Medium-high	Medium-high	High	High	Medium-high	<ul style="list-style-type: none"> <li>➤ Hydrophobicity</li> <li>➤ Molecular size</li> <li>➤ Structure</li> <li>➤ Functional group</li> </ul>	<ul style="list-style-type: none"> <li>➤ Relatively high financial costs</li> <li>➤ Lower efficiency in the presence of NOMs</li> <li>➤ Need for regeneration</li> <li>➤ Disposal of used carbon</li> </ul>	Used material
AOPs	Medium-high	Medium-high	High	High	Medium-high	<ul style="list-style-type: none"> <li>➤ Compound structure</li> </ul>	<ul style="list-style-type: none"> <li>➤ High energy consumption</li> <li>➤ Formation of byproducts</li> <li>➤ Interference of radical scavengers</li> </ul>	Residual oxidants
Nanofiltration	Medium-high	High	Medium-high	Medium	Medium-high	<ul style="list-style-type: none"> <li>➤ Hydrophobicity</li> <li>➤ Molecular size</li> </ul>	<ul style="list-style-type: none"> <li>➤ High energy demand</li> <li>➤ Membrane fouling</li> <li>➤ Disposal of concentrate</li> <li>➤ Desorption of sorbed chemicals from membrane</li> </ul>	Concentrate
Coagulation	Low-medium	Medium-high	Low	Low	Low-high	<ul style="list-style-type: none"> <li>➤ Hydrophobicity</li> <li>➤ Molecular size</li> </ul>	<ul style="list-style-type: none"> <li>➤ Ineffective MP removal</li> <li>➤ Large amount of sludge</li> <li>➤ Introduction of coagulant salts in aqueous phase</li> </ul>	Sludge

### 3 Plasma Technology

---

To get a better understanding why plasma discharges in contact with water is a promising technique to compete with alternative AOPs, it is important to understand its nature. Basically, plasma is partially or fully ionized gas which is considered to be the fourth state of matter (Figure 3-1). It consists of electrons, free radicals, ions and neutrals and is produced by electrical discharges (Jiang et al. 2014).

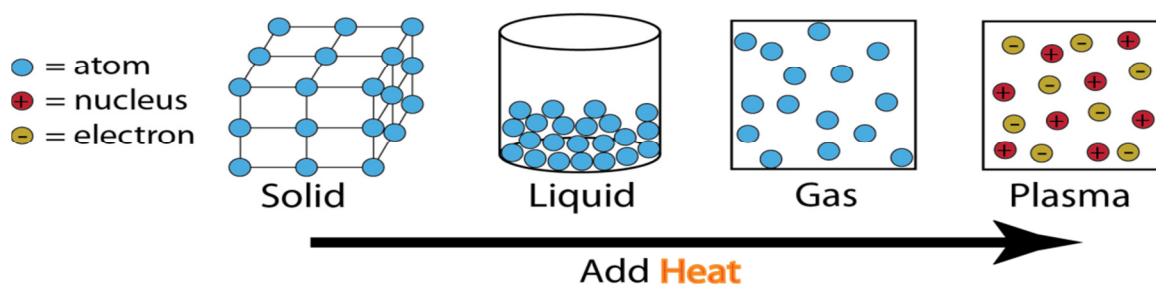


**Figure 3-1:** The four states of matter (solid, liquid, gas and plasma)

Transition from gas to plasma is based on ionization reactions. That is why plasma is defined as ionized gas. Macroscopically, plasma is considered electrically neutral, which means that there is an equal amount of positive and negative charges, but because of high energy addition, particles like ions and electrons will get separated. The electron velocity will be much higher than the ion velocity due to their lower mass and higher mobility (Wang et al. 2007).

#### 3.1 Plasma parameters

---

Important parameters that characterize plasma are density and temperature of composing species and electron Debye length (Wang et al. 2007).

##### 3.1.1 Density

---

Plasma density refers to degree of ionization. This is also known as electron density ( $n_e$ ) or number of electrons per unit of volume. As mentioned before a plasma is electrically neutral, which means that electron density is equal to ion density.

##### 3.1.2 Temperature

---

Three types of temperature are defined for plasma: electron temperature, ion temperature and gas temperature (Zhu and Pu 2008). These relative temperatures divide plasma into either thermal plasma and non-thermal plasma. For non-thermal plasma, as used in this work, electron temperature will be higher than the ion and gas temperature, whereas ion and gas temperature will be approximately equal. For thermal plasma, thermal equilibrium is reached. Electron temperature can be determined using optical emission spectroscopy.

### 3.1.3 Debye Length

The maximum length an electron can move away from an ion without being electrostatically screened is called Debye length. When plasma is induced by an arc discharge in atmospheric-pressure, Debye length will be  $10^{-7}$  m whereas space plasma will have one of 1 m (Wang et al. 2007).

### 3.2 Discharge types

Plasma is generally an electric discharge, formed by passing electrical current through a gas. To review the possible discharges a current-voltage characteristic is made (Figure 3-2). This graph is not representative for every setup, but gives a good image of different stages of a discharge (Chu and Lu 2013).

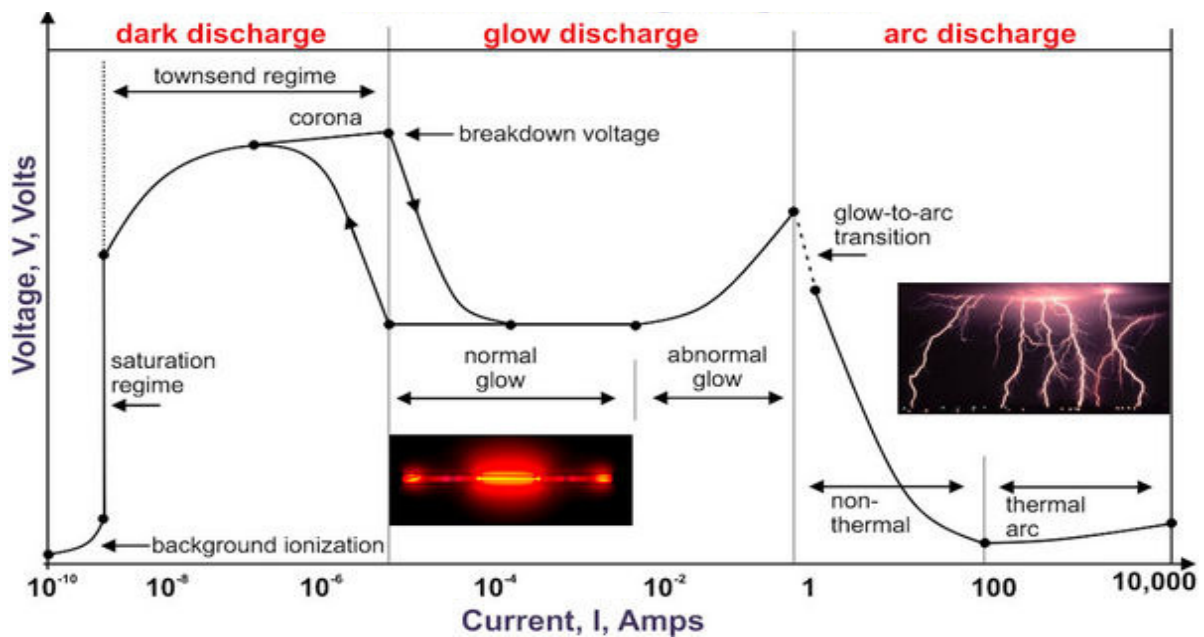


**Figure 3-2:** Current-voltage characteristic (Plasma Universe 2014)

When a certain voltage is achieved, the electric field will be large enough to accelerate electrons. These electrons will cause ionization. When current rises, Townsend discharge will be developed. It is characterized by collision of electrons to another molecule, resulting in a cleavage of an atom or molecule. This will result a chain reaction so more free electrons will reach the anode, as described in Figure 3-3.

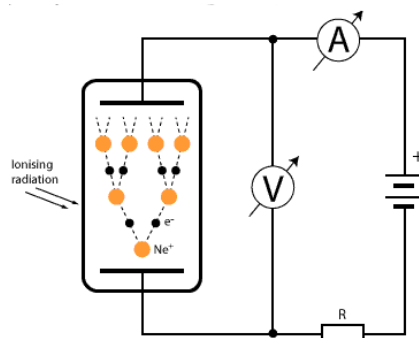


**Figure 3-3:** Illustration of electron chain reaction in Townsend discharge (Saltechtips 2014)

At higher current, discharge starts to be self-contained. This is called glow discharge. Here, charge density is large enough to produce its own electric field, hence the self-containing properties. When current density is rising, transition from normal to abnormal glow discharge is observed. Abnormal glow discharge will undergo a lot of influence of the plasma heating. At a certain point, an arc discharge is obtained. Because an arc discharge is highly conductive, a drop in voltage can be observed (Schutze et al. 1998).

Different types of plasma exist and are listed in Table 3-1. These various types of plasma already have found their way into industrial applications. For example, solid waste treatment has more benefit of thermal plasma. High gas temperature and pressure meet the melting and evaporating requirements in this kind of application. Depending on the pollutants, low temperature and high gas pressure plasma can be more beneficial for water treatment (Chang 2009).

**Table 3-1:** Type of industrial plasmas (Chang 2009)

Type	Pressure		Gas Temperature		Electron Temperature		Typical Applications
	Low	High	Low	High	Low	High	
Low pressure Plasma	×		×			×	<ul style="list-style-type: none"> <li>- Semiconductor</li> <li>- Lamp and lasers</li> <li>- Display</li> </ul>
Non-Thermal Plasma		×	×			×	<ul style="list-style-type: none"> <li>- Air pollution control</li> <li>- Waste treatment</li> <li>- Polymer coating</li> <li>- Polymer treatment</li> </ul>
Thermal Plasma		×		×		×	<ul style="list-style-type: none"> <li>- Solid waste treatment</li> <li>- Coating</li> <li>- Ceramic process</li> <li>- Water treatments</li> <li>- Cutting &amp; welding</li> </ul>
Nuclear Fusion Plasma	×			×		×	<ul style="list-style-type: none"> <li>- Energy</li> <li>- Military</li> </ul>

### 3.3 Non-thermal plasma

Thermal plasma will introduce high electrical energy that will destroy most of the waste through thermal destruction process. When non-thermal plasma is used a higher selectivity and energy efficiency can be achieved (Jiang et al. 2014). For this research non-thermal plasma will be used because of its selectivity and the lower current that is required. Essentially non thermal plasma means that the division of energy to light electrons and heavy particles (ions and neutrals) will not be equal. Power applied to the plasma will favor electrons, which results in higher electron temperature (Chu and Lu 2013).



This type of plasma can be generated by glow, arc, corona, capacitively coupled and inductively coupled discharge. Stable non-thermal plasma is easy to produce under low pressure conditions and gas temperature below room temperature. When atmospheric pressure is used, plasma will become unstable and will form arcs, sparks or microfilaments instead of glow discharge. To make sure a stable plasma is achieved, special geometries and electrodes have to be used (Chu and Lu 2013). This plasma in contact with water produces a lot of active species which is favorable in order to remove organics compounds such as micropollutants.

### 3.4 Dielectric barrier discharge

---

Water treatment with plasma can be designed in different electrode configurations. Based on the plasma-phase distribution these discharges can be subdivided into 3 main groups (Locke et al. 2006):

- Direct electrical liquid discharges
- Electrical discharges above the liquid surface
- Discharges in bubbles/vapor in liquid

The first type of discharge is very complex because water as discharge medium is much denser than gas. Also, the transfer of current is highly affected by conductivity and purity of the water. The second type, where the electrical discharge is above the liquid surface, the liquid itself acts as an electrode. Because of the gas-liquid interface, oxidative reagents (OH radicals, O<sub>3</sub>, ...) can diffuse easily into the water and initiate chemical reactions, so diffusion will not be a limiting factor. When bubbles are used, similar effects can be observed, as with electrical discharges above the liquid surface. The main advantage of using bubbles is that the gas-liquid contact surface is much larger. This allows for more chemical reagents to transfer into the water.

To make the setup more convenient electrical discharges above the liquid surface where chosen under the form of dielectric barrier discharge (DBD).

### 3.5 Plasma chemistry

---

Plasma generated in the air, in contact with water will generate a number of active species in the gas phase. These active species will induce formation of secondary species in water (Machala et al. 2013). The compounds made by the plasma can then be divided into 2 different groups: reactive oxygen (ROS) and nitrogen species (RNS). Due to the reactivity, a lot of the active components have a short lifetime. That is why only the most important ones will be discussed (Lukes et al. 2014).

Research shows that electrical discharges could dissociate H<sub>2</sub>O into OH and H (Figure 3-4). This could lead to the formation of hydroxyl radicals, which is one of the most important chemical oxidants. This oxidant can help to destroy persistent compounds (Locke and Shih 2011).

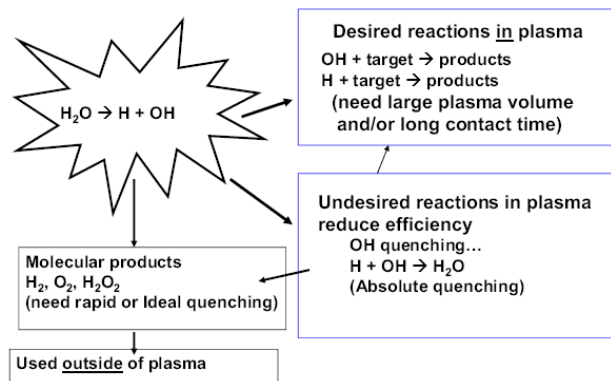
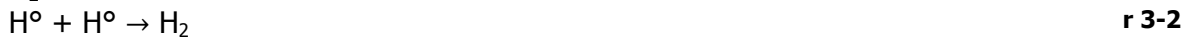


**Figure 3-4:** Schematic representation of OH radical formation by plasma (Locke and Shih 2011)

### 3.5.1 Hydrogen Peroxide

Hydrogen peroxide is an important oxidizer formed by a recombination reaction after the decomposition of water molecules (Vasko et al. 2014). This reaction is also known as the hydroxyl radical recombination reaction and consists of 2 main reactions: decomposition (r 3-1) and recombination (r 3-2, r 3-3 and r 3-4) (Vasko et al. 2014).



$\text{H}_2\text{O}_2$  can also be formed in the gas phase, where the plasma comes in contact with water vapor. Because the concentration of oxygen is a lot higher than  $\text{OH}^\circ$  radicals concentration,  $\text{H}_2\text{O}_2$  is formed by recombination of hydroperoxyl radicals (r 3-6) (Vasko et al. 2014).



Hydrogen peroxide however is more of importance when used in low power discharge reactors than in high power ones. The main reason is that in low power reactors, there will be less radicals to interfere with the stability of the hydrogen peroxide (Locke and Shih 2011). High temperature is the next parameter that will drastically decrease the  $\text{H}_2\text{O}_2$  concentration.

### 3.5.2 Ozone

Dry air, will flow between 2 electrodes which are separated by an insulating barrier (hence the name, dielectric barrier discharge). In this air flow, ionization will occur, plasma will be formed and oxygen molecules will split into oxygen atoms. These atoms then recombine with the O<sub>2</sub> in the air and will form ozone. With M, the micropollutants.



The single oxygen atoms can also react with each other, resulting in a less desirable recombination reaction, to form dioxygen (Pekárek 2014).



Ozone is transferred from the gas phase into the liquid, where ozone will react selectively with organic compounds. This is only when direct oxidation occurs, ozone will then attack unsaturated and aromatic compounds. When high pH is observed, ozone will decompose and generate OH radicals, which will react more randomly with those organic compounds (Dobrin et al. 2014).

### 3.5.3 Nitric acid

Because of the presence of nitrogen in air, all types of nitrogen derivates (NO<sub>x</sub>, NO<sub>2</sub><sup>-</sup>, NO<sub>3</sub><sup>-</sup>, ...) are formed. The formation of NO begins with bond breaking of nitrogen gas with electrons (r 3-9) or reaction with oxygen atoms (r 3-11) (Brisset et al. 2011).



From there on NO<sub>2</sub> can be formed, either through thermal oxidation or through a reaction with ozone. Because the system is in close contact to water, NO will dissolve in water, with similar diffusion as O<sub>2</sub> in water (Zacharia and Deen 2005). The formation of nitric acid itself is described in Figure 3-5.

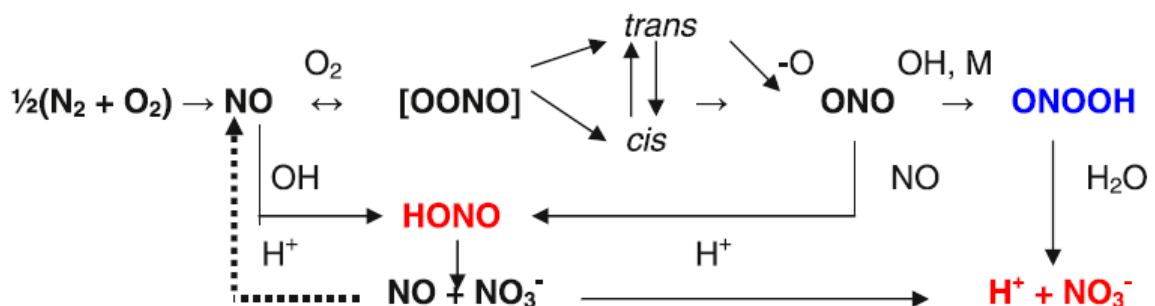
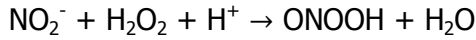


**Figure 3-5:** Formation path of nitric acid (Brisset et al. 2011)

The decomposition of NO<sub>x</sub> and the formation of NO<sub>2</sub><sup>-</sup>, NO<sub>3</sub><sup>-</sup> is responsible for the acidification of the solution (Machala et al. 2013).

### 3.5.4 Other active species

Other active species are a lot more difficult to measure due to their short lifetimes and fast disproportionation. One of these species is peroxyxynitrite, which is formed through the reaction between hydrogen peroxide and nitrous acid (r 3-12).



r 3-12

Peroxyxynitrite, however, is not stable in acidic conditions and will decompose (Figure 3-5) (Lukes et al. 2014). A complete overview of all known reactions can be found in Figure 3-6. These nitrogen and oxygen species can react with organic compounds and degrade them to less harmful components.

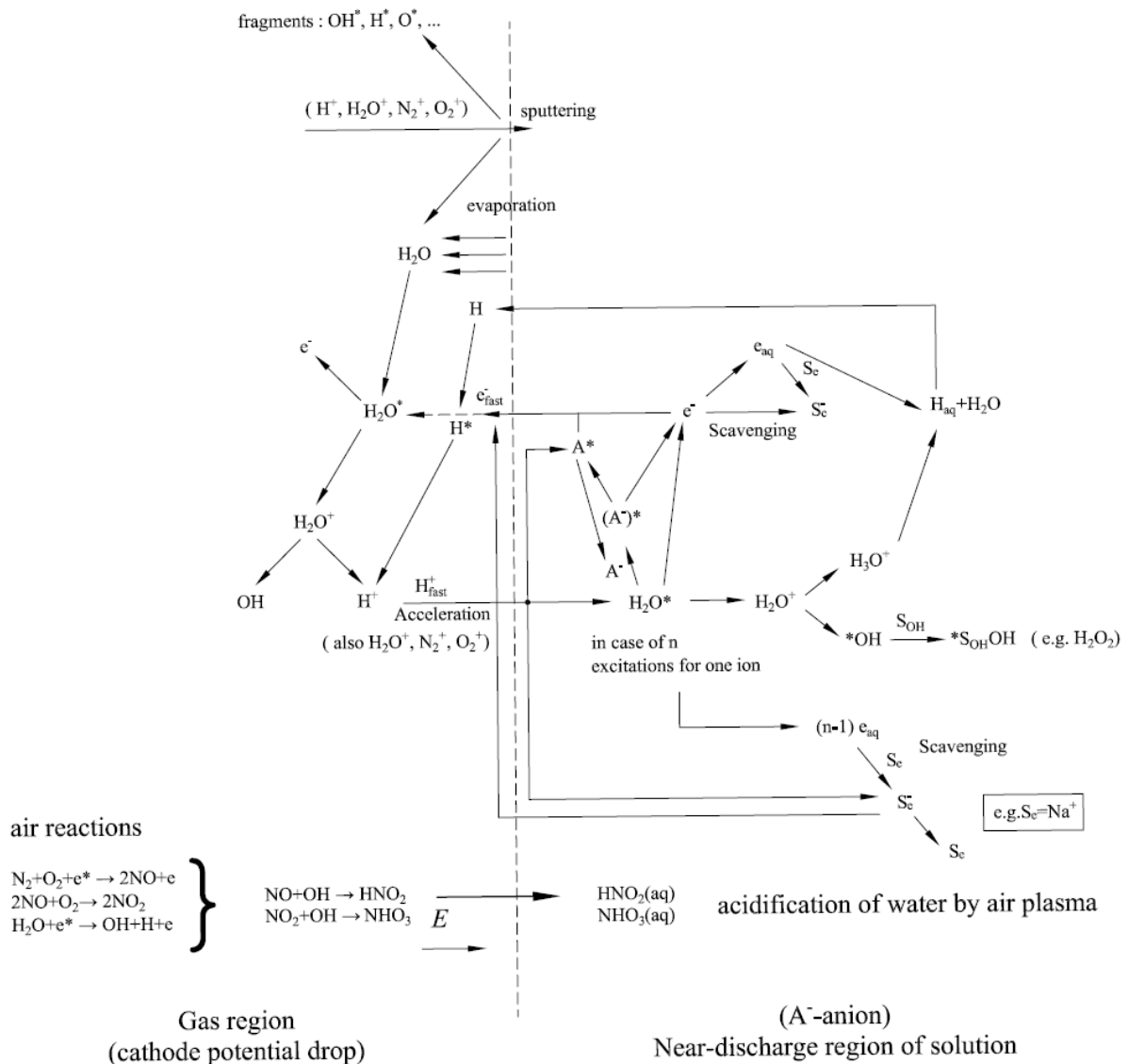


**Figure 3-6:** Complete overview of all reactions occurring in and around water (Bruggeman and Leys 2009)

---

## *II. Experimental setup, methods and materials*

---

## 4 Materials and experimental setup

This chapter describes the different chemicals and measuring equipment, used throughout this thesis. It also gives the full design specifications of the plasma reactor with the motivation for this design.

### 4.1 List of chemical products

In Table 4-1, an overview of the used chemicals can be found, together with their purity and manufacturer.

**Table 4-1:** List of all used chemicals throughout this thesis

Name	Chemical formula	Purity	Manufacturer
Ammonium monovanadate	$\text{NH}_4\text{VO}_3$	99.3%	VWR International
Potassium indigotrisulfonate	$\text{C}_{16}\text{H}_7\text{K}_3\text{N}_2\text{O}_{11}\text{S}_3$	Unknown	Sigma-Aldrich
Phosphoric acid	$\text{H}_3\text{PO}_4$	85%	Sigma-Aldrich
Sodium Phosphate	$\text{NaH}_2\text{PO}_4 \cdot 2\text{H}_2\text{O}$	Pure	VWR International
Sulphuric Acid	$\text{H}_2\text{SO}_4$	95.0%	RPL Leuven
Methylene Blue	$\text{C}_{16}\text{H}_{18}\text{N}_3\text{SCl}$	Unknown	Unknown
Alpha hexachlorocyclohexane	$\text{C}_6\text{H}_6\text{Cl}_6$	99.8%	Sigma-Aldrich - Fluka
Pentachlorobenzene	$\text{C}_6\text{HCl}_5$	100%	Sigma-Aldrich - Fluka
Hexachlorobenzene	$\text{C}_6\text{Cl}_6$	99.9%	Sigma-Aldrich - Fluka
Naphthalene	$\text{C}_{10}\text{H}_8$	Unknown	Unknown
Ethyl acetate	$\text{C}_4\text{H}_8\text{O}_2$	99.8%	VWR International
Methanol	$\text{CH}_3\text{OH}$	99.8%	VWR International
Dichloromethane	$\text{CH}_2\text{Cl}_2$	99.9%	Carl Roth
Acid Blue	$\text{C}_{20}\text{H}_{13}\text{N}_2\text{NaO}_5\text{S}$	45%	Sigma-Aldrich
Sodium Hydroxide	$\text{NaOH}$	>95%	Acros Organics
Humic Acid	Unknown	30-40%	Carl Roth
Isopropyl alcohol	$\text{C}_3\text{H}_8\text{O}$	99.8%	Chem-Lab nv

### 4.2 Measuring instruments and devices

#### 4.2.1 Oscilloscope and probes

Using a dual channel Tektronic TDS 1002 oscilloscope with a maximum frequency of 60 MHz, voltage and current can be monitored simultaneously in real time. Voltage is measured with a Tektronix P6015 HV probe, connected to channel 1 of the oscilloscope. On the second channel, a Pearson 2877 current probe is connected. Data from the monitor of the oscilloscope can then be transferred over a RS232 port to a Dell latitude D829 laptop, running Windows XP.

#### 4.2.2 Ozone monitor

---

Ozone concentrations in gas phase were measured with a M450 Ozone monitor from Envitec. This monitor uses the absorption of 254 nm UV light for detection of ozone molecules. With the gas moving through a quartz tube, the ozone monitor acts as a spectrometer for gases. Because the concentration of ozone is dependent on temperature and pressure, these factors are implemented in the calculations of the device itself. This way the device can measure concentrations of ozone from 1 to 1000 ppmv with an error of 0.1%.

#### 4.2.3 UV-VIS spectrometer

---

The absorption spectra of different types of compounds were measured using a UV mini 1240 spectrometer from Shimadzu. Spectral data can be acquired over a wavelength range of 190 nm to 1100 nm. This range is possible with 2 different type of lamps: 20 W halogen lamp (visible light) and a deuterium lamp (UV light).

#### 4.2.4 GC-MS

---

Quantification of micropollutants was possible with a gas chromatograph coupled to a mass spectrometer (GC-MS). This is a computer controlled Agilent HP 5973 6890 GC-MS with an 100 position auto-sampler (Model 7683). Further details about the settings can be found in the next chapter.

### 4.3 Experimental setup: the reactor

---

#### 4.3.1 Design

---

Because of the versatility of the reactor, it can be changed in many configurations. That way, different components of the setup can be examined individually.

##### 4.3.1.1 Standard design

---

The standard model of the reactor can be seen as a closed system, where the same water will continuously be transfer from one chamber to the other. Air flow however will act as an open system. The schematics for this type of design can be found in Figure 4-1. The setup can be filled with contaminated water via a valve (9) and by reversing the direction of the Roth pump (6). With the same valve, samples can be taken for further research. At this point all water is collected in the ozonation chamber (left part of the reactor).

The complete reactor can be put to work by turning both pumps on (in the direction as illustrated) and by turning on the high voltage power supply. Water will then be pumped out of the ozone chamber, into the bottom of the plasma chamber. Here it rises through the metal tube until it reaches the holes at the top. Because the holes are covered with activated carbon cloth, water will be evenly distributed around the outside of the same tube. Eventually it passes through the plasma where a lot of the active species will diffuse and form into the water. In the last step, water gets pumped back into the ozone chamber to avoid flooding. Gas, in form of dry air will first pass through the plasma chamber. There it will transport the excess active species into the ozone chamber.

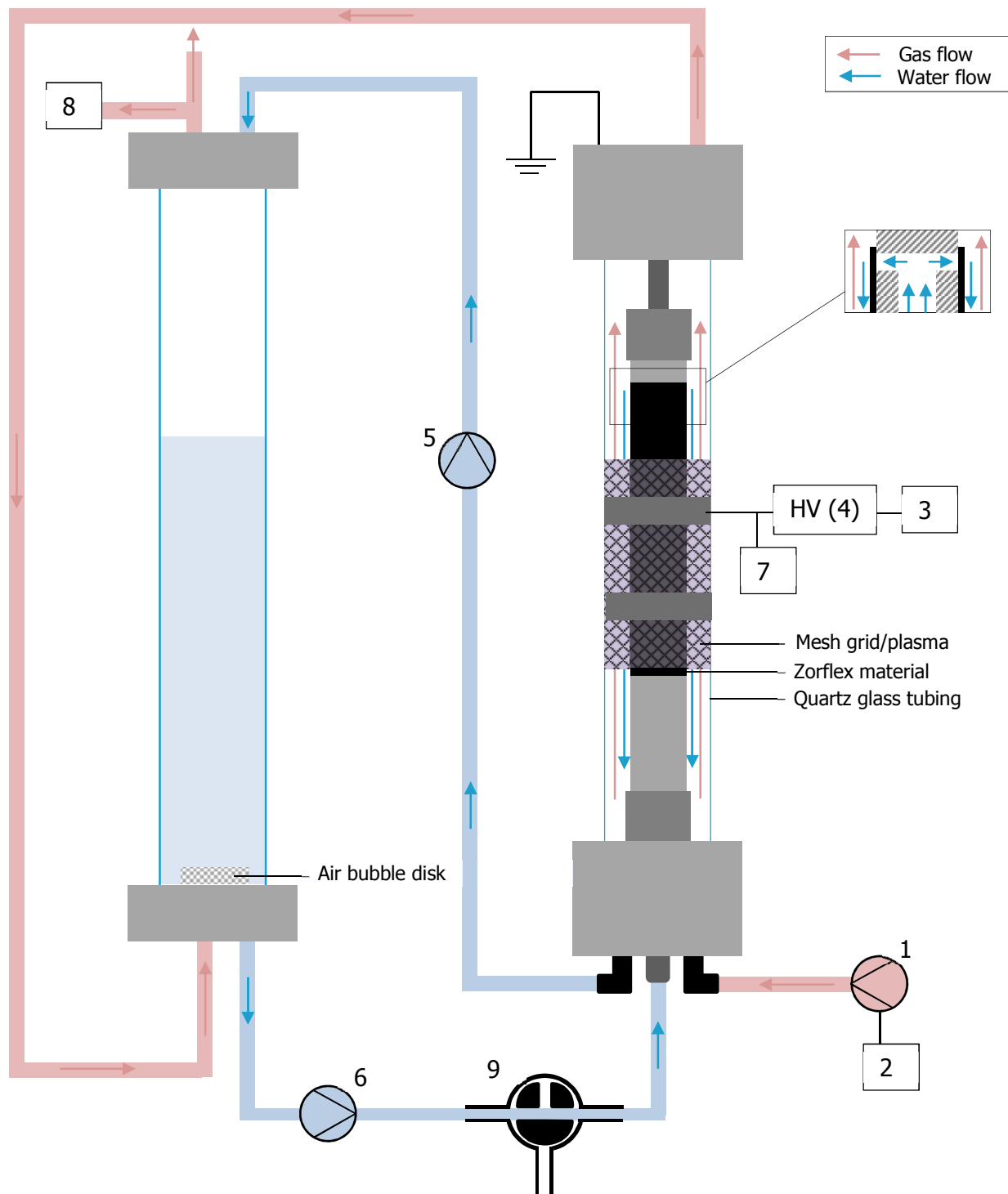


**Figure 4-1:** Schematic overview of the reactor. 1 Mass flow controller; 2 PR 4000 controller; 3 TGP 110 pulse generator; 4 High voltage power generator; 5 custom peristaltic pump; 6 Roth cyclo II peristaltic pump; 7 Tektronic TDS 210 oscilloscope; 8 M450 ozone monitor and 9 T- shaped 3 way ball valve



### 4.3.1.2 Alternative designs

When a continuous process is required, the system can be easily adapted. This level of versatility can be used to mimic industrial applications, such as in waste water treatment plants. This alternative version can be subdivided into 2 alternatives:

- The water passes the plasma reactor first and then the reservoir
- The water passes the reservoir first and then the plasma reactor.

The latter is illustrated in Figure 4-2.

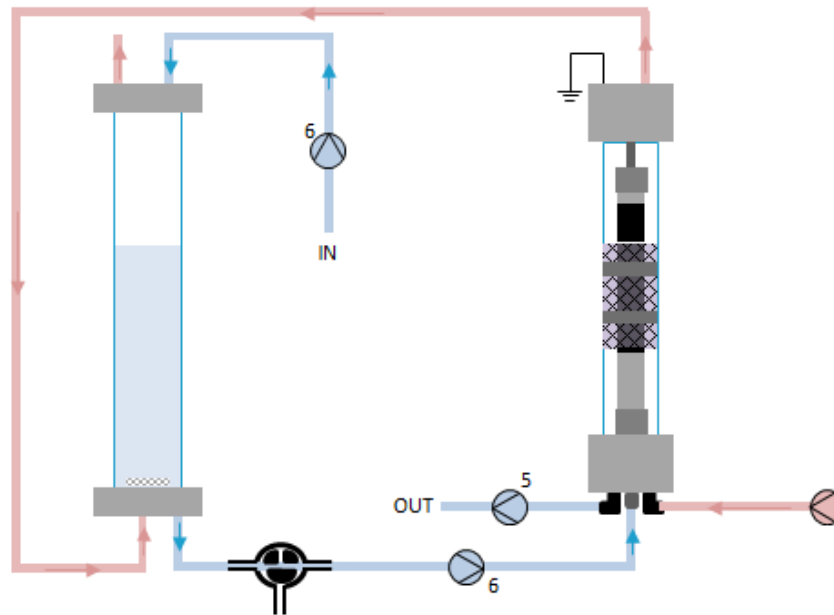


**Figure 4-2:** Schematic of the setup for single pass experiments

### 4.3.2 Specifications

The plasma reactor consists of 2 chambers, one being the plasma chamber, where the plasma is formed. The other one is where gaseous ozone from the plasma chamber runs through the water solution and is called the ozone chamber. In this reactor, about 500 ml of water can be treated by an AC driven dielectric barrier discharge. The dielectric barrier is made from quartz glass (1 mm thick) and creates a discharge gap of about 2 mm where dry air passes through.

#### 4.3.2.1 Power supply

Power can be varied in two different ways. First, this can be done by varying the current on the high voltage power supply itself (Table 4-2). The setup has a periodically interrupted power input (so the reactor does not get damaged, due to overheating). It is possible to change interruption time and which is referred to as duty cycle. Duty cycle is achieved by connecting a pulse generator (TGP 110, 10 MHz pulse generator) to the power supply.

**Table 4-2:** Technical details about the power supply

Electrical parameter	Value/Description
Discharge Voltage	Up to 15.5 kV
High Voltage	AC
AC frequency	50 kHz
Input power	20 – 100 W

#### 4.3.2.2 Pumps

Water is transferred from the reservoir to the plasma reactor at a rate of approximately 95.2 ml/min. This is done with a peristaltic Roth cyclo II pump. To prevent the plasma reactor from getting flooded, a custom peristaltic pump is used at a higher rate than the Roth pump to transfer the fluid back to the ozone chamber.

Plasma is generated in dry air, that is continuously pumped from the plasma reactor through the reservoir, to the outlet. The gas goes from the gas tank to the pump at a pressure of 5 bar. Using a PR 4000 mass flow controller (MKS instruments), a standard rate of 1000 SCCM can be obtained throughout the experiments.

#### 4.3.2.3 Reactor membrane

The reactor membrane acts as a guiding material to let the water run evenly over the central electrode. This prevents the water from falling uncontrollably and makes sure an air gap is preserved. In the standard layout of the reactor Zorflex, an activated carbon cloth supplied by Chemviron Carbon, is used (Figure 4-3). The material itself is designed for military operations, where it provides protection against a wide variety of chemical, biological and nuclear agents.

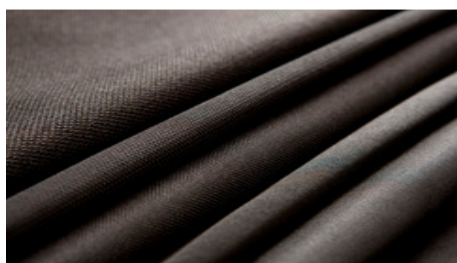


**Figure 4-3:** Activated carbon cloth (Zorflex)

In this setup, a Zorflex knitted cloth model FM50K is used. This material has a surface density of 130 g/m<sup>2</sup>, a thickness of 0.5 mm and a carbon tetrachloride activity of 55-70 %ww. The latter is a measure for the activation level of activated carbon and is defined as the ratio (in percent) of the weight of CCl<sub>4</sub> absorbed by the carbon to the weight of the sample (ASTM D3467).

Another, more industrial textile material that was used, is glass fiber. It is resistant against most chemicals and has little to no absorbing properties. This material is well suited to compare with Zorflex in its influence on the overall process.

### 4.3.3 Design motives

---

Designing a reactor that is both effective, energy efficient and inexpensive to build always encounters some tradeoffs. The design features that are associated with better energy yield (first column) have not been used, as they contribute to higher operation and installation costs and lower sustainability. Table 4-3 shows how much the energy yield is affected by some of the design factors (underlined parts indicates the current reactor).

**Table 4-3:** Requirements for an energy efficient plasma source based on (Muhammad Arif Malik 2010)

<b>Energy yield</b>	Good	Moderate	Poor
<b>Power input</b>	Pulsed DC	<u>Pulsed AC</u>	Continuous AC of DC
<b>Discharge type</b>	Pulsed corona discharge	<u>Pulsed dielectric barrier discharge</u>	DC Discharges
<b>Plasma medium</b>	Oxygen	<u>Air</u>	Liquid
<b>Treated solution as</b>	Fine droplets	<u>Thin film</u>	Deep layer

## 5 Analysis techniques

In this work, chemical, optical and electrical techniques have been used to measure concentrations, powers, pH, conductivities and temperatures. To ensure correctness of all parameters, it is necessary to validate and verify these analysis techniques, as discussed in this chapter.

### 5.1 Power measurements

Voltage and current are both measured with previously described probes (see Chapter 4) and attached oscilloscope. Data is then transferred to a laptop with a dedicated cable. Normally, voltage and current are sine waves. But due to the plasma discharge, the signal gets distorted (Figure 5-1). An average of 128 of these sine waves are used in order to calculate average input power. This can be done automatically by the oscilloscope.

The power ( $P_0$ ) is calculated from voltage and current data from the oscilloscope (Eq 5-1). Because the reactor has a periodically interrupted power output, the duty cycle has to be taken into account when calculating the actual power ( $P$ ). This can be done by multiplying power per period ( $P_0$ ) and duty cycle (Eq 5-3). The duty cycle can be defined by Eq 5-2 and is illustrated in Figure 5-2. The calculation of the power is done numerically using Microsoft Excel. This method is verified using integration with Origin 8.

$$P_0 = \frac{1}{\Delta T} \int_{T_1}^{T_2} I \cdot V dt \quad \text{Eq 5-1}$$

$$D_C = \frac{T_{on}}{T_{on} + T_{off}} \quad \text{Eq 5-2}$$

$$P = P_0 \cdot D_C \quad \text{Eq 5-3}$$

With  $T_1$  and  $T_2$  respectively the lower and upper limit of the measured range. For duty cycle,  $T_{on}$  means the time that power is turned on and  $T_{off}$  the time it is off.

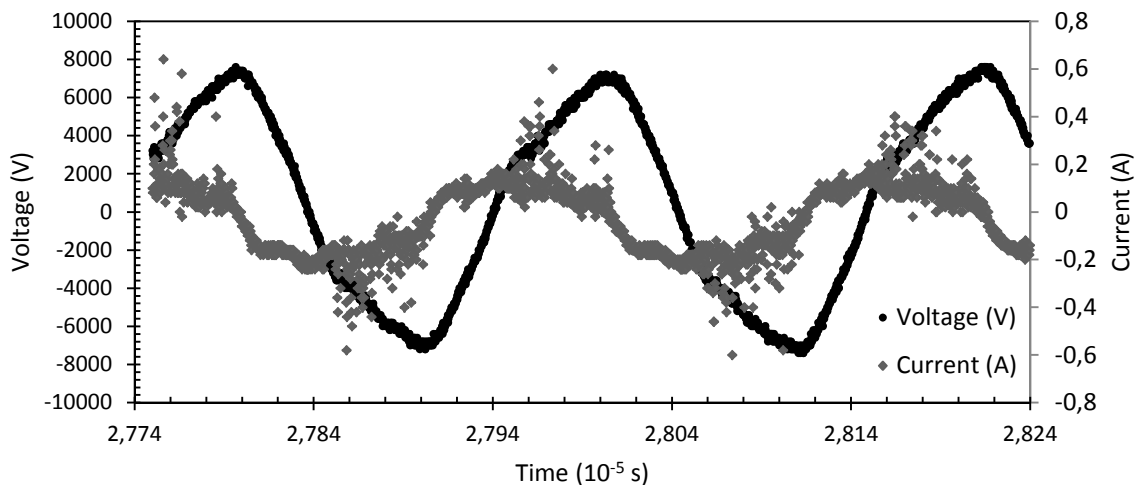


**Figure 5-1:** Voltage and current signal with noise during  $T_{on}$  (measured with oscilloscope)

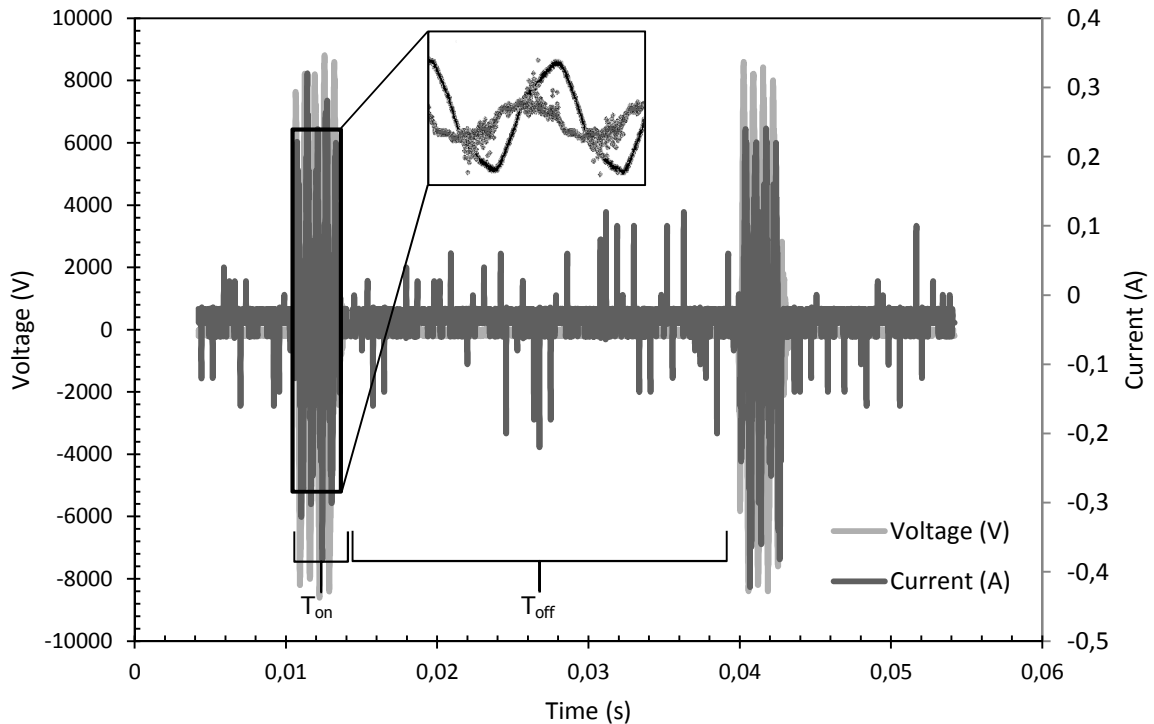


**Figure 5-2:** Illustration of duty cycle (0.15) with  $T_{on}$  and  $T_{off}$  respectively 4.5 and 25.5 ms

## 5.2 Ozone measurements

The reactor produces ozone in air because of reaction of oxygen radicals with oxygen gas. The produced ozone gas is in close contact with water, which allows ozone molecules to dissolve into the liquid phase. Therefore, ozone can be found in water and in gas phase. Ozone in water can be determined using the indigo method, described by Bader and Hoigné (Bader and Hoigné 1981).

### 5.2.1 Ozone in water

#### 5.2.1.1 Method

Ozone in water is determined using the Indigo method by Bader and Hoigné (Bader and Hoigné 1981). This method is based on the reaction of ozone and the double bond of the indigo molecule. This reaction results in decolorization of blue indigo trisulfonic acid solution and can be found in Figure 5-3. The difference in color can be determined with a UV-VIS spectrometer at an absorbance of about 600 nm.

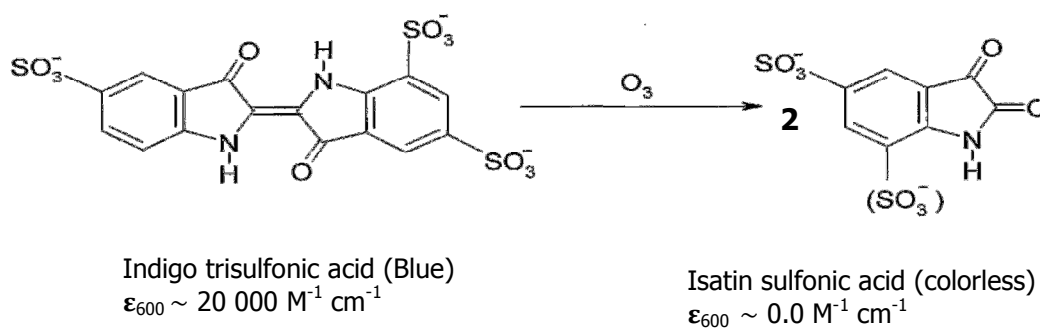


**Figure 5-3:** Reaction of Indigo trisulfonic acid with ozone and corresponding molar absorptivity  $\epsilon_{600}$  at 600 nm

The stock solution of indigo reagent is prepared by dissolving 0.6 g/l (1 mM) potassium indigo trisulfonate in 20 mM phosphoric acid. The 20 mM phosphoric acid solution is prepared by diluting 99 % phosphoric acid 1000 times (19 mM) with deionized water. To stabilize the ozone and keep the pH to around 2, a phosphate buffer was used. This buffer is made by dissolving 15.83 g  $\text{NaH}_2\text{PO}_4 \cdot 2\text{H}_2\text{O}$  in 500 ml of deionized water and subsequently adding 17.1 ml of  $\text{H}_3\text{PO}_4$  (85 %), according to the instructions of Bader and Hoingé.

The measurement itself is executed using 1 ml of phosphate buffer and adding 10  $\mu\text{l}$  of the indigo reagent (9.9  $\mu\text{M}$ ). Then 1 ml of ozone sample is added. Because this sample is not stable, it is necessary to mix the solution firmly. Mixing assures that ozone reacts immediately with indigo, making the solution longer tenable, otherwise ozone will degrade over time. The last step is to add 1 ml of water to match the procedure. This mixture is then added to a cuvette so the absorbance can be measured with a wavelength between 500 and 700 nm (Figure 5-4). Concentration of  $\text{O}_3$  is then calculated with the absorbance at a wavelength of 600 nm.

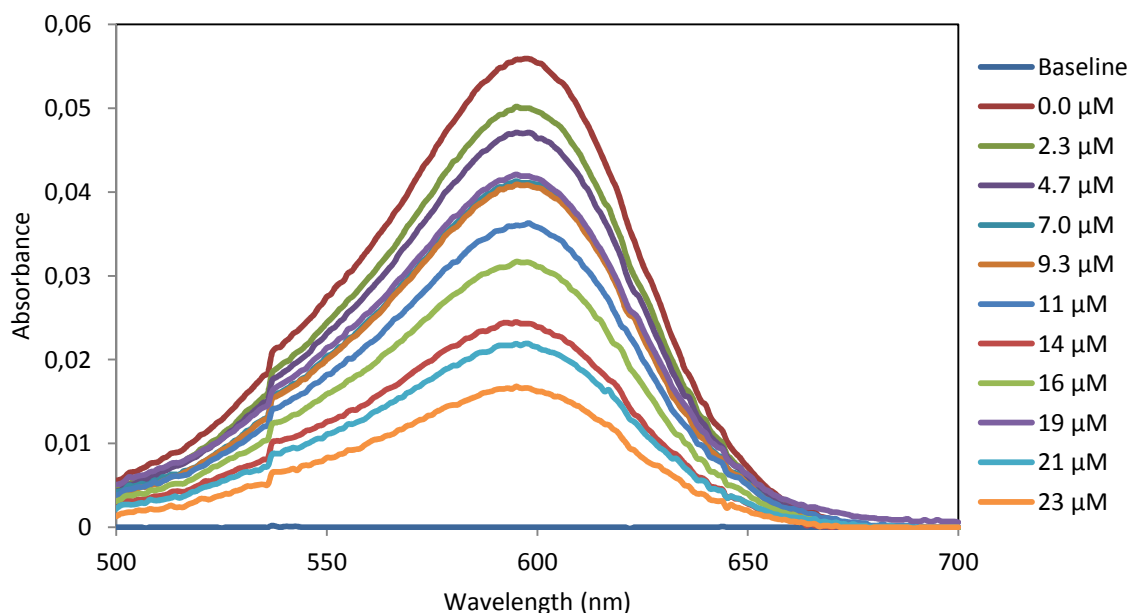


**Figure 5-4:** Indigo absorbance spectrum after adding a certain amount of ozone (ml).

### 5.2.1.2 Calibration

Ideally, the indigo method is calibrated using the iodine method. This iodine method uses potassium iodide which will react with ozone to iodine. The concentration of iodine can then be determined with a titration of sodium thiosulphate. Because the concentration of ozone produced by the reactor is too low for the iodine method, it was not possible to calibrate the indigo method this way.

Therefore, the UV-method has been used to determine the concentration of the ozone solution. Because ozone is not stable, a stock solution has to be made by bubbling ozone from the reactor to a glass tube. This bubbling was done for half an hour to make sure the water was saturated. Then a sample of 1 ml was taken out of the stock solution and put into a quartz cuvette. With a UV-VIS spectrometer, the absorbance was measured at a wavelength of 260 nm. Using the molar absorption coefficient  $3300 \text{ M}^{-1} \text{ cm}^{-1}$  (Hart et al. 1983), ozone concentration in the stock solution can be calculated.

This calculation can be done with the Lambert Beer law (Eq 5-4). An example can be found in the equation below (Eq 5-5). Where A is absorbance, C the concentration,  $\epsilon$  the molar absorption coefficient and b the path length of UV-VIS meter.

$$A = \epsilon \cdot C \cdot b \quad \text{Eq 5-4}$$

$$C = \frac{A}{\epsilon \cdot b} = \frac{0,03894}{3300 \text{ M}^{-1} \text{ cm}^{-1} \cdot 1 \text{ cm}} = 11.8 \cdot 10^{-6} \text{ M} \quad \text{Eq 5-5}$$

This measurement was done 6 times to get an accurate concentration. An overview of this data can be found in Table 5-1. The average of these values will then be used to set up a calibration curve.

**Table 5-1:** Overview of the different concentrations using the UV method.

Absorbance (260 nm)	C <sub>O<sub>3</sub></sub> (µM)	C <sub>O<sub>3</sub></sub> (mg/l)
0.03894	11.80	0.5664
0.03845	11.65	0.5593
0.03869	11.72	0.5628
0.03833	11.62	0.5575
0.03845	11.65	0.5593
0.03820	11.58	0.5556
Average:	11.67 ± 0.081	0.5601 ± 0.0039

With the same ozone stock solution, a dilution sequence is made. This sequence (Figure 5-4) is measured using the indigo method and results in a calibration curve (Figure 5-5).

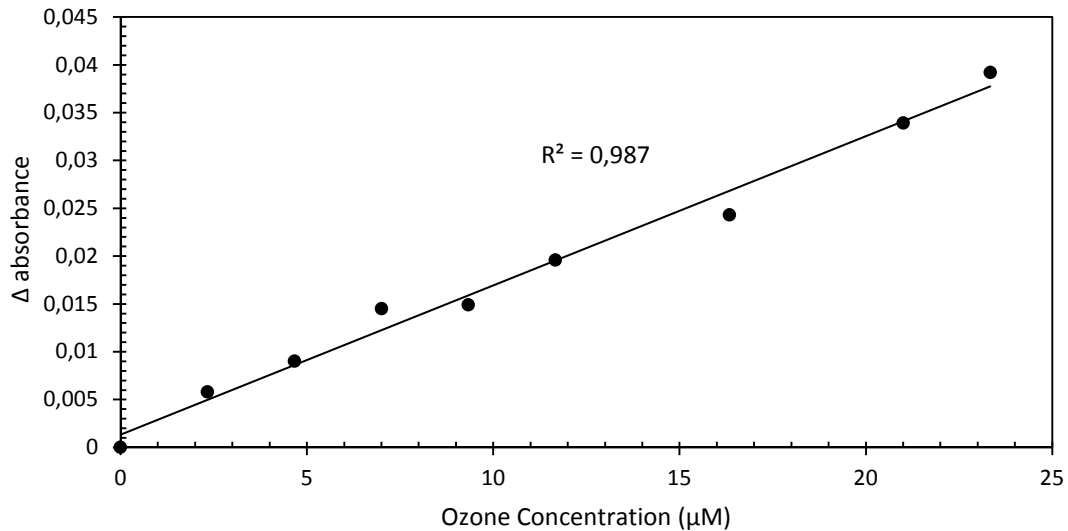


**Figure 5-5:** Calibration curve of the indigo method, absorbance at 600 nm in function of concentration of ozone. On x-axis the ozone concentration and on the y-axis the absorbance of the indigo solution without ozone minus the absorbance with ozone.

### 5.2.1.3 Calculation

Aqueous ozone concentration is directly proportional to the difference of the absorbance with a blank sample of pure water at a wavelength of 600 nm. The concentration of ozone in water is obtained with the Lambert Beer law with a molar absorption coefficient of  $0.001651 \mu\text{M}^{-1} \text{cm}^{-1}$  for indigo (Eq 5-6). Where  $A_0$  represents the absorbance at  $C_{O_3} = 0$  and  $A_x$  the absorbance of the sample. The molar absorption coefficient is obtained from the calibration curve (Figure 5-5).

$$C_{O_3} = \frac{A}{\varepsilon \cdot b} = \frac{A_0 - A_x}{0,00165 \mu\text{M}^{-1}\text{cm}^{-1} \cdot 1 \text{ cm}} \quad \text{Eq 5-6}$$

### 5.2.2 Ozone in air

Ozone concentration in air is constantly monitored and is displayed in ppmv. It is important to note that flow rate in the monitor has to be lower than the flow rate of the dry air through the system. Otherwise, erroneous values are obtained for ozone concentration. In these experiments, ozone in air was measured at the exhaust of the setup.



## 5.3 Hydrogen peroxide measurements

### 5.3.1 Method

The analysis of hydrogen peroxide is based on the method proposed by (Nogueira et al. 2005). This spectrophotometric method uses the reaction between metavanadate and  $\text{H}_2\text{O}_2$  to determine  $\text{H}_2\text{O}_2$  concentration. The method is based on reaction (r. 5.1).



In this reaction, the formation of a red-orange colored peroxovanadium cation will be related to the  $\text{H}_2\text{O}_2$  concentration. As can be derived from the reaction equation, an acidic medium has to be used. The most optimal concentration of the metavanadate ammonium and the acid ( $\text{H}_2\text{SO}_4$ ) were determined in previously discussed paper (Nogueira et al. 2005) and can be found in Table 5-2. This solution is diluted with deionized water and will eventually be referred to as the metavanadate solution. The compounds and their purities used for the metavanadate solution are stated in Table 4-1.

**Table 5-2:** Concentration of the necessary compounds to make 100 ml of the metavanadate solution

	n (mmol)	m (mg)	V (ml)
Ammonium monovanadate	0.62	72.5	-
Sulfuric acid ( $\text{H}_2\text{SO}_4$ )	0.0058	-	0.644

To measure the concentration of peroxovanadium cation, an UV-VIS spectrophotometer is used. The wavelength of the spectrometer is put on a range of 350 to 550 nm, with the concentration measured at 450 nm. This absorbance will be matched to an actual concentration during calibration.

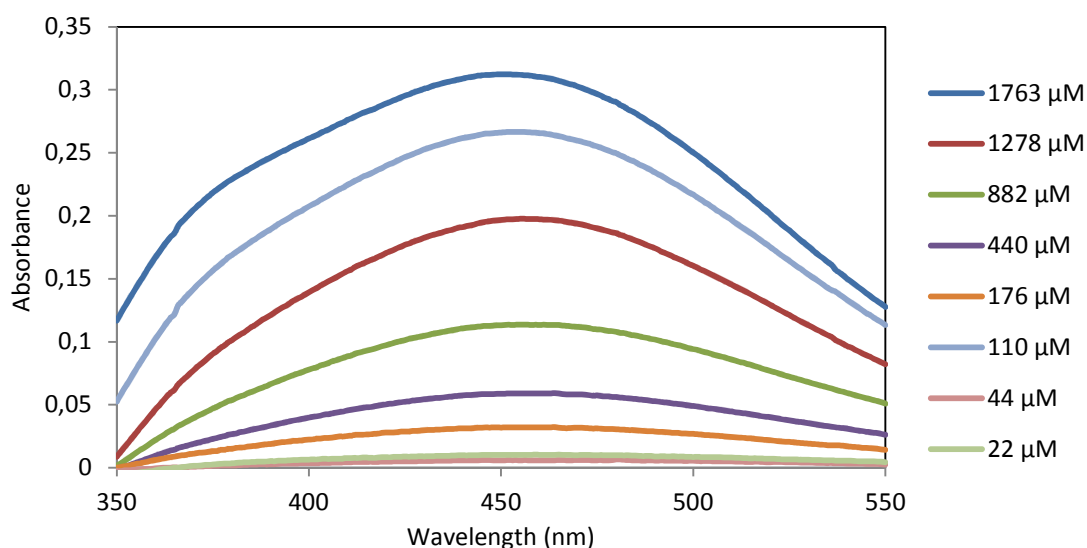


**Figure 5-6:** Spectrum of vanadate solution after addition of  $\text{H}_2\text{O}_2$  diluted samples (presented as dilution ratios of  $\text{H}_2\text{O}_2$ )

Calibration is based on a dilution series of a known solution of hydrogen peroxide (3% of 0.88 M). The dilution series and matching spectrum can be found in Figure 5-6. Absorbance at a wavelength of 450 nm can then be plotted against the matching concentration. This calibration curve can be found in Figure 5-7.

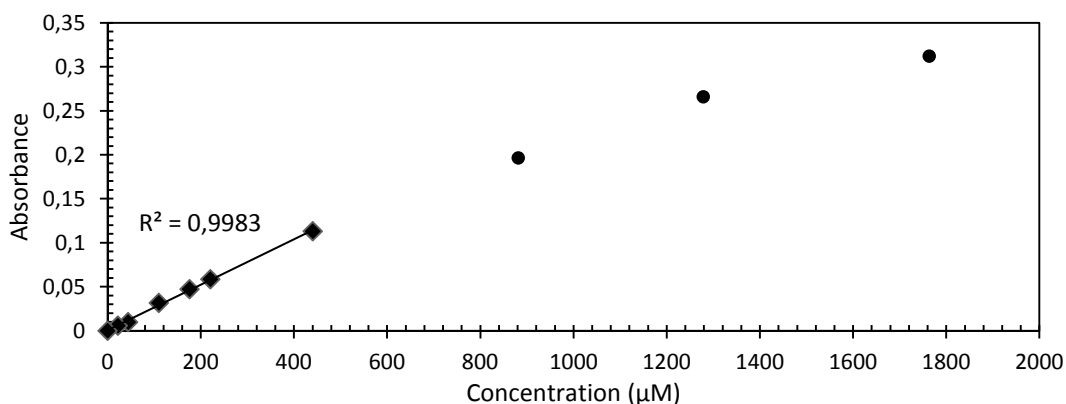


**Figure 5-7:** Calibration curve of H<sub>2</sub>O<sub>2</sub> metavanadate method

Using Lambert Beer law (Eq 5-4), a formula to calculate the concentration can be made with linear regression. There is an error of about 5% on the calculations of the concentration. This value was determined by measuring the calibration curve in duplo.

To be able to use Lambert Beer law, the graph has to be linear and go through the origin. With *A* the absorbance,  $\epsilon$  the molar absorbance ( $\text{l mol}^{-1} \text{cm}^{-1}$ ), *C* the concentration (M) and *b* the path length. For this calibration, it means that Lambert Beer law is only valid to a concentration of about 440 µM. Because the cuvette is 1 cm wide, *b* is 1 cm. So the concentration can be calculated with following equation (Eq 5-7). For concentrations higher than 440 µM, interpolation will be used.

$$C = \frac{A}{\epsilon \cdot b} = \frac{A}{0.261 \text{ mM}^{-1} \text{cm}^{-1} \cdot 1 \text{ cm}} \quad \text{Eq 5-7}$$

### 5.3.2 Calculation

Using equation 5.7, concentrations between 0 and 441 µM can be calculated when the absorbance is known. For example, an absorbance of 0,0314 will give a concentration of 120 µM. When the concentration exceeds 441 µM or the absorbance exceeds 0,113, interpolation is needed. For example, an absorbance of  $A = 0,145$  lies between 0,1132 (441 µM) and 0,1967 (882 µM) on the calibration curve. Using Eq 5-8 and Eq 5-9, these higher concentrations can be calculated. Where index 1 denotes a point on the calibration curve lower than *A* and index 2 denotes a higher one.

$$C = \frac{C_2 - C_1}{A_2 - A_1} \cdot (A - A_1) + C_1 \quad \text{Eq 5-8}$$

$$C = \frac{882 \frac{\mu\text{mol}}{\text{l}} - 441 \frac{\mu\text{mol}}{\text{l}}}{0.1967 - 0.1132} \cdot (0.145 - 0.1132) + 441 = 609 \frac{\mu\text{mol}}{\text{l}} \quad \text{Eq 5-9}$$

## 5.4 Analysis of methylene blue

Because methylene blue (MB) has a typical blue color, photo spectroscopy can be used to measure its concentration. The kinetics of this model compound will be mostly based on the relative concentration, i.e. determination percentage of removal. Although absolute concentration is not required, a calibration curve is needed to assure the absorbance is linear to the concentration.

To be able to find the correct peak that represents methylene blue, the absorbance is measured over the complete measurable spectrum (220 – 700 nm). The peaks are validated on their linearity with the concentration (Figure 5-8).

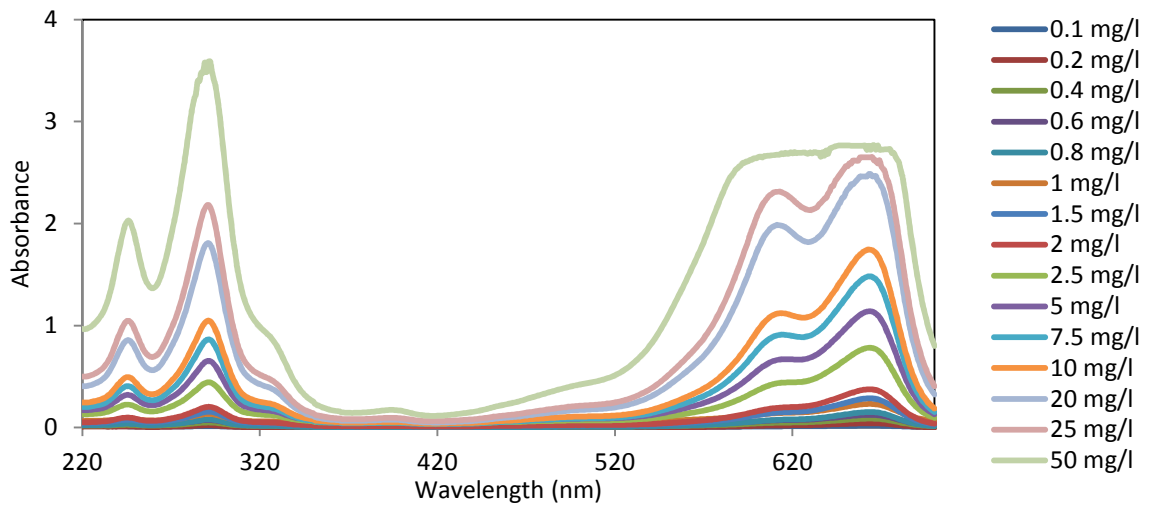


**Figure 5-8:** Spectrum of methylene blue, for different concentrations

On basis of the spectrum above, 2 wavelengths are chosen to check the linearity. The first one being at 660 nm and the second one at 290 nm. This results in 2 calibration curves, respectively Figure 5-9 and Figure 5-10. Based on the determination coefficients (0.9936 for 660 nm and 1 for 290 nm), the wavelength of 660 nm can be used for concentrations up to 10 mg/l. For higher concentrations, up to 25 mg/l, the absorbance at a wavelength of 290 nm is suitable. A wavelength of 660 nm is not suitable for concentrations higher than 10 mg/l due to flattening of the spectrum. Because degradation can follow a different path, only one wavelength is used throughout the experiments.

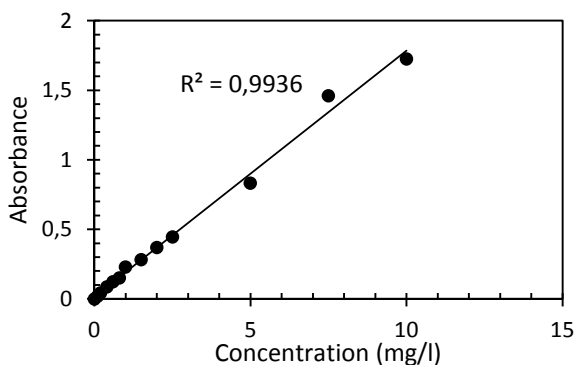


**Figure 5-9:** Calibration curve MB, 660 nm

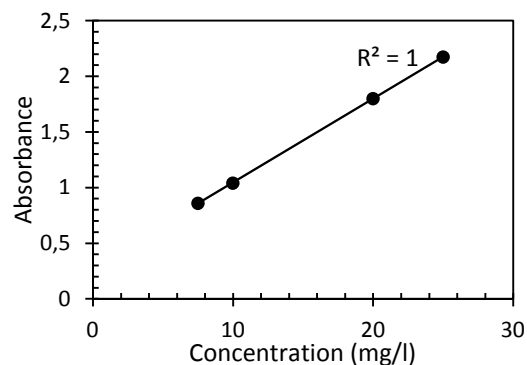


**Figure 5-10:** Calibration curve MB, 290 nm

## 5.5 GC-MS calibration and preparation

Before any measurements of micropollutants can be done, a GC-MS method and calibration curve have to be made. This method is based on a multi pesticide analysis for GC-MS-MS. This thesis only focuses on 3 micropollutants ( $\alpha$ -HCH, PeCB and HCB), so the method has to be compressed for these compounds. For these micropollutants, a concentration of maximum 4000  $\mu\text{g/l}$  has been opted. This is to ensure concentrations of up to 300  $\mu\text{g/l}$  can be measure, even after concentrating 10 times.

### 5.5.1 Optimizing the method

Validation of a method with GC-MS, the apparatus has to run in scanning mode. Scan mode is used for identification of chemical components by using mass spectroscopy. With this method it is possible to identify multiple components, which allows analyses of several components simultaneously. Identification is done using the library that is built into the software.

First, an oven program is chosen. Standard solution, for optimization of the oven program, has to contain all components such as the internal standard and the pollutants. It is also important to make sure that every pollutant is added in a high concentration. This is to ensure that the peaks will show up clearly to give a good mass spectrum. The first solution that was made contained:

- Internal standard, Naphthalene (3.3 mg)
- PCB (1.1 mg)
- $\alpha$  - HCH (0.9 mg)
- HCB (1.1 mg)

All of these components where dissolved in 1 ml of ethyl acetate so the concentration was around 1000 mg/l. This solution was put into a vial, ready for the GC-MS validation. With the standard solution, a method can be developed and optimized. Starting in scan mode, with a wide temperature range and a slow heating rate, it is possible to search for every peak in the spectrum. Constant parameters for the GC-MS are presented in Table 5-3.

**Table 5-3:** Constant parameters of GC-MS

Column		MS parameters	
Model	HP-5MS	Solvent delay (min)	2.00
Model number	Agilent 19091s-433	MS quad ( $^{\circ}\text{C}$ )	150 (max 200)
Nominal length (m)	30	MS source ( $^{\circ}\text{C}$ )	230 (max 250)
Nom. diameter ( $\mu\text{m}$ )	250	<b>Back inlet</b>	
Nom. film thickness ( $\mu\text{m}$ )	0.25	Pressure (kpa)	81.1
<b>Injector parameters</b>		Purge flow (ml/min)	9.9
Injection volume ( $\mu\text{l}$ )	1.0	Total flow (ml/min)	13.8
Syringe size ( $\mu\text{l}$ )	10.0	Gas type	Helium

When every peak is identified, the method can be optimized by changing one parameter at a time. The progress of this optimization can be found in Table 5-4. Because of the high concentrations, the method starts with a split 1:100. This means that only one

hundredth of the total injected volume is transferred to the column. The hold is to make sure the solvent (ethyl acetate or dichloromethane) cannot be found on the chromatogram. Next thing to change is the rate (°C/min) at which the temperature rises. In the first methods, a slow rate is opted to assure all components can be retrieved. The final method (method 4) is represented by Figure 5-11.

**Table 5-4: Overview of the progress of the optimization of the oven program**

	Method 1	Method 2	Method 3	Method 4
Split	Split 1:100	Split 1:100	Split 1:100	Splitless
Start (°C)	50	115	125	125
Hold (min)	1.50	1.50	0.00	0.00
Rate (°C/min)	10.00	10.00	15.00	25.00
Maximum (°C)	300	210	195	195
Hold (min)	4.00	1.00	0.00	0.00
Rate (°C/min)			10	10.00
Maximum (°C)			210	210
Hold (min)			1.00	1.50
Total time (min)	30.50	12.00	7.17	5.80

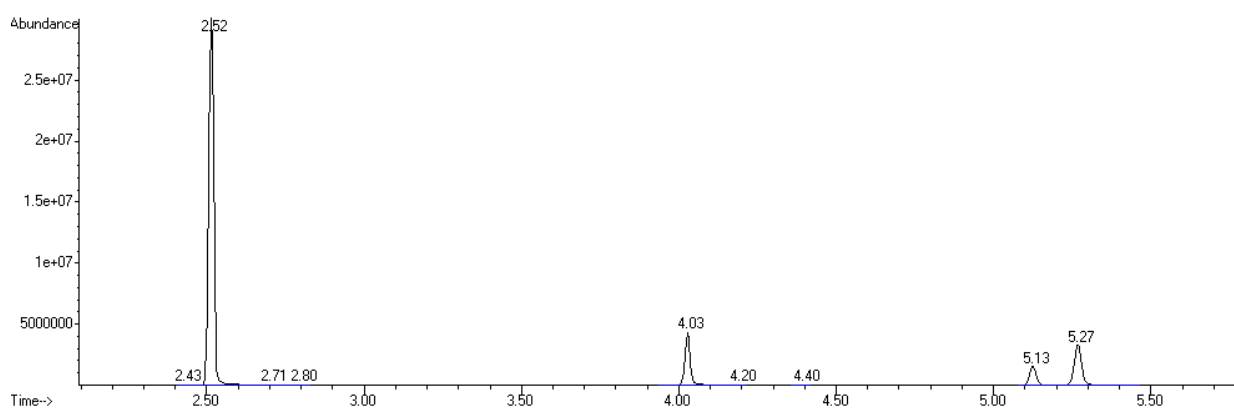


**Figure 5-11:** Retention time for all standards, represented in the chromatogram. On the x-axis time (min) is presented and on the y-axis the signal intensity

Important to note is that the method first ran with a split of 1:100. The split is of great importance when high concentrations are used. This makes sure that the components will not saturate which could have a bad separation as consequence. After optimization, the components have to be tagged. This can be done by using the mass spectrum (MS) (Figure 5-12). An important parameter is the retention time, this is the time it takes for a component to leave the column. This information can be found in the gas chromatogram (Figure 5-11).

With this MS spectrum, a target and two qualifier ions have to be determined (tagging). The target ion will be the one with the strongest signal, in the case of pentachlorobenzene that is the ion with mass charge ratio ( $m/z$ ) of 250. Mass charge ratio is based on the behavior of different ions in a magnet field. These target ions will characterize the target component, in this example, pentachlorobenzene.

The qualifier ions will ensure that the correct target component is identified. This identification is based on the ratio of the amount of qualifier ions and target ions. Because this is unique for every component, a 100 % positive identification can be achieved. In this case, qualifiers ions are the second and the third largest signals in the TIC. For pentachlorobenzene, the qualifiers are the ones with a mass/charge ratio of respectively 247 and 252.

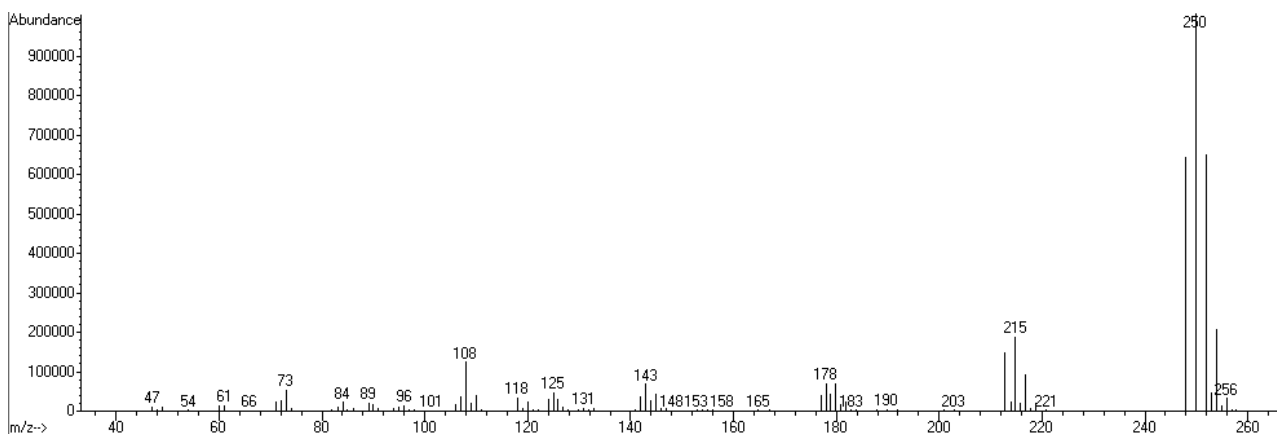


**Figure 5-12:** Mass spectrum of Pentachlorobenzene. On the x-axis mass charge ratio is presented and on the y-axis the signal intensity.

With these data, summarized in Table 5-5, it will be possible to run the method in SIM (Single ion monitoring) mode. SIM mode allows for a higher sensitivity, thus lower detection limits. This higher sensitivity can be obtained in SIM mode because the MS only gathers data for the masses of interest. The mass spectrometer will look at only 3 ions (target and qualifiers) per component (this is done more thoroughly than in scan mode, because the mass spectrometer will look for these specific ions multiple times instead of just once) and compare the ratios of those ions.

**Table 5-5:** Overview of the retention time and mass/charge ratios for the pollutants and the internal standard

	Retention time (min)	Mass/charge ratio		
		Target ion	Qualifier 1	Qualifier 2
Naphthalene (internal standard)	2.513	128	127	129
PCB	4.027	250	247	252
$\alpha$ -HCH	5.127	219	181	183
HCB	5.266	284	286	282

## 5.5.2 Calibration

In order to use the GC-MS to quantify the micropollutants, calibration is needed. This can only be done with a valid method and when all the molecules of preference are retrieved on the chromatogram. Here, the internal standard comes to use. The internal standard is a component with similar properties as the micropollutants, so it has a retention time, close to these pollutants. Its purpose is to be added, in about the same concentration (the concentration of the highest point in the calibration curve, 2000  $\mu\text{g/l}$ ) to all of the standard samples. In that way the internal standard acts as a correction of errors and variations during the extractions and measurements.

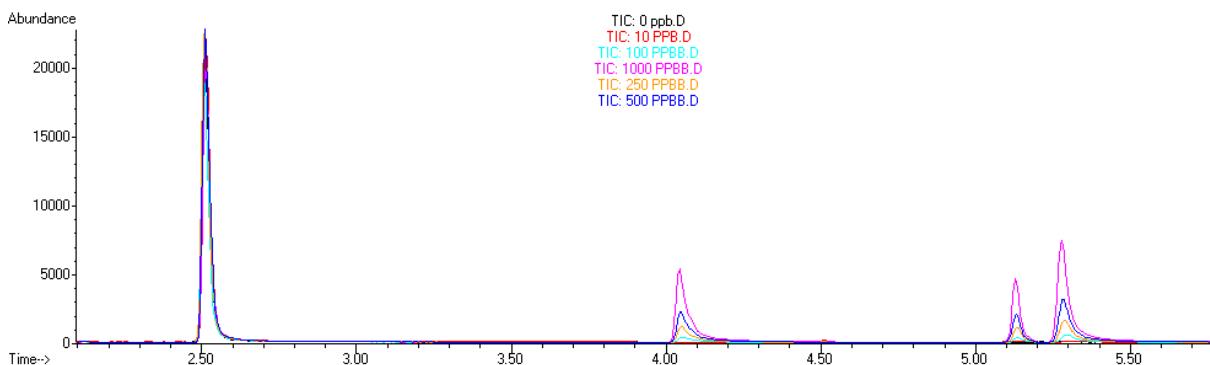


**Figure 5-13:** Overlay of all points of the calibration curve. On the x-axis time (min) is presented and on the y-axis the Abundance.

To make a good calibration curve, a minimum of 5 points is needed. These points have to be chosen in a way that the concentration of future samples lies within its boundaries. Because concentration of the micropollutants will be around 300  $\mu\text{g/l}$ , standards from 0 to 4000  $\mu\text{g/l}$  (500, 1000, 2000 and 4000  $\mu\text{g/l}$ ) were chosen. Taking into account that the samples will be approximately 10 times more concentrated after extraction (see next section), allowing higher accuracy.

To validate the extraction method, a calibration sample series is made in ethyl acetate. This solvent allows all of the pollutants and the internal standard to dissolve easily and without interference on the chromatogram. The internal standard is applied in the calibration by dividing the response of the pollutants with the response of the added internal standard (response ratio  $A/A_i$ ). Also concentrations have to be divided by initial concentration  $C_i$  (concentration ratio  $C/C_i$ ). By doing so, a calibration curve such as Figure 5-14 is achieved.

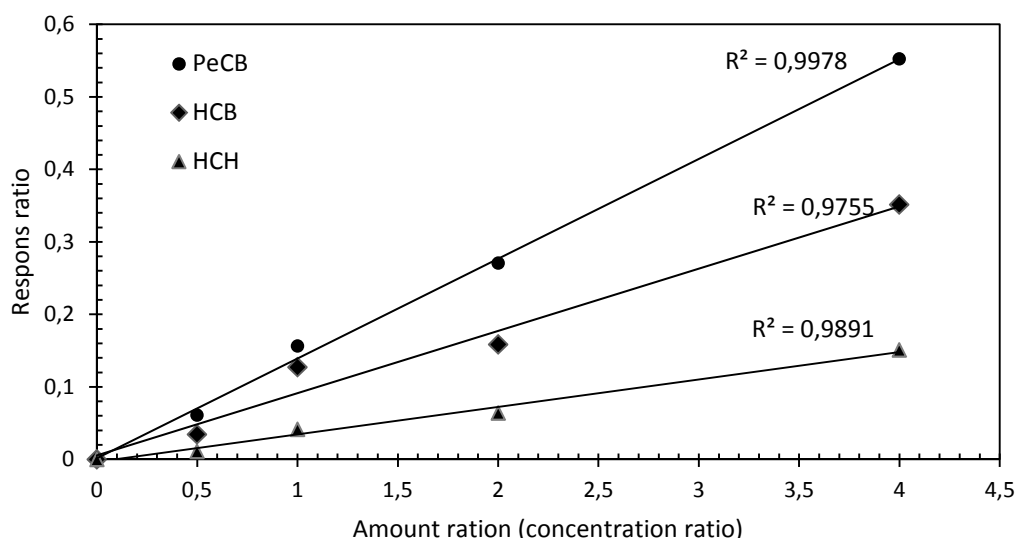


**Figure 5-14:** Calibration curves of alpha hexachlorocyclohexane, pentachlorobenzene and hexachlorobenzene.

Once an extraction method is optimized, the calibration curve is made using pollutants, dissolved in water. Due to low solubility in water, high concentrations can be achieved by dissolving the organic pollutants (400 mg/l) in methanol first. Methanol solutions are then diluted with water to the desired concentration. The calibration curve is made using the extraction method. By doing so, the method becomes more reliable and a correction is made for component recovery. Methanol is only used to test extraction methods, not in plasma related experiments.

To make sure that the method is still valid, a new calibration curve is made every time a new batch of samples is measured. Therefore 4 determination coefficients are shown in Table 5-6 as illustration of how well the data fits the statistical linear model. The first 2 columns represent  $r^2$  for the calibration in ethyl acetate, while the next 2 represent the calibration after extraction procedure. Calibration curves can be found in Annex A and B.

**Table 5-6:** Different determination coefficients for different calibrations

	Determination coefficient			
	Calibration in ethyl acetate 1	Calibration in ethyl acetate 2	Calibration after extraction 1	Calibration after extraction 2
PCB	0.9947	0.9993	0.9760	0.9983
$\alpha$ -HCH	0.9761	0.9973	0.9961	0.9978
HCB	0.9948	0.9988	0.9960	0.9948

### 5.5.3 Extraction

The HP 5MS UI column, which is a nonpolar column used in GC-MS, in which water is not allowed. Therefore extractions are used, to transfer the compounds of interest into a nonpolar solvent. Because micropollutants have a low concentration ( $\mu\text{g/l}$  range), extraction will also help to concentrate these pollutants. This results in a better quantification and eliminates working on the limit of detection.



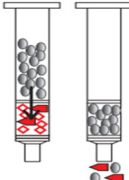
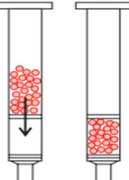
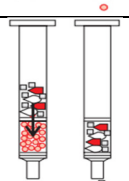
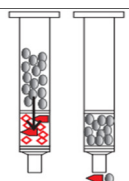
### 5.5.3.1 Solid Phase Extraction

Based on 2 papers (Matamoros et al. 2012, Robles-Molina et al. 2014), solid phase extraction (SPE) was used to extract the micropollutants. An example of a SPE cartridge can be found in Table 5-7. Such cartridge consists of 3 main parts, namely:

- ✓ Reservoir, to contain membrane, filter and solutions
- ✓ Membrane, to extract the component of interest
- ✓ Filter, to prevent any particles in the water from clogging the system.

Because the micropollutants have to be extracted out of a water solution, reversed phase SPE is used. Reversed phase basically means the system consists of a polar liquid phase and a nonpolar modified solid phase. Hereby relying on hydrophobic interactions to eliminate the pollutants out of its original solvent. The membrane itself has to be nonpolar as well, that is why a C 18 cartridge is used. The latter is a hydrophobic silanol group that is chemically modified with an alkyl group (C 18). The procedure of extraction itself is based on a paper (Matamoros et al. 2012) and consists of a five-step procedure. The way this procedure was executed can be found in Table 5-7.

**Table 5-7:** Full procedure for solid phase extraction

Step	Description	Representation	Implementation
Pre washing	To elute all remaining compounds for a second use of the cartridge		10 ml of elution solvent: Ethyl Acetate
Conditioning the SPE tube or disk	To wet the surface of the sorbent and penetrates bonded alkyl phases		10 ml of ethyl acetate 10 ml of methanol 10 ml of water
Adding the sample	The complete sample is poured over the cartridge		20 ml of sample at a rate of 2-3 ml/min
Drying the cartridge	To prevent that water gets in the way when eluting		2 min drying with vacuum
Elute compound of interest	To transfer the compounds to the organic solvent		4 times 0,5 ml ethyl acetate for small cartridges and 2 times 1 ml ethyl acetate for larger cartridges

In Table 5-8 a summary is made of the recoveries after the solid phase extraction. The component used for these tests is pentachlorobenzene (PeCB). The recovery is used to estimate how much of the actual concentration can be retrieved after extraction. Recoveries are calculated by dividing the measured concentration by the expected concentration. The initial concentration (in water) was 50 µg/l which is then supposed to be concentrated to 500 µg/l (in ethyl acetate) after extraction. This concentration is unfortunately not met, not even with 3 different types of SPE cartridges. Also when the wastewater was examined, no PeCB was retrieved. That is why another extraction technique is adopted, namely liquid-liquid extraction.

**Table 5-8:** Overview of different recoveries for 3 types of SPE cartridges

	<b>Empore disk C18 3 ml</b>		<b>Chromabond C18 500 mg, 6 ml</b>		<b>Envi C18 2000 mg, 12 ml</b>	
	C (µg/l)	Recovery (%)	C (µg/l)	Recovery (%)	C (µg/l)	Recovery (%)
PeCB internal calibration	215.5	43.6	296.7	60.0	198.9	40.2
PeCB external calibration	194.2	39.3	344.5	69.7	386.9	78.3

### *5.5.3.2 Liquid-Liquid Extraction*

Liquid-liquid extraction (LLE) makes also use of the polarity of the component. The main idea is that a nonpolar component will be more likely to dissolve in a nonpolar solvent than in a polar component. In this case the nonpolar components are the pollutants and the polar solvent is water. As extraction solvent, dichloromethane was used. This solvent is recommended in most standard procedures (Yrieix et al. 1996).

The procedure for LLE is much more straightforward than SPE. In this case 20 ml of the sample (sample + internal standard) is put into a vial. Then 2 ml of dichloromethane is added to the vial. The closed vial is shaken for about 5 minutes by hand. When the extraction solvent has sunk to the bottom, a glass Pasteur pipette can be used to remove as much of the solvent as possible. To make sure no water is left in the solvent, 2 grains of dry CaCl<sub>2</sub> are used to absorb the water. Now the solution is ready to be analyzed by the GC-MS. Because the GC-MS only needs 10 µl per sample, it is not necessary to get all of the dichloromethane transferred, although a maximum of the solution is recommended.

A water sample with concentration of 50 µg/l of each micropollutant and 100 mg/l of naphthalene was used to determine the percentage of component recovery during sequential extraction steps. Pollutant concentration in the resulting dichloromethane samples was measured after every extraction step of the corresponding peak in the GC-MS chromatogram. Figure 5-13 shows the efficiency of every additional extraction step. In this figure, it is clear that after 2 extraction steps, nearly 99% of all the components are transferred. Every step of extraction transfers about 91% of all components. The recovery rates are found to be reproducible, with an error of less than 1.2%.

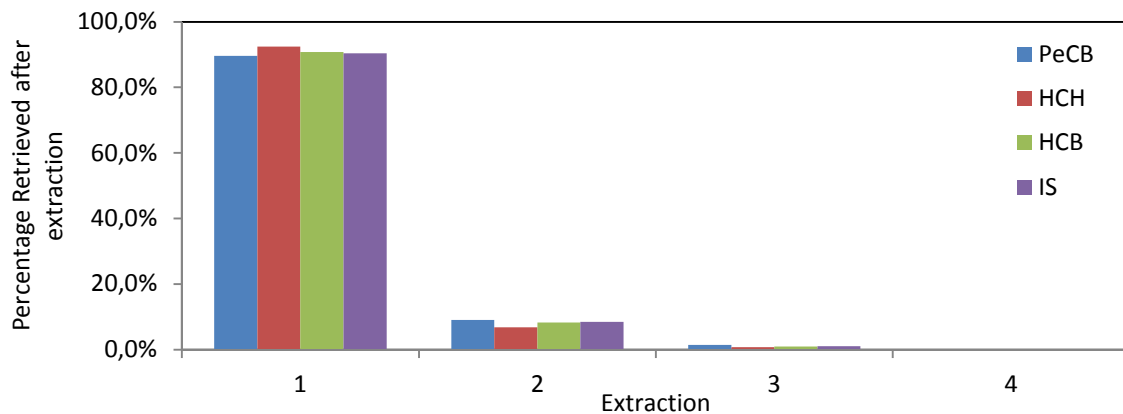


**Figure 5-15:** Percentage retrieved after sequential extraction steps

## 5.6 Statistical analysis

Evaluating several graphs and determining whether or not these graphs are different from one another can usually be done visually. However, in certain cases statistical methods are needed. In this thesis paired T-tests and nonparametric Wilcoxon tests will be used (Weiss and Weiss 2012). For the first test data points have to be normally distributed. This can be checked with the Kolmogorov Smirnov test. The null hypothesis states that the data is normally distributed. So when the p-value of the Kolmogorov Smirnov test, obtained with the statistical program SPSS (IBM, [www.ibm.com](http://www.ibm.com)), is greater than or equal to 0.05, normality can be assumed. If there is normality, a T-test is used. Otherwise a nonparametric Wilcoxon test is opted.

A one tailed, paired T-test is opted, because of the possibility to conclude whether or not one curve is greater than the other. The null hypothesis for this test means that the two graphs are equal. For this statement to be true, p-values have to be greater than 0.05. When the data point are not normally distributed, the Wilcoxon test is an alternative. The null hypothesis is the same as with the T-test. As previously stated, all of these tests are conducted with SPSS Statistics, a software package used for statistical analysis. For convenience, linear regressions and error intervals are calculated with Microsoft Excel 2010.

---

## *III. Experimental results*

---

## 6 Parameters and active species

Prior to the removal of any components, a study about different reactor characteristics was done. In this study, influences of pH, conductivity, power and active species will give better insight in how the system functions. This will help explain certain removal patterns in the next chapters.

A study on active species focused on ozone and hydrogen peroxide, since reactors in literature are typically characterized with production efficiency of these long living oxidants. Conductivity and pH were measured to give an global view on the active species as well.

### 6.1 Parameters

#### 6.1.1 Conductivity and pH

In this part, a relationship between pH and conductivity will be investigated. A pH drop can be partially explained by formation of  $\text{HNO}_3$  under influence of plasma discharge and the high concentration of nitrogen gas. Formation of this acid in the water gives rise in conductivity, due to the presence of more ions in the water. Investigating these parameters are important because a lower pH due to  $\text{HNO}_3$  can decrease radical formation by ozone. Figure 6-1 gives a graphical presentation of pH and conductivity changes in function of time. A total time of 30 min was chosen because all other experiments will lie within this range.

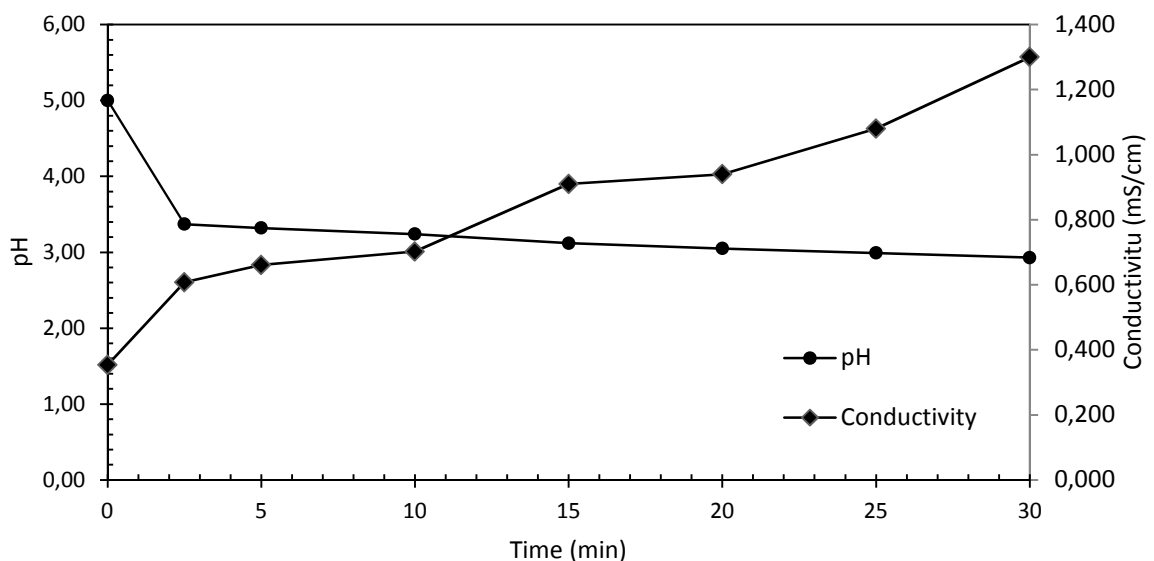


**Figure 6-1:** pH and conductivity in function of time (standard settings: Power 49.7 W and DC 0.15)

Neglecting all other influences, conductivity can be calculated from the concentration of  $\text{HNO}_3$  (and thus pH). Using tabular values (Haynes 2013) a conversion from mass percent of  $\text{HNO}_3$  to conductivity can be made (Eq 6-2) with G the conductivity in mS/cm. The conversion from pH to mass percent  $\text{HNO}_3$  can be done with the pH-formula for strong acids (Eq 6-1).

$$\% HNO_3 = (10^{-pH}) \cdot MM_{HNO_3} \cdot 0.1 \quad \text{Eq 6-1}$$

$$G = \frac{\% HNO_3}{0.0189} + 0.046 \quad \text{Eq 6-2}$$

In Table 6-1, calculated values of the conductivity are compared to the actual conductivity. Based on these values, it is clear that there are other influences to lower pH. This means the influence of other species such as ozone and hydrogen peroxide is not neglectable. To accurately link the conductivity of the water to the pH, it will be necessary to work with the activity of ozone, hydrogen peroxide, HNO<sub>3</sub> and other species. This is out of the scope of this thesis. Nevertheless HNO<sub>3</sub> will certainly play a role. In one research (Tarabova 2014) it was found that the changes of pH and electrolytic conductivity can be correlated with the production of reactive oxygen and nitrogen species.

In a study where air (N<sub>2</sub>/O<sub>2</sub>) was compared to a Ar/O<sub>2</sub> atmosphere showed that, nitrous species such as NO<sub>2</sub><sup>-</sup> and NO<sub>3</sub><sup>-</sup> decreased drastically below pH 3.5. Also, overall activity of the water decreased due to less aqueous active species (Lukes 2014).

**Table 6-1:** Comparison between calculated and actual conductivity

Time (min)	Calculated conductivity (mS/cm)	Actual conductivity (mS/cm)
2,5	2,576	0,608
5	2,593	0,661
10	2,625	0,702
15	2,686	0,910
20	2,731	0,940
25	2,775	1,080
30	2,825	1,300

To explain further degradations paths and influences, pH was measured in the ozone chamber, with only the ozone gas bubbled through it. In this setup, the water did not come in contact with the plasma. What is observed from Figure 6-2, is that pH will be a lot more stable and will only reach a pH of 3.90 after 30 minutes. Where under normal conditions pH had already dropped to 2.90. Ozone will not be scavenged as much by nitrogen species.

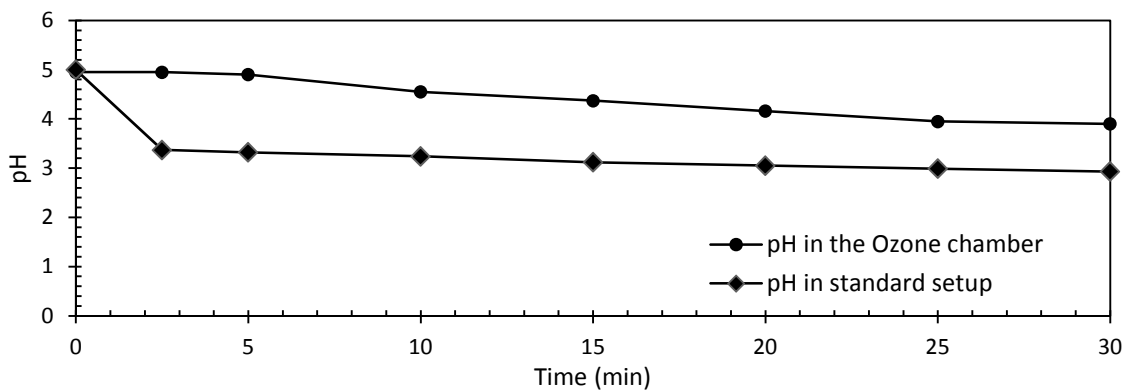


**Figure 6-2:** Comparison between pH in standard setup and pH in ozone chamber

### 6.1.2 Relation between pH, conductivity and power

Conductivity and pH of water entering wastewater treatment plants, can vary. Therefore, the effect of different starting pH and conductivity are important factors to consider. As can be seen from Table 6-2, starting conductivity and pH have little to no influence on the pH and conductivity after 30 minutes.

**Table 6-2:** Influence of initial pH and conductivity on pH and conductivity after 30 minutes

	Starting conductivity (mS/cm) At a pH of 5		Starting pH At a conductivity of 350 mS/cm	
	5	1000	4	10
Conductivity after 30 minutes	1.190	1.560	1.090	0.990
pH after 30 minutes	2.86	3.13	2.93	3.01

The power can be varied in two ways. The first way is to increase the average power is by increasing the voltage of the power source. The second way is by changing duty cycle. Throughout all experiments, the period will not be changed. When only the voltage is changed, there will be a slight increase in conductivity (Figure 6-3). However, when the duty cycle is changed, there will be a much larger change. This is due to the introduction of more active species in the water. The same observation can be made about the pH in function of power (Figure 6-4). When voltage is changed, power (P) is what will be the important parameter. That is why change in voltage will be expressed in watt as opposed to in volt.

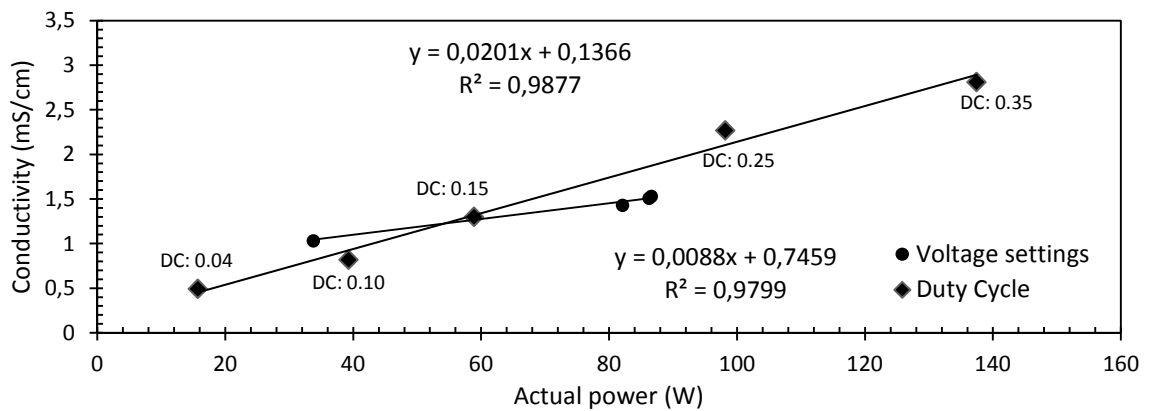


**Figure 6-3:** Conductivity in function of power for different voltage (DC: 0.15) and duty cycle settings

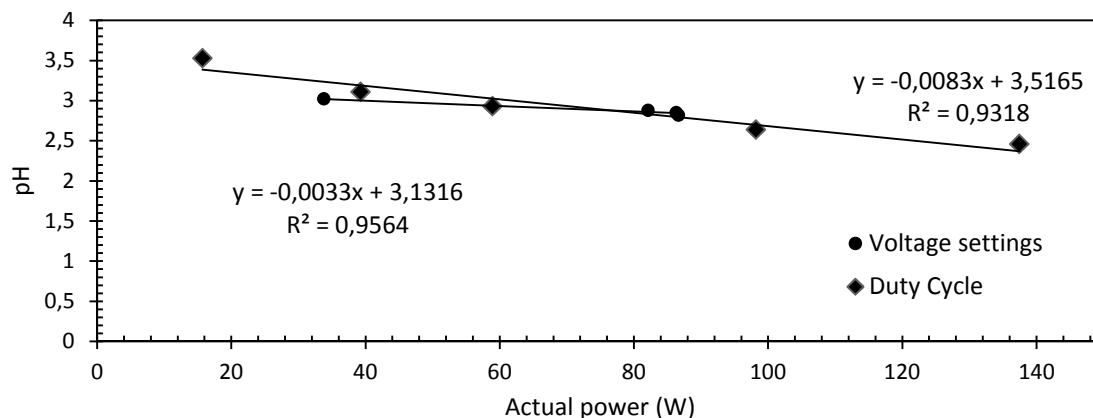


**Figure 6-4:** pH in function of power for different voltage (DC: 0.15) and duty cycle settings

### 6.1.3 Voltage and duty cycle

Table 6-3 gives a visual understanding of the concept duty cycle. Basically, duty cycle represents the percentage of time that power is activated. Visually, this means that the brightness of the plasma will be influenced. A higher duty cycle means an increased brightness and vice versa. Change in voltage influences the distribution of the plasma over the metal mesh. A higher power will get the plasma to spread more evenly than a low power. Because change in duty cycle also influences the actual power, distribution of the plasma over the metal mesh will also vary. For the voltage parameter, a duty cycle of 0.15 will be used.

**Table 6-3:** Visual representation of excitation of active species for different voltage and duty cycle settings

Duty Cycle Power 50 W	0.04	0.15	0.35
Voltage Duty cycle 0.15	29.0 W	49.7 W	68.3 W

Another visual aspect of plasma to consider is the purple light that is emitted. This color, at a wavelength of around 450 nm represents the relaxation of electrons from a excited state to a lower state. Figure 6-5 is a spectrum of the plasma, which clearly shows different peaks, at different wavelengths. These peaks represent mostly excited nitrogen species. This excited state of nitrogen ( $N_2^*$ ) can react with dioxygen to form other active compounds ( $O_3$ ,  $OH$ , etc.). It can be found that an increase in voltage does not increase the amount of active species locally, but instead spreads the plasma more evenly over the mesh grid. Duty cycle on the other hand will increase active species locally, while spreading more evenly when increased.



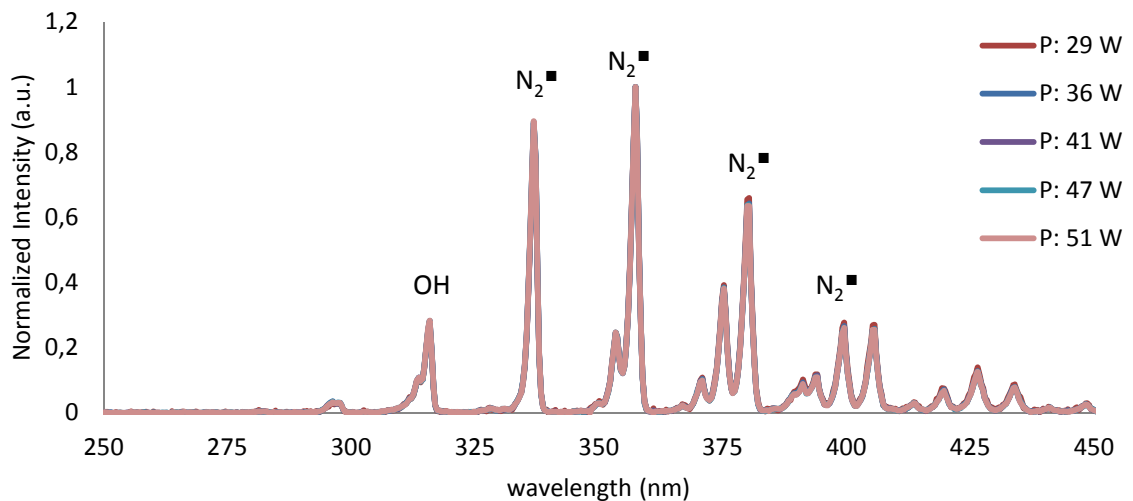


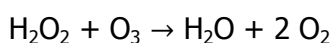
**Figure 6-5:** Plasma spectrum with designation of different active species

## 6.2 Active species

There are a lot of active species, produced by the plasma, but only  $\text{H}_2\text{O}_2$  and  $\text{O}_3$  where measurable with the available resources. These are long living active species and are often used to characterize plasma reactors.

### 6.2.1 Hydrogen peroxide and ozone comparison

The amount of ozone and hydrogen peroxide in water is highly depending on voltage amplitude. The amount of hydrogen peroxide and ozone will increase linear in time. In both graphs (Figure 6-7 and Figure 6-6), linearity drops after about 15 minutes. From thereon, interaction between hydrogen peroxide and ozone prevent increase of the concentration (r 6-1) (Taube and Bray 1940, Thevenet et al. 2010).



**r 6-1**

Another explanation for the drop in linearity is mass transfer or the net movement from the gas phase to the liquid phase. Here, limitations such as diffusion can be responsible because of a not optimal gas flow rate.

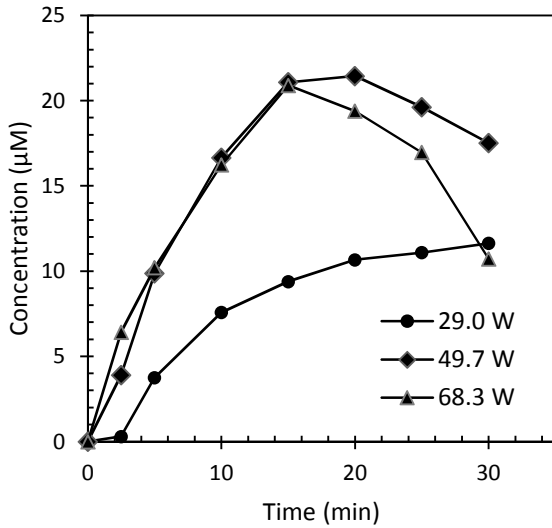


**Figure 6-6:** Concentration of ozone in function of time, for different voltage settings

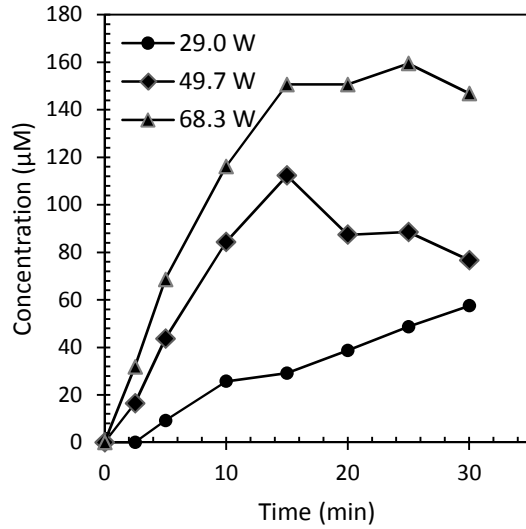


**Figure 6-7:** Concentration of hydrogen peroxide in function of time, for different voltage settings

Energy efficiency is calculated using the concentrations at 15 minutes, because for most voltage settings, this is when the maximum concentration is obtained (Eq 6-3). With P the power in watt, C the concentration of H<sub>2</sub>O<sub>2</sub> or O<sub>3</sub> in M and MM the molar mass of the component in g/mol.

$$\text{Power efficiency} = \frac{4000 \cdot C \cdot MM}{P} \quad \text{Eq 6-3}$$

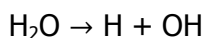
These efficiencies can be found in Table 6-4 and are expressed in mg kWh<sup>-1</sup>. Maximum efficiency is obtained at a power of about 70 W for both H<sub>2</sub>O<sub>2</sub> and O<sub>3</sub>.

**Table 6-4:** Power efficiency of H<sub>2</sub>O<sub>2</sub> and O<sub>3</sub>

Power (W)	H <sub>2</sub> O <sub>2</sub>	O <sub>3</sub>
	Power efficiency (mg kWh <sup>-1</sup> )	Power efficiency (mg kWh <sup>-1</sup> )
29.0	0.0143	0.0065
49.7	0.0950	0.0252
68.3	0.2103	0.0412

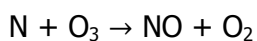
For different duty cycles, only H<sub>2</sub>O<sub>2</sub> concentration was measured (Figure 6-8). Something that strongly stands out is the linearity after 15 minutes for both a duty cycle of 0.25 and 0.35, where below these values the concentration stagnated at around 15 minutes. This could mean that either more H<sub>2</sub>O<sub>2</sub> is produced in the water or H<sub>2</sub>O<sub>2</sub> is not degraded by ozone.

The first explanation, where more H<sub>2</sub>O<sub>2</sub> is produced due to a higher power can be explained because plasma is longer active in a given pulse. Resulting in more water molecules decomposing into hydrogen and hydroxyl radicals (r 6-2) for a given time. This can eventually lead to a higher hydrogen peroxide formation (Locke and Shih 2011).

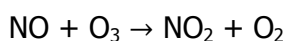


r 6-2

Assuming there is a correlation between the ozone concentration in the gas phase and in the liquid phase, a drop in ozone concentration can be observed at a duty cycle of 0.35 (Figure 6-9). This suggests that less ozone is produced or reaches the water. This decrease leads to less interference between ozone and H<sub>2</sub>O<sub>2</sub> molecules. Thus resulting in a unrestrained H<sub>2</sub>O<sub>2</sub> supply. At high power, NO<sub>x</sub> poisoning can play a role and result in a drop of ozone. Because dry air is used, presence of nitrogen will cause ozone destruction due to formation of nitrogen oxides (r 6-3 and r 6-4) (Kogelschatz et al. 1988, Pekárek 2003).



r 6-3



r 6-4

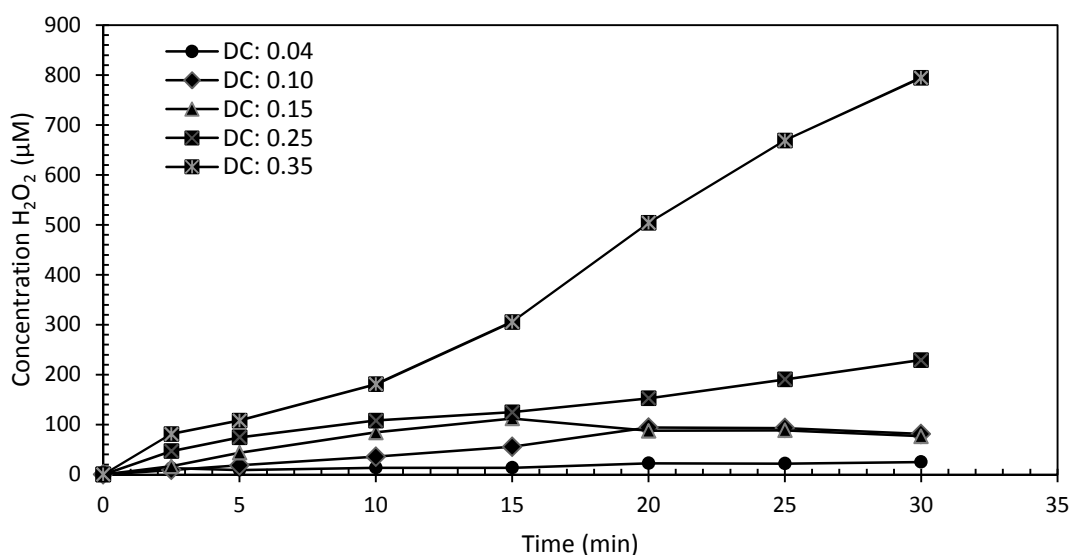


**Figure 6-8:** Concentration of H<sub>2</sub>O<sub>2</sub> for different duty cycles

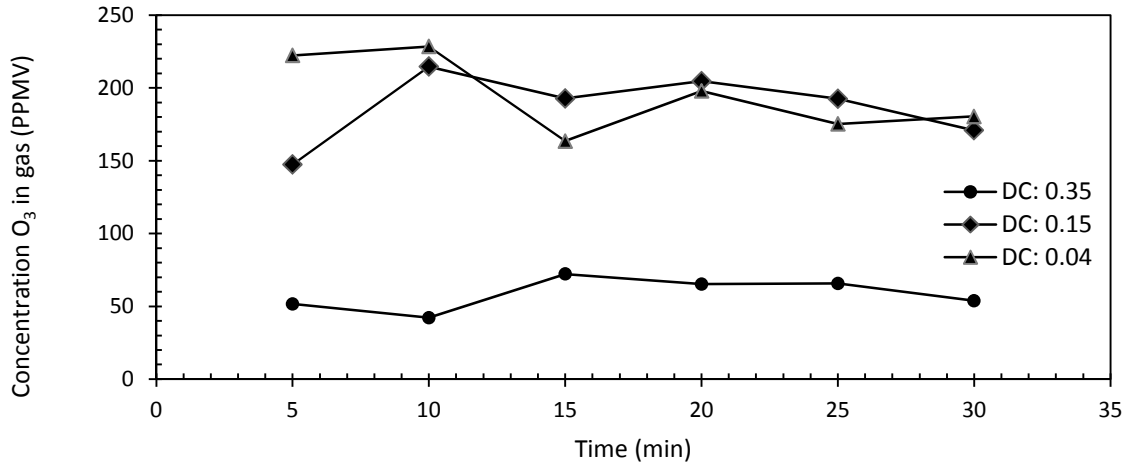


**Figure 6-9:** Concentration of ozone in gas phase for different duty cycles

## 6.2.2 Gas phase

Ozone is measured both in gas (measured at the exhaust) and liquid phase. This means, a correlation between the gas and liquid phase can be expected. When there is a correlation and an equilibrium is achieved, a link to Henry's law can be made.

Because the ozone monitor needs some stabilization time, a correlation is sought only after 5 minutes of running time. This gives a coefficient of determination of 0.8702 and is plotted in Figure 6-10. This means the ratio between the aqueous and gaseous concentration is 1.59 and given by the equation (Eq 6-4) below, with  $C_A$  the concentration in the aqueous phase and  $C_G$  the concentration in the gas phase.

$$\frac{C_A}{C_G} = 1.59 \quad \text{Eq 6-4}$$

This equation can be compared to the Henry's constant expressed as  $H_{CC}$ , which stands for the ratio of  $C_A$  and  $C_G$ . In literature, Henry's constants are expressed as  $H_{CP}$  (for ozone:  $1.13 \cdot 10^{-4}$  in  $\text{mol m}^{-3} \text{Pa}^{-1}$ ). This representation of the henry constant is in essence the same as  $H_{CC}$ . At a temperature  $T$  of approximately 293 K (20°C). Conversion of  $H_{CC}$  to  $H_{CP}$  can be done with the next equation (with  $R$  the ideal gas constant) (Eq 6-5).

$$H_{CC} = H_{CP} \cdot R \cdot T = 1.13 \cdot 10^{-4} \cdot 8.31 \cdot 293 = 0.424 \quad \text{Eq 6-5}$$

However, this value of  $H_{CC}$  of 0.424 does not match the experimental determined ratio of 1.59. Comparing these numbers, it was found that there is more ozone in the water than the equilibrium would allow. This can be explained because the supply of aqueous ozone comes primarily of the plasma chamber as illustrated in (Figure 6-11). Because of the limitations of the setup, ozone in gas was measure at the top of the liquid while ozone in water was measured at the bottom. As such, both concentrations are not in equilibrium. This is why the expected concentration is lower than the measured concentration.

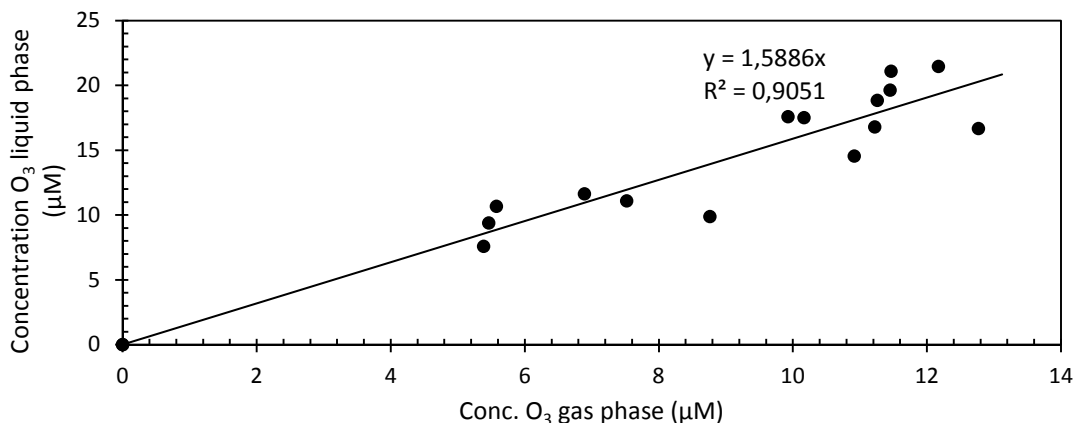


**Figure 6-10:** Concentration of aqueous ozone in function of gaseous ozone

Besides the ozone concentration, hydrogen peroxide was also measured with and without bubbling ozone gas in the ozone chamber (Figure 6-12). It can be found that both concentrations of ozone and hydrogen peroxide drop without bubbling. This proves the assumption that ozone and hydrogen peroxide are partially introduced through the gas phase.

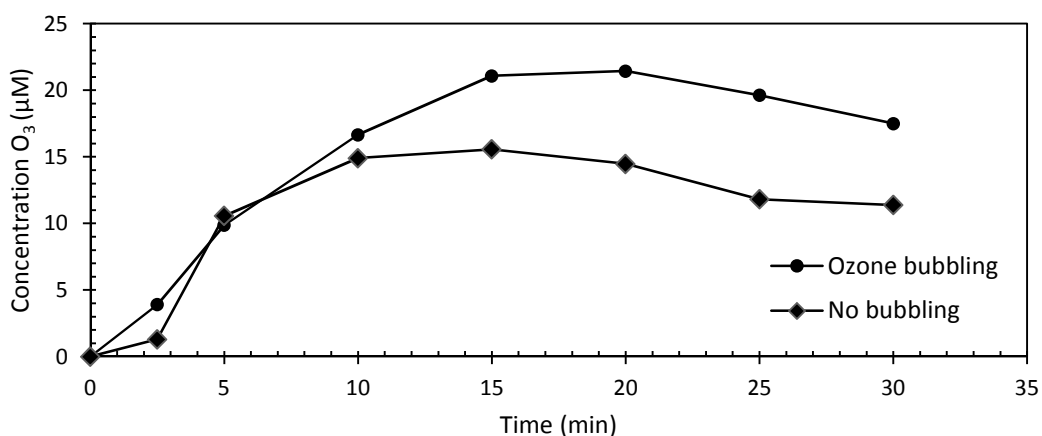


**Figure 6-11:** Concentration of ozone in water, with and without gas bubbling

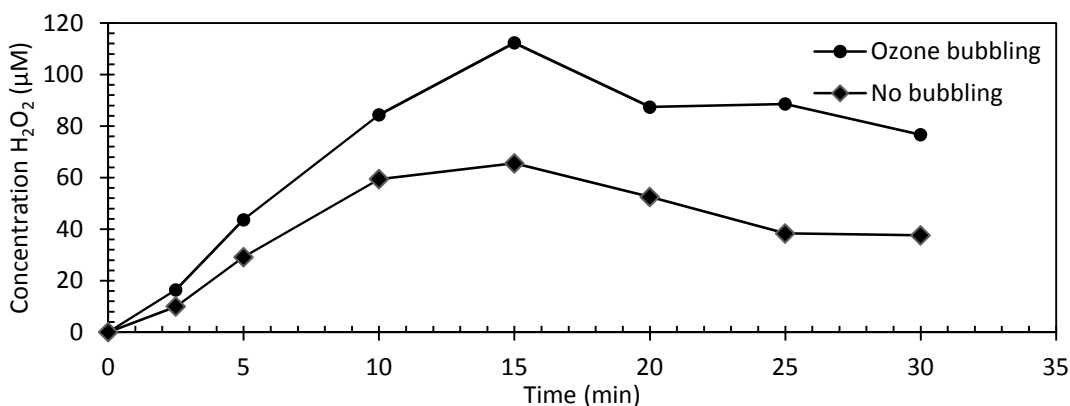


**Figure 6-12:** Concentration of hydrogen peroxide in water, with and without gas bubbling

### 6.2.3 Activated carbon cloth

Activated carbon (AC) is known for its adsorbing properties (Karimi et al. 2012), but it also has a catalytic effect on  $\text{H}_2\text{O}_2$  and  $\text{O}_3$  production. Activated carbon will decompose hydrogen peroxide by exchanging a surface hydroxyl group with a  $\text{HO}_2^-$  anion (r 6-5 and r 6-6). This will increase the oxidation potential of AC which can decompose another  $\text{H}_2\text{O}_2$  molecule and regenerate the AC surface while releasing oxygen.



Besides this decomposition reaction, AC can function as an electron-transfer catalyst, forming hydroxyl radicals ( $\text{OH}$ ) (r 6-7 and r 6-8). In these equations AC and  $\text{AC}^+$  are the oxidized and reduced catalyst states (Affam and Chaudhuri 2011, Paternina et al. 2009).



The removal of hydrogen peroxide was investigated by comparing the concentration of hydrogen peroxide with and without the presence of the Zorflex cloth ( $100 \text{ cm}^2$ ). The starting concentration was approximately a 700 times dilution of a 3% hydrogen peroxide solution with a volume of 200 ml ( $920 \mu\text{M}$ ). Both test solutions were continuously stirred at 430 rpm. Figure 6-13 shows that with Zorflex the concentration of  $\text{H}_2\text{O}_2$  dropped 95% in 15 minutes. This test was conducted outside of the setup.

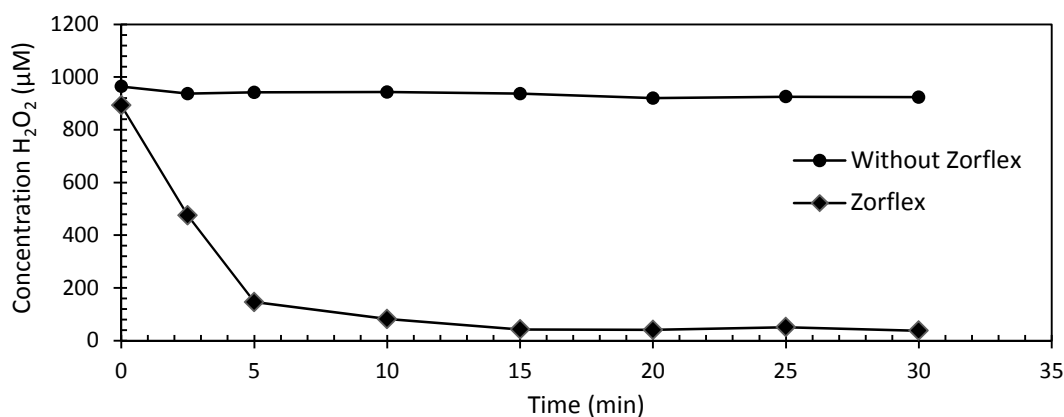


**Figure 6-13:** Effect of the addition of active carbon cloth on hydrogen peroxide concentration

This experiment does not provide any evidence of the formation hydroxyl radicals. However, these experiments show an expected change in concentration of  $\text{H}_2\text{O}_2$ . Literature is used to back up the assumption that active species ( $\text{OH}$  and  $\text{HO}_2$ ) are formed.

Also ozone concentrations are highly influenced by the activated carbon cloth. Presence of activated carbon accelerates the decomposition of ozone. This leads to the formation of active species such as hydroxyl radicals (Faria et al. 2006).

To determine the influence of activated carbon, a similar experiment was conducted as with hydrogen peroxide (Figure 6-14). Ozone, made by the reactor, was bubbled in a beaker with 200 ml of distilled water for about half an hour. Self-decomposition of ozone was observed without any added AC. However, the addition of the Zorflex cloth definitely accelerates the process.

Such drop in ozone and hydrogen peroxide in presence of activated carbon can be considered as a positive factor. Especially since ozone and hydrogen peroxide decompose through active species in a place where the concentration of micropollutants is highest (directly at the active carbon surface).

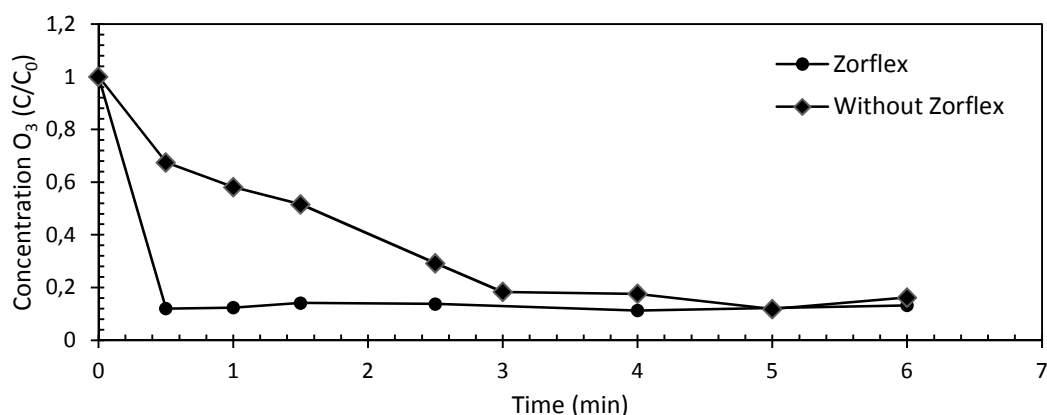


**Figure 6-14:** Effect of the addition of active carbon cloth on ozone concentration

### 6.3 Conclusion

Effect of pH, conductivity and power has been studied. It was found that initial pH and conductivity have little to no effect on the overall process. Also, active species such as ozone and hydrogen peroxide were measured. These two long living active species have a strong correlation in the liquid phase. Considerable amount of hydrogen peroxide is produced in gas phase and transferred to liquid phase during a second step of gas transfer.

It was also clear that pH in the ozone chamber drops much more slowly when water does not come in contact with the plasma (Figure 6-2). This can have some positive consequences on the active species such as ozone, which is highly pH dependable.

Also a correlation between ozone in gas phase and liquid phase was measured. However, no equilibrium was obtained, so Henry's law does not apply. This can be explained due to ozone in gas phase was measured at the top of the liquid, while aqueous ozone was measured at the bottom.

The active carbon cloth, used in the system, plays a crucial role not only in micropollutant adsorption, but also in hydrogen peroxide and ozone transformation. That way, active carbon acts as a catalyst and as an adsorbent.

## 7 Methylene blue

Before discussing micropollutants, a model compound is used to check the removal rate of the reactor. This model compound, methylene blue, will give a better understanding of the degradation mechanics and chemistry. Methylene blue, just as any dye, can be analyzed with a spectrometer.

### 7.1 Spectrum

Concentrations of methylene blue were measured at a wavelength of 660 nm, at the absorption peak of the monomer (Figure 7-1). High concentrations lead to molecular aggregation, when this occurs, absorption peaks at 610 and 570 nm start to appear, respectively representing dimers and trimers of the methylene blue molecule. A decrease in pH suggests a rise in absorption at 740 nm, but was not observed due to the limited range (700 nm) (Cenens and Schoonheydt 1988, Contineanu et al. 2009, Liu et al. 2012). The absorption peaks at 250 and 290 nm also indicate methylene blue. Reason for these peaks is the aromatic structure of methylene blue, which absorbs well in this spectral region (Shimadzu 2015). After about 3 minutes of plasma treatment, the absorbance starts to increase between 220 and 250 nm, indicating phenol and carboxyl group formation by the plasma reactor (Huang et al. 2010).

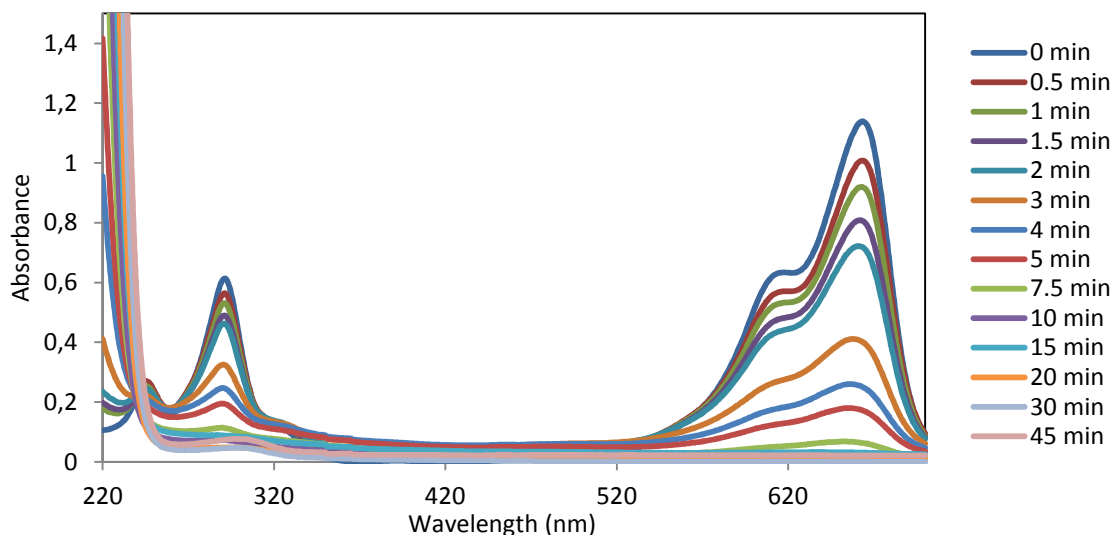


**Figure 7-1:** Full spectrum of methylene blue degradation for different stages in the process



## 7.2 Kinetics

### 7.2.1 Order determination

First parameter that is investigated is the initial concentration (Figure 7-2). This parameter will give better insight of methylene blue degradation kinetics and can be used to determine the reaction order. Reaction order determination is based on the graphical method (Lachheb et al. 2002).

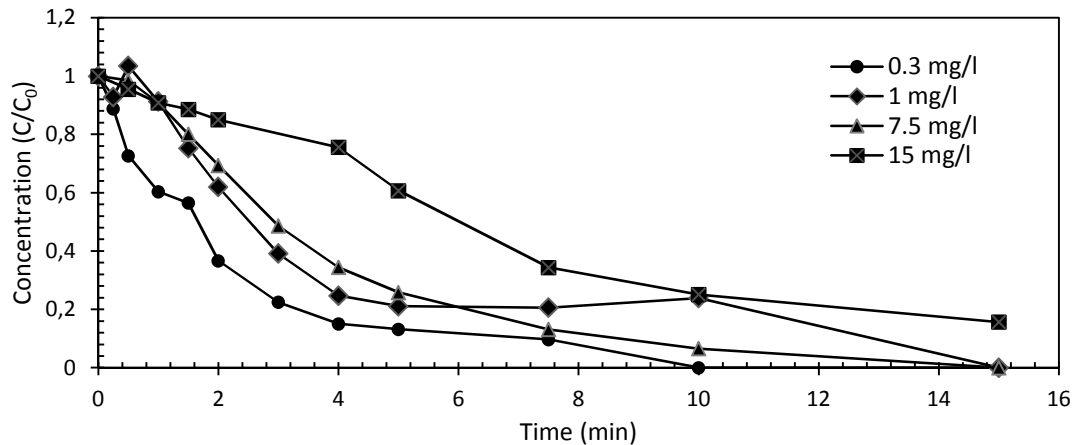


**Figure 7-2:** Methylene blue degradation in function of time for different initial concentrations

With the graphical method, the response (concentration), natural logarithm of the response and inverted of the response is plotted against time. These graphs will respectively represent zero, first and second order. Linear regression is used to determine which of those plots fit the linear model the most. Thus the one with the highest determination coefficient (Table 7-1) determines the order. For the methylene blue degradation, a first order reaction (Figure 7-3) is observed. Reaction rate constant ( $k$ ) was calculated using following relation with  $C_t$  the concentration at any given time and  $C_0$  the initial concentration (Eq 7-1).

$$\ln\left(\frac{C_t}{C_0}\right) = -k \cdot t \quad \text{Eq 7-1}$$

A first order reaction has a constant half-life, regardless of the initial concentration (Eq 7-2). When looking at Figure 7-2, this statement is clearly not met.

$$t_{1/2} = \frac{\ln(2)}{k} \quad \text{Eq 7-2}$$

**Table 7-1:** Overview of determination coefficients ( $r^2$ ) for different reaction orders and initial concentrations.

	0.3 mg/l	1 mg/l	7.5 mg/l	15 mg/l
0th order	0.6487	0.7252	0.8027	0.9394
1st order	0.9268	0.7703	0.9951	0.9761
2nd order	0.9797	0.7703	0.8771	0.9444

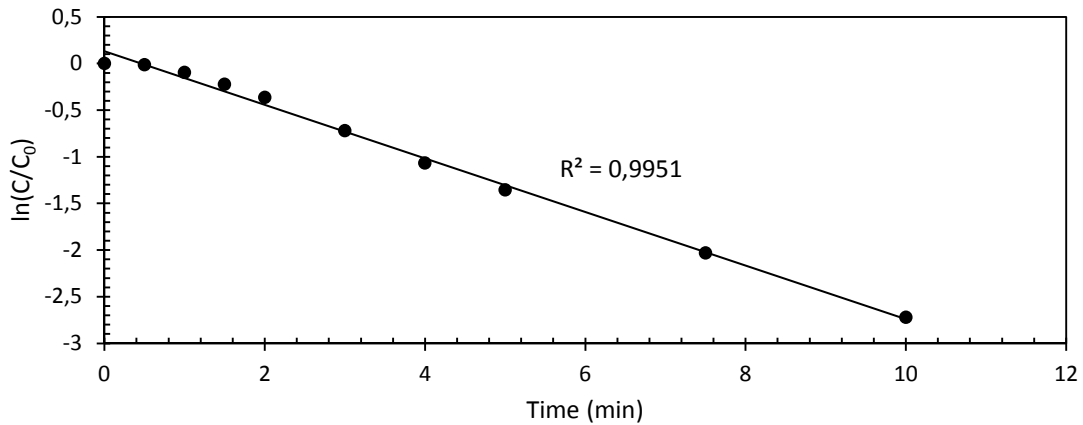


**Figure 7-3:** Visual representation of the graphical method (first order reaction) with an initial concentration of 7.5 mg/l

To determine the true reaction order, method of initial reaction rate is used. At different starting concentrations, the slope of concentration versus time will be determined at  $t_0$  (Figure 7-2). This slope is the initial reaction rate and can be plotted against initial concentration. To calculate the order of reaction ( $n$ ), it is necessary to start from the basic formula of reaction rate (Houas et al. 2001) (Eq 7-3).

$$\text{rate} = k \cdot C_0^n \quad \text{Eq 7-3}$$

The order of reaction can be seen as the tangent of the logarithm of reaction rate in relation (Eq 7-4) to the logarithm of the initial concentration (Figure 7-4).

$$\log \text{rate} = \log k + n \cdot \log C_0 \quad \text{Eq 7-4}$$

According to Figure 7-4 and Eq 7-4, the order of this reaction is 1,61. Because MB degradation is close to a first order reaction, this is the one that will be worked with. So for other calculations, the degradation will be assumed to be a first order reaction.

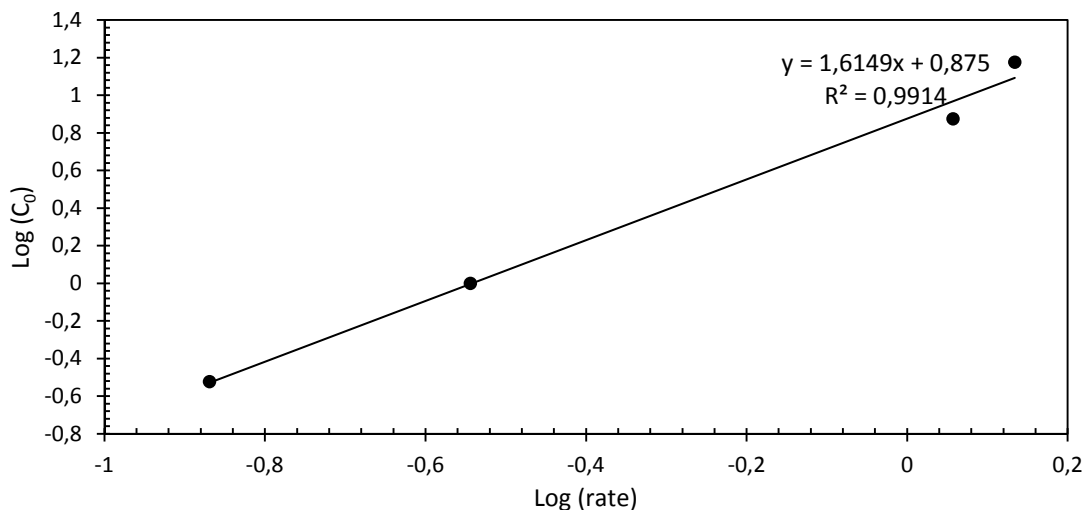


**Figure 7-4:** Determination of actual order

### 7.2.2 Reaction rate constants

For real life applications it is important to see the amount of decolorization for a given power at certain rate. The ideal situation is one where there is a maximum decolorization at a maximum rate, but at a minimum cost (power). The experiments with methylene blue (Table 7-2) show that when decolorization was high, so was the rate, but at the cost of a high power. This means there are some tradeoffs when it comes to power efficiency. Based on this data, it can be found that a duty cycle of 0.35 has the best removal.

**Table 7-2:** Overview of decolorization and first order reaction rate constants of methylene blue for different parameters.

$C_0$ (mg/l)	Voltage setting (W)	Duty Cycle	% of decolorization	Rate constant $k$ ( $\text{min}^{-1}$ )	$R^2$
0.3	49.7	0.15	90.32	0.3800	0.9626
7.5	29.0	0.15	91.85	0.2518	0.9986
	49.7	0.04	93.28	0.2563	0.9890
	49.7	0.15	93.43	0.2659	0.9926
	49.7	0.35	98.55	0.3212	0.8669
	68.3	0.15	96.61	0.2659	0.9874
	15	49.7	0.15	74.90	0.1253

### 7.2.3 Influence of ozone

The decolorization of methylene blue can mainly be divided into two parts. The first, being the reaction of ozone and other active species transferred through the gas phase with methylene blue. And the second one being due to direct contact of the dye with the ionized gas (plasma). The last differentiation is hard to make, because ozone is also formed at the plasma-water surface.

However, it is possible to change the setup in a way, so no ozone gas can be bubbled through the reservoir in the ozone chamber. This results in a fairly low degradation of methylene blue, compared to the standard experiment (complete setup) (Figure 7-5).

The plasma chamber can also be disconnected from the ozone chamber and only ozone gas can flow through the dye solution ( $C_0 = 7.5$  mg/l). This way the dye removal solely depends on the active species, that where transferred through the air, such as ozone and hydrogen peroxide. According to Figure 7-5, this results in a higher removal rate. This can be explained by the fact that pH does not drop as fast as with the plasma chamber connected. Therefore, ozone can be far more active than with lower pH, thus having a greater removal. In terms of reaction rate constants, effect of plasma only has the lowest value of  $k$ ,  $0.069 \text{ min}^{-1}$ . The combination of ozone and plasma was conducted at standard settings (Voltage setting: 49.7 W and DC: 0.15), therefore reaction rate constant is  $0.266 \text{ min}^{-1}$ . With only the ozone reactor at work, a  $k$ -value of  $0.434 \text{ min}^{-1}$  was obtained.

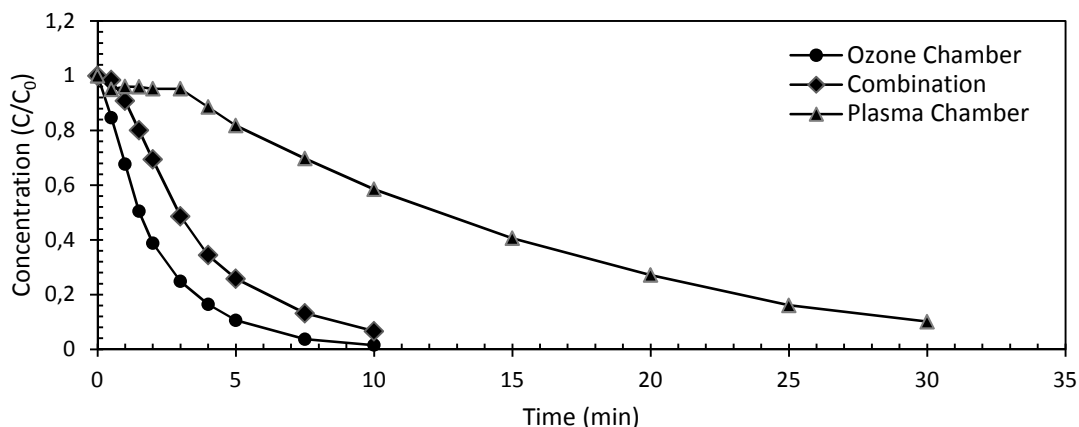


**Figure 7-5:** Influence of plasma (plasma chamber), ozone bubbling (ozone chamber) and combination of both on MB degradation

### 7.3 Influence of voltage waveform

Future use of DBD based reactors, depends on the energy efficiency of the process, because cost effectiveness of this reactor highly depends on energy and gas consumption. Since the latter will not change throughout the experiments, main focus will be the electricity consumption.

#### 7.3.1 Effect of voltage

For energy efficiency, parameters such as voltage, duty cycle and scavengers will be used. Graphical presentation of the first one can be found in Figure 7-6. This figure indicates that a higher voltage setting induces a higher removal of the dye. Lower power however, shows little to no difference in decolorization.

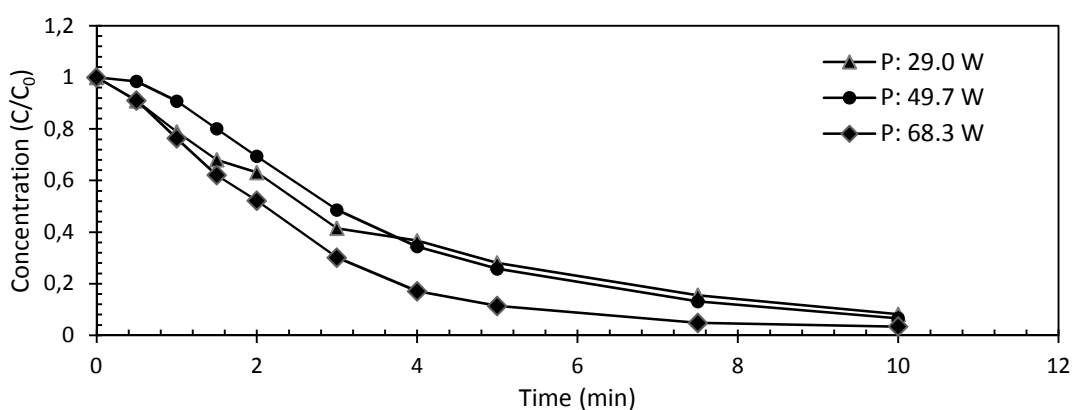


**Figure 7-6:** Concentration of methylene blue in function of time for different voltage settings

### 7.3.2 Effect of duty cycle

Duty cycle was changed as well and its influence on degradation is rather low. However, it can be found that a higher duty cycle (Figure 7-7), eventually results in a higher degradation of methylene blue. It is also expected to see a higher removal rate for the highest value of duty cycle. This higher rate is only observed after 4 min and can be explained by a malfunction (longer stabilization time, air supply, etc.) of the plasma reactor.

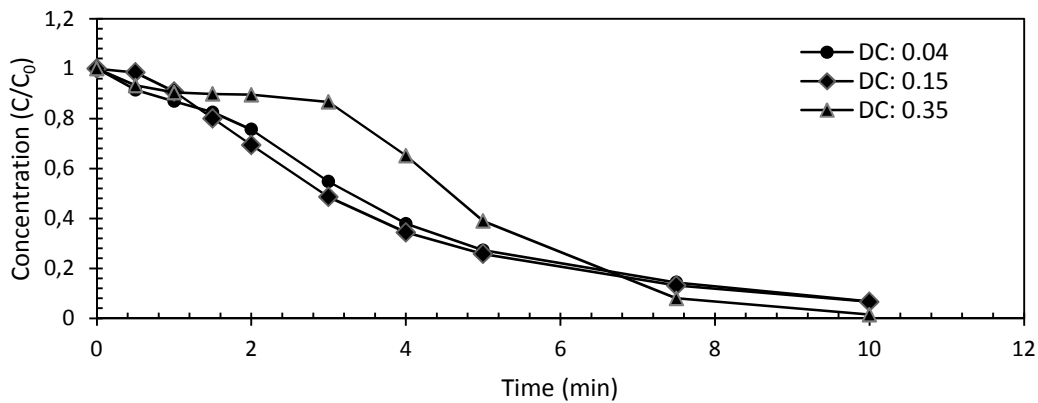


**Figure 7-7:** Concentration of methylene blue in function of time for different duty cycle

### 7.3.3 Power efficiency

#### 7.3.3.1 $G_{50}$

In plasma research  $G_{50}$  is a frequently used parameter to express energy efficiency.  $G_{50}$  is defined as the amount of dye in grams that is removed per kWh to get a 50% reduction (Eq 7-5).

$$G_{50} = \frac{6.0 \cdot 10^4 \cdot C_0 \cdot V_0 \cdot MM \cdot 1/2}{P \cdot t_{50}} \quad \text{Eq 7-5}$$

With  $C_0$  the initial concentration in M, MM the molar mass in g/mol,  $V_0$  volume of the initial solution in liter, P the power in Watt and  $t_{50}$  treatment time in minutes for removal of 50% of the component.  $t_{50}$  can be calculated using Eq 7-2 (MuhammadArif Malik 2010). Because concentration of methylene blue is expressed in mg/l the formula can be simplified to Eq 7-6. In this case,  $C_0$  is the initial concentration in mg/l. By implementing Eq 7-2, k is introduced and is the reaction rate constant in  $\text{min}^{-1}$ .

$$G_{50} = \frac{30 \cdot C_0 \cdot V_0 \cdot k}{P \cdot \ln 2} \quad \text{Eq 7-6}$$

For the standard experiment with initial concentration of 7.5 mg/l and a power consumption of 49.7 W, calculation of  $G_{50}$  will be elaborated. The calculated efficiency is then 0.87 g/kWh. Important to note for  $G_{50}$  is that bigger is better. Thus the higher  $G_{50}$ , the higher decolorization will be per unit of energy (kWh).

$$G_{50} = \frac{3.0 \cdot 10^4 \cdot 7.5 \text{ mg/l} \cdot 0.5 \text{ l} \cdot 0.2659}{49.7 \cdot \ln 2} = 0.87 \text{ g/kWh} \quad \text{Eq 7-7}$$

For different settings of voltage and duty cycle,  $G_{50}$  was calculated and summarized in Table 7-3. With this data, it is clear that a lower actual power increases the energy efficiency drastically. Efficiency rises with about 350 % when duty cycle is lowered from 0.15 to 0.04. However, increasing this duty cycle (0.35) lowers the efficiency with about the same amount. By changing the power settings from minimum to maximum, energy yield drops approximately 15 times. The  $G_{50}$  formula is in correlation with the initial concentration, that is why the use of low concentrations such as 0.3 mg/l have a low efficiency. On the other hand 15 mg/l as initial concentration has a lower degradation rate, but still has a decent efficiency. Assuming a cost of 0.1 euro per kWh, a diagram can be made where the cost per volume ( $m^3$ ) is compared to the value of  $G_{50}$  (Figure 7-8). This diagram shows that a lower duty cycle (0.04) is both cost effective and has a high efficiency, compared to the lower efficiency of a higher duty cycle (0.35) and the higher cost.

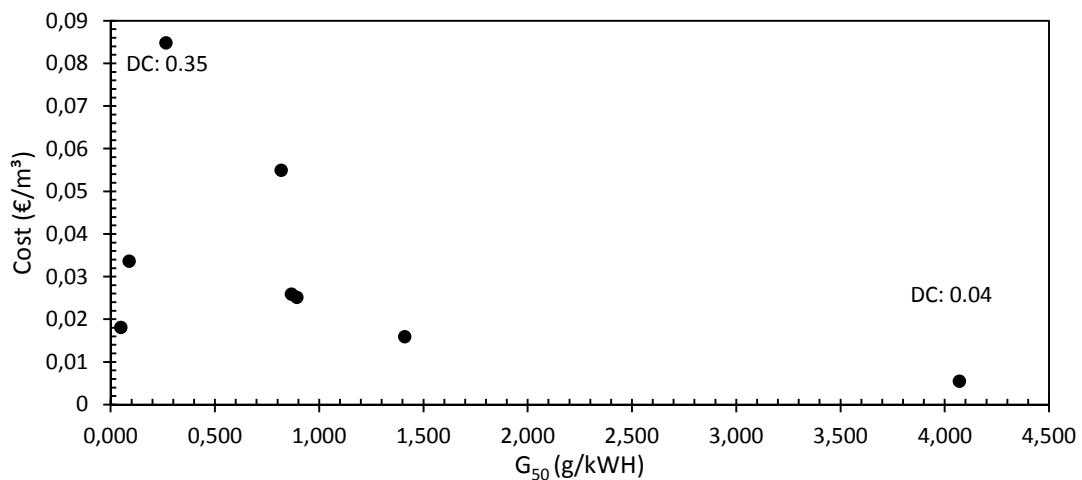


**Figure 7-8:** Cost per volume ( $m^3$ ) versus energy efficiency.

**Table 7-3:**  $G_{50}$  for different power settings (voltage and duty cycle)

$C_0$ (mg/l)	Voltage setting (W)	Duty Cycle	Actual power $P_0$ (W)	$k$ ( $min^{-1}$ )	$G_{50}$ (g kWh <sup>-1</sup> )
0.3	49.7	0.15	49.72	0.3800	0,05
7.5	29.0	0.15	28.96	0.2518	1.41
	49.7	0.04	10.22	0.2563	4.07
	49.7	0.15	49.72	0.2659	0.87
	49.7	0.35	196.7	0.3212	0.27
	68.3	0.15	68.33	0.2659	0.89
	15	49.7	0.15	49.72	0.1253

To compare this DBD reactor, the most energy efficient settings were used. According to Table 7-4 this reactor is about 2 orders of magnitude more efficient than most reactors. Important to note is that the  $G_{50}$  formula depends on the initial concentration, however reactors with a higher initial concentration still have a lower efficiency. When the DBD reactor would use  $O_2$  instead of air, a significant increase would be observed. Due to the usage of pure  $O_2$  instead of air, more ozone can be produced. Also the usage of  $O_2$

eliminates nitrogen species in the water. Those 2 factors affect the ozone production a lot, hence the methylene blue degradation.

**Table 7-4:** Comparison of efficiency between different reactors using  $G_{50}$  for MB degradation

Type of reactor	$C_0$ (mg/l)	$G_{50}$ (g kWh <sup>-1</sup> )	Reference
DBD on thin layer of water	7.5	4.071	
Radio Frequency Discharge in water	5	0.037	(Maehara et al. 2008)
Diaphragm Discharge in water	12	0.042	(MuhammadArif Malik 2010)
Pulsed Corona Discharge in water	13	0.064	(Malik et al. 2002)
Pulsed Corona Discharge in water with O <sub>2</sub> bubbling	13.25	0.341	(Malik et al. 2002)
Pulsed Corona Discharge on water surface in O <sub>2</sub>	15	1.500	(Stará et al. 2009)

### 7.3.3.2 Electric energy per order

Because this plasma technique has a promising future in waste water treatment. Energy efficiency expressed as electrical energy per order (EEO) is more appropriate to compare different AOPs. This implementation is defined as the number of kWh of electrical energy required to reduce one order of magnitude (90%) of the pollutant in 1 m<sup>3</sup> of contaminated water (Cater et al. 2000, Daneshvar et al. 2005) and is represented by Eq 7-8. Where P is the power (kW), t is the residence time (min), V is the volume (l) of the water in the reactor,  $C_0$  and  $C_f$  are the initial and final concentration of methylene blue.

$$EEO = \frac{P \cdot t \cdot 1000}{V \cdot 60 \cdot \log\left(\frac{C_0}{C_f}\right)} \quad \text{Eq 7-8}$$

EEO is calculated for the standard experiment, using all the standard settings for the reactor. In contrast to  $G_{50}$ , with EEO a low value has to be pursued. As with  $G_{50}$ , EEO shows that a lower actual power is more efficient (Table 7-5).

**Table 7-5:** EEO for different power settings (power and duty cycle)

Voltage setting (W)	Duty cycle	Actual power (W)	K (min <sup>-1</sup> )	$C_f$ (mg/l)	EEO (kWh m <sup>-3</sup> order <sup>-1</sup> )	Cost (€ m <sup>-3</sup> order <sup>-1</sup> )
49.7	0.04	10.22	0.2563	0.50	2.90	0.29
29.0	0.15	28.96	0.2518	0.61	8.87	0.89
49.7	0.15	49.72	0.2659	0.49	14.02	1.40
68.3	0.15	68.33	0.3764	0.25	15.50	1.55
49.7	0.35	196.7	0.3212	0.11	35.64	3.56

Data on methylene reduction was compared with a couple of AOPs. Again, it was found that the DBD system was most effective. However, not many studies were found on methylene blue degradation to compare this reactor to.

**Table 7-6:** Comparison of efficiency between different AOPs using EEO

Process	C <sub>0</sub> (mg/l)	EEO (kWh m <sup>-3</sup> order <sup>-1</sup> )	Reference
DBD on thin layer of water	7.5	2.90	
UV-LED light irradiation + TiO <sub>2</sub> coated quartz tube	5	3000	(Natarajan et al. 2011)
UV/ H <sub>2</sub> O <sub>2</sub>	20	38.09 -107.31	(Zhang et al. 2013)

### 7.3.3.3 Scavenger effect

Use of a natural matrix such as humic acid and isopropyl alcohol can give better insight on the actual process. These scavengers will inhibit the active species in water and will mimic the water matrix for which the system is intended.

Scavenger effect on the methylene blue degradation was tested using organic compounds such as isopropyl alcohol (2%) and humic acid (10 and 50 mg/l). Because reactive species such as OH radicals and ozone will react with various types of organic components, these scavenger molecules will compete with methylene blue.

Table 7-7 shows the addition of 2% isopropyl alcohol (333 mM) induces a 33% drop on energy efficiency at a 50% degradation of methylene blue. Efficiency had dropped 50% for 90% removal of methylene blue. Isopropyl is used as a more overall scavenger. To get a more realistic view on the effect of organic matter in this reactor, 10 and 50 mg/l humic acid solutions were used. This concentration corresponds to wastewater effluent samples (Jarusutthirak et al. 2002). With humic acid as scavenger, 20% decrease in efficiency is observed. It can be found that the role of organic matter in wastewater is important to remove compounds such as methylene blue.

When cost effectiveness is taken under consideration, it is necessary to take the whole treatment of waste water into account. According to a survey (Waterworld 2015) it was found that treatment of water costs about 2.06 \$ per 1000 gallon of water. At the current exchange rate (1 \$ = 0.89 €) this means about 0.48 €/m<sup>3</sup>. The addition of a plasma reactor will already increase the price drastically, so scavengers have a huge impact on the cost of water treatment.

**Table 7-7:** Overview on the effect of scavengers on the G50 and EEO on methylene blue decolorization (Initial concentration MB of 7.5 mg/l)

	k (min <sup>-1</sup> )	r <sup>2</sup>	G50 (g kWh <sup>-1</sup> )	% less efficient	EEO (kWh m <sup>-3</sup> order <sup>-1</sup> )	Cost € m <sup>-3</sup> order <sup>-1</sup>	% less efficient
Standard	0.2659	0.9926	0.8681	0	14.01	1.40	0
10 mg/l HA	0.2126	0.9866	0.6942	20.0	17.29	1.73	23.3
50 mg/l HA	0.2112	0.9912	0.6894	20.6	16.93	1.69	20.8
IPA 2%	0.1777	0.9960	0.5801	33.2	21.03	2.10	50.1



## 7.4 Single pass

In industrial applications, a continuous water flow through the reactor is more appropriate. The alternative design of chapter 4 is used to simulate that. With this continuous flow, a steady state is expected. In terms of the reactor in closed circuit, this means all of the water in the ozone chamber has to pass one single time through the whole system. At a flowrate of 95.3 ml/min, 500 ml will have passed through in 5 minutes, in other words hydraulic retention time (HRT) will be 5.22 min. At 5 minutes 68.42% of the methylene blue is degraded for standard settings and a closed circuit (power of 50 W, duty cycle of 0.15 and MB concentration of 7.5 mg/l).

A steady state is achieved at 5 minutes (Figure 7-9). This corresponds to the estimated time for one pass through in the closed circuit setup. Higher degradation is observed than in the single pass setup, 74.21% and 91.35% when MB solution respectively passes first through plasma and ozone. By changing the configuration from plasma chamber first to ozone first, efficiency will increase with 23%.

The difference in effectiveness can be explained with pH change. From the pH experiments, it is known that when water does not pass through the plasma chamber, pH will be at least one pH unit higher. Therefore, ozone and other pH dependable active species can have a higher oxidative potential to destroy the dye.

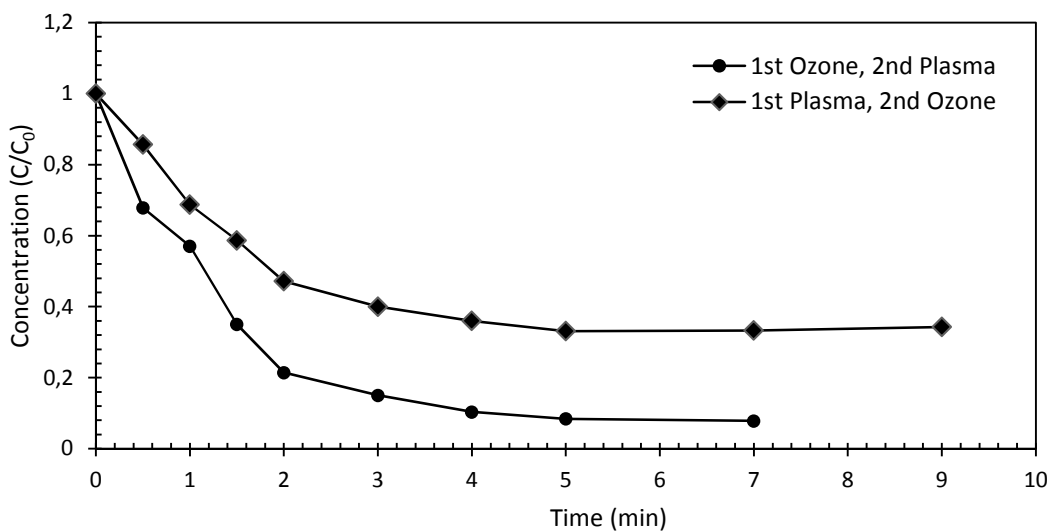


**Figure 7-9:** Decolorization of methylene blue in function of time for a continuous flow configuration, with an initial concentration of 7.5 mg/l

## 7.5 Conclusion

---

The use of methylene blue offers a great insight in how the system performs under different circumstances. First of all, decolorization has a reaction order of 1.61. This means that the process is influenced by multiple factors. For sake of simplicity the process can be divided into plasma and ozone gas reactions. In case of MB, the latter reaction had the upper hand.

Efficiency was calculated using  $G_{50}$  and EEO, respectively compared to other plasma reactors and AOP's. It was seen that for methylene blue, this setup was the most efficient. Also the effect of scavengers such as humic acid and isopropyl alcohol were investigated. For concentrations of 10 and 50 mg/l humic acid, the efficiency only dropped about 20%. Isopropyl alcohol on the other hand made the efficiency drop 33 to 50%.

Lastly, a continuous system was mimicked, where water could pass first through the ozone chamber followed by the plasma chamber and vice versa. After 5 minutes an expected steady state was observed. At this steady state, it was found that the use of an ozone reactor first, the system was 23% more effective at decoloring the water.

## 8 Micropollutants

Micropollutants such as chlorinated hydrocarbons have been tested to show the removal efficiency of the system on more persistent molecules. This will give a more realistic view on future applications where this type of reactor can be put to use. In this chapter, the removal of micropollutants will be compared to decolorization of the model compound. It is important to know that initial concentration of the micropollutants will be 2 orders of magnitude lower than initial concentration of the blue dye.

Graphical data of either alpha hexachlorocyclohexane ( $\alpha$ -HCH) and pentachlorobenzene (PeCB) will be compared throughout this chapter. All these comparisons are substantiated with statistical tests, discussed in chapter 5.

Concentration of PeCB and  $\alpha$ -HCH were kept as low as possible, while still maintaining measurable on the GC-MS. Therefore, concentrations of about 70 and 300  $\mu\text{g/l}$  respectively for PeCB and  $\alpha$ -HCH were used. Due to technical difficulties, experiments with HCB have not been done.

### 8.1 Kinetics

#### 8.1.1 Order determination

Kinetics are used to make a distinction between PeCB and  $\alpha$ -HCH in terms of removal rate and to compare with the decolorization of methylene blue. A visual representation of the degradation for PeCB and  $\alpha$ -HCH can be found in Figure 8-1. Again, order determination was done using the graphical method. With this method, zeroth, first and second order were checked with their corresponding plots. The best fit was can be found using the determination coefficient ( $r^2$ ) to give an approximation of the reaction order. Values of  $R^2$  are presented in Table 8-1 with the highest values for PeCB and  $\alpha$ -HCH being underlined to designate the order.

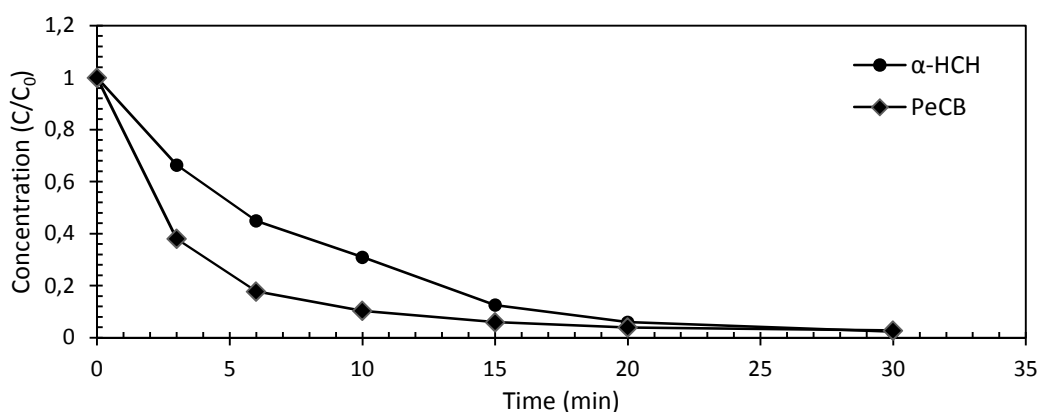


**Figure 8-1:** Degradation of PeCB ( $C_0$ : 155  $\mu\text{g/l}$ ) and  $\alpha$ -HCH ( $C_0$ : 308  $\mu\text{g/l}$ ) for standard settings (49.7 W and DC: 0.15)

According to Table 8-1,  $\alpha$ -HCH follows a first order reaction, while PeCB follows a second order reaction (underlined). This makes it a little bit more difficult to compare both components using the reaction order constant because the units will be different. However, half-life and energy efficiency can be calculated and compared.

As for methylene blue, it can be seen that the reaction order can be strongly different from first order kinetics. Resulting in the fact that there is more than one reaction to dominate, but series of reactions that are almost indistinguishable in this research. Parameters are changed relative to standard conditions (49.3 W and DC: 0.15).

**Table 8-1:** Overview of determination coefficients ( $r^2$ ) to determine reaction order of PeCB and  $\alpha$ -HCH. Unless mentioned otherwise, initial concentrations for PeCB and  $\alpha$ -HCH are respectively 155  $\mu\text{g/l}$  and 308  $\mu\text{g/l}$ .

		Duty cycle (P: 50 W)			Voltage (DC: 0.15)		Concentration ( $C_0$ )		Adsorption
		0.04	0.15	0.35	29 W	68 W	150 $\mu\text{g/l}$	75 $\mu\text{g/l}$	
<b>0<sup>th</sup> order</b>	PeCB	0.5619	0.5061	0.4477	0.5467	0.3889	-	-	0.6232
	$\alpha$ -HCH	0.8093	0.8041	0.6995	0.7863	0.8285	0.7959	0.7472	0.9160
<b>1<sup>st</sup> order</b>	PeCB	0.8002	0.8661	0.8618	0.8307	0.8703	-	-	0.9227
	$\alpha$ -HCH	<u>0.9941</u>	<u>0.9526</u>	<u>0.9572</u>	<u>0.9868</u>	<u>0.9885</u>	<u>0.987</u>	<u>0.9577</u>	<u>0.9939</u>
<b>2<sup>nd</sup> order</b>	PeCB	<u>0.9164</u>	<u>0.9897</u>	<u>0.9115</u>	<u>0.915</u>	<u>0.9181</u>			<u>0.9843</u>
	$\alpha$ -HCH	0.8905	0.8532	0.9113	0.9046	0.8365	0.9066	0.9542	0.9001

### 8.1.2 Reaction rate constant

Table 8-2 shows an overview of the reaction rate constants, half-life and percent degraded for PeCB and  $\alpha$ -HCH. To compare the micropollutants, half-life can be used. It can be stated that PeCB takes less time to degrade to 50% with a maximum of 1 min, while the average of  $\alpha$ -HCH lies around 5.96 min. For both components half-life drops as duty cycle goes up. In terms of voltage settings, only a great distinction can be made between 49.7 W and 68.3 W.

Compared to methylene blue, half-life of PeCB is a lot lower, where the average of methylene blue lies around 2.5 to 3 minutes. However, compared to  $\alpha$ -HCH, methylene blue reaches its half-live earlier. One thing that definitely stands out is the decolorization of methylene blue does not prove to be a lot faster, than the micropollutants. But on the other hand, methylene blue has higher concentration compared to the micropollutants.

**Table 8-2:** Overview of reaction rate constants, half-life and percentage degraded after 30 minutes of runtime for PeCB and  $\alpha$ -HCH <sup>(1)</sup> measured at 15 minutes)

	PeCB			$\alpha$ -HCH		
	k (M/min)	$t_{1/2}$ (min)	% Degraded	k ( $\text{min}^{-1}$ )	$t_{1/2}$ (min)	% Degraded
Duty cycle 0.04	$3.62 \cdot 10^6$	1.00	96.68	0.104	6.68	95.41
Duty cycle 0.15	$4.39 \cdot 10^6$	0.82	97.20	0.129	5.37	97.65
Duty cycle 0.35	$1.31 \cdot 10^7$	0.28	97.91 <sup>(1)</sup>	0.155	4.47	98.64
Power 29.0 W	$4.98 \cdot 10^6$	0.94	96.46	0.109	6.34	95.97
Power 68.3 W	$1.78 \cdot 10^7$	0.13	99.02 <sup>(1)</sup>	0.128	5.41	97.53
Adsorption	$1.00 \cdot 10^6$	2.01	93.71	0.0877	7.90	92.34
$C_0$ 150 $\mu\text{g/l}$	-	-	-	0.112	6.21	95.94
$C_0$ 75 $\mu\text{g/l}$	-	-	-	0.0958	7.23	94.11

## 8.2 Influence of voltage waveform

To make degradation of the micropollutants more comparable to methylene blue, energy efficiency expressed as  $G_{50}$  and EEO can be used.

### 8.2.1 Effect of voltage

Again, power was varied with duty cycle and voltage for PeCB and  $\alpha$ -HCH. When voltage is varied, the graphs are very similar.  $\alpha$ -HCH has a degradation path that's analogous for most voltage settings. Possible explanation is that the distribution of the power is too low since the maximum difference is only 40 W. PeCB has only a better degradation for 68.3 W, whereas powers of 49.7 and 29.0 W show no significant difference.

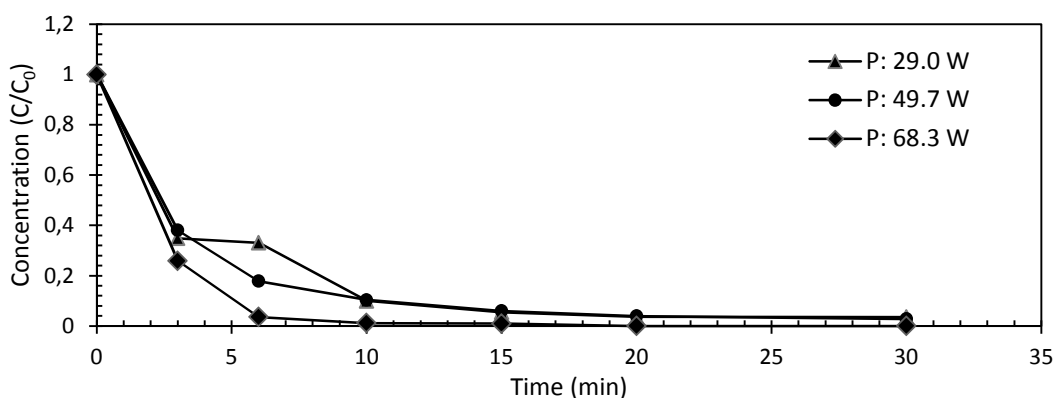


**Figure 8-2:** Degradation of pentachlorobenzene over time for different voltages

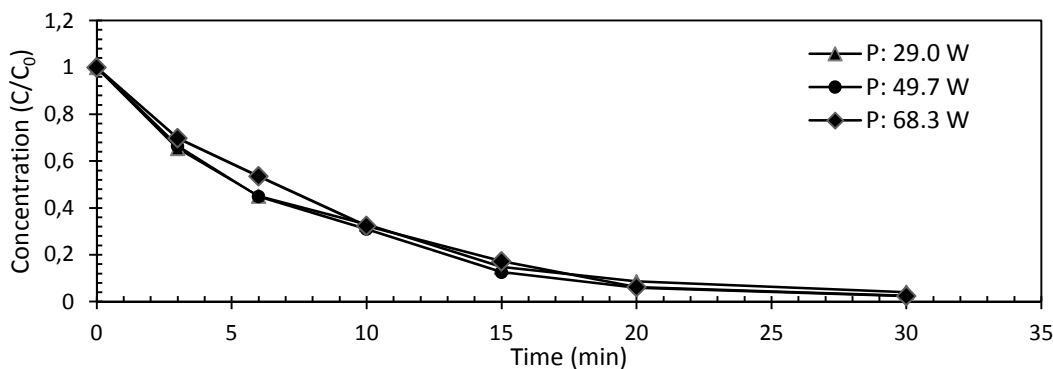


**Figure 8-3:** Degradation of alpha hexachlorocyclohexane over time for different voltages

### 8.2.2 Effect of duty cycle

Duty cycle of 0.35 induces a higher removal of the micropollutants. For PeCB no difference is observed for duty cycle 0.04 and 0.15, while degradation of  $\alpha$ -HCH is slightly better at a duty cycle of 0.15 than for 0.04. Because little dissimilarities are observed, a prediction can be made that energy efficiency will be higher for a duty cycle of 0.04.

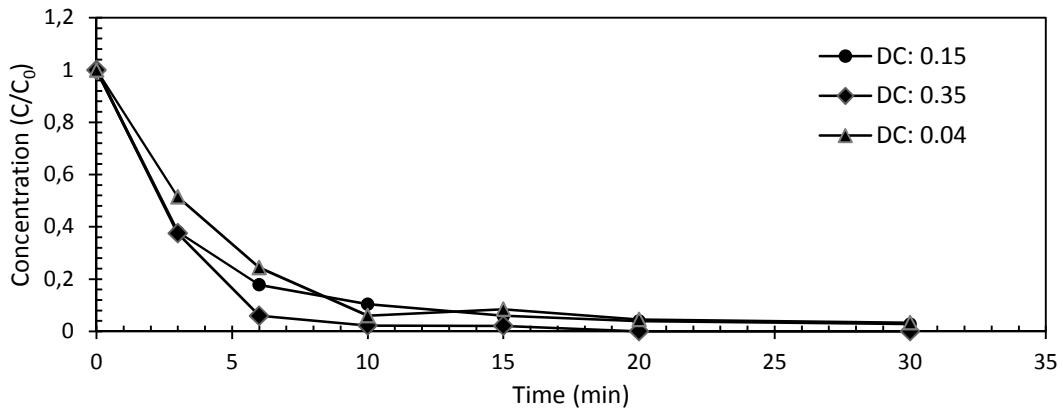


**Figure 8-4:** Degradation of pentachlorobenzene over time for different duty cycles

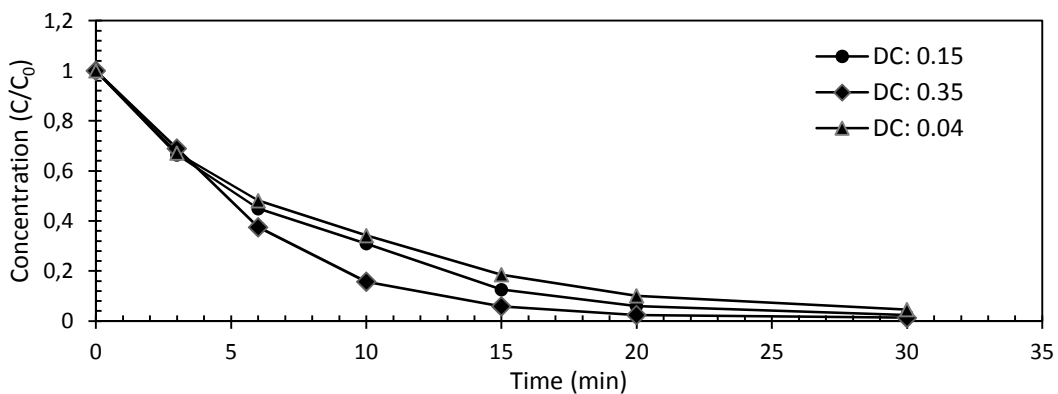


**Figure 8-5:** Degradation of alpha hexachlorocyclohexane over time for different duty cycles

### 8.2.3 Power efficiency

As discussed in previous chapter,  $G_{50}$  and EEO can be used to describe the energy efficiency. This can also be done for micropollutants. When reviewing Table 8-3,  $G_{50}$  shows that a duty cycle of 0.04 and a power of 68.3 W are most efficient for pentachlorobenzene. With a duty cycle of 0.04 it is obvious, because the lowest actual power was used (10 W). For a power of 68.3 W degradation time was a lot lower, compared to other voltage settings. Micropollutant  $\alpha$ -HCH has a similar outcome for duty cycle. However, voltage settings showed little influence on the degradation process, thus leaving the lowest power to be more efficient.  $G_{50}$  is also proportional to the initial concentration when nothing else changes, which is the case for  $\alpha$ -HCH. So a higher concentration of 300  $\mu\text{g/l}$  is almost double as efficient as an initial concentration of 150  $\mu\text{g/l}$ .

Since  $G_{50}$  is strongly dependable on the initial concentration, EEO will give a more arbitrary view on energy efficiency. It will also be easier to compare to the model compound. As with methylene blue, a duty cycle of 0.04 is the most efficient, in terms of energy consumption versus removal. Although a higher degradation was obtained with a power of 68.3 W or a duty cycle of 0.35, it does not outweigh the fact that 7 to 20 times the power was needed.

**Table 8-3:** Overview of energy efficiency ( $G_{50}$  and EEO) for PeCB and  $\alpha$ -HCH

	PeCB			$\alpha$ -HCH		
	G50 (g/kWh)	EEO (kWh/m <sup>3</sup> /order)	Cost €/m <sup>3</sup>	G50 (g/kWh)	EEO (kWh/m <sup>3</sup> /order)	Cost €/m <sup>3</sup>
Duty cycle 0.04	$10.24 \cdot 10^{-3}$	6.91	0.69	$67.64 \cdot 10^{-3}$	7.64	0.76
Duty cycle 0.15	$2.55 \cdot 10^{-3}$	32.01	3.20	$17.28 \cdot 10^{-3}$	30.52	3.05
Duty cycle 0.35	$1.92 \cdot 10^{-3}$	58.54	5.85	$5.25 \cdot 10^{-3}$	35.14	3.51
Power 29.0 W	$2.97 \cdot 10^{-3}$	19.97	2.00	$25.13 \cdot 10^{-3}$	20.77	2.08
Power 68.3 W	$11.88 \cdot 10^{-3}$	17.00	1.70	$12.49 \cdot 10^{-3}$	14.17	1.42
C <sub>0</sub> 150 µg/l	-	-	-	$7.81 \cdot 10^{-3}$	35.73	3.57
C <sub>0</sub> 75 µg/l	-	-	-	$3.29 \cdot 10^{-3}$	40.43	4.04

### 8.3 Influence of active cloth

To determine the influence of the active carbon cloth, an experiment was conducted where plasma was turned off. Assistance of the carbon fiber cloth in the removal of micropollutants plays a major factor for both PeCB and  $\alpha$ -HCH. Although visually there is little difference between the standard experiment and the one where the plasma is turned off, statically, a significant difference (p-value of 0.04 for  $\alpha$ -HCH and 0.025 for PeCB) was observed for both micropollutants (Figure 8-6 and Figure 8-7).

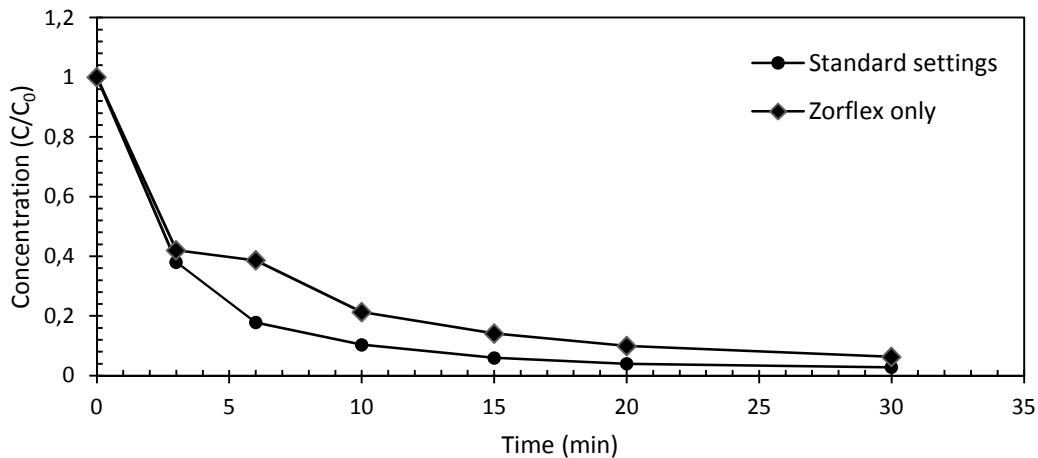


**Figure 8-6:** Influence on the removal of PeCB when plasma is turned off

Removal of micropollutants might be great without the plasma, but degradation cannot be guaranteed. The carbon cloth can act solely as a filter so the addition of plasma is still necessary. Another point to take in consideration is that activated carbon will be saturated after some time while plasma can aid in the removal of adsorbed pollutants.

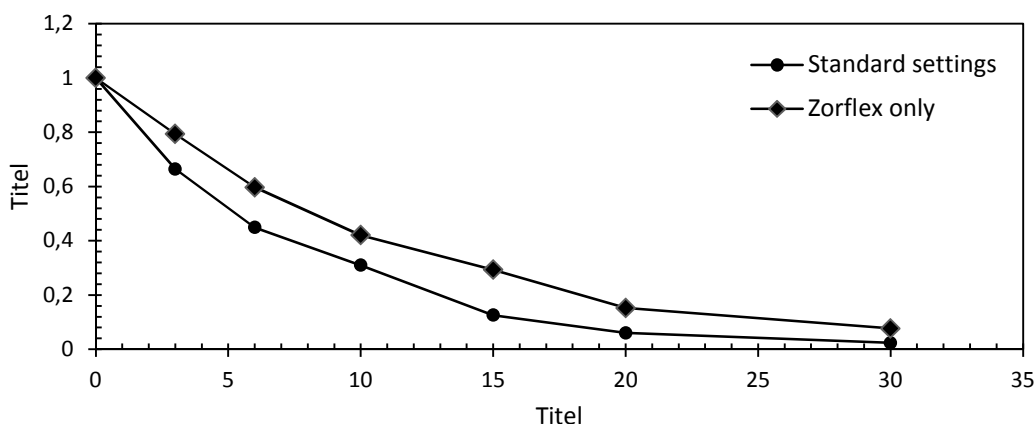


**Figure 8-7:** Influence on the removal of  $\alpha$ -HCH when plasma is turned off

#### 8.4 Single pass

The implementation of this reactor into a wastewater treatment plant requires some degree of continuity. This can be achieved with the alternative design. As with methylene blue, the ozone chamber can be placed before or after the plasma chamber.

When ozone is used first in a single pass configuration (HRT: 5.22 min), the removal of PeCB is significantly higher than when the plasma chamber is the first one in the chain. A steady state is for both configurations achieved between 0 and 3 min. A removal of 79% was reached with the plasma chamber first, in comparison to a removal of 91% with the ozone chamber first.

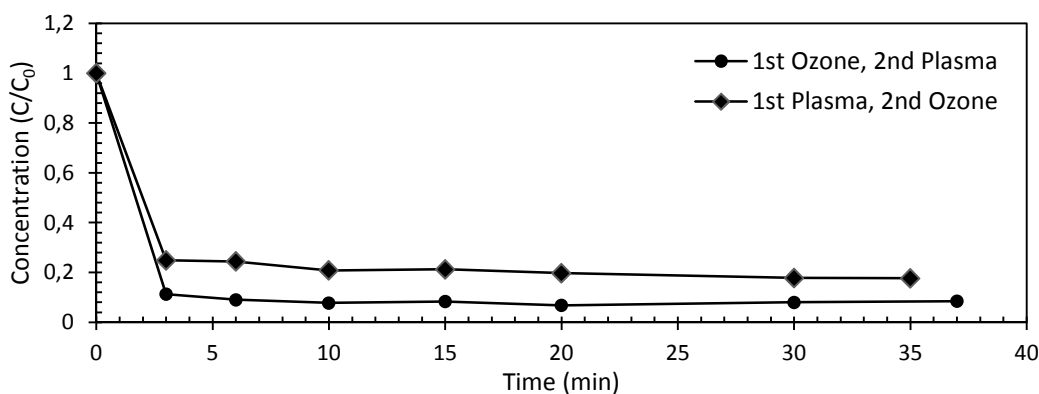


**Figure 8-8:** Degradation of pentachlorobenzene in function of time for a steady state configuration

For  $\alpha$ -HCH, similar results were found. Although the overall removal of  $\alpha$ -HCH was slightly lower than PeCB. At a steady state, removal of  $\alpha$ -HCH reached 57% with the plasma chamber first. When this reactor was put last in line, degradation went up to 64%.



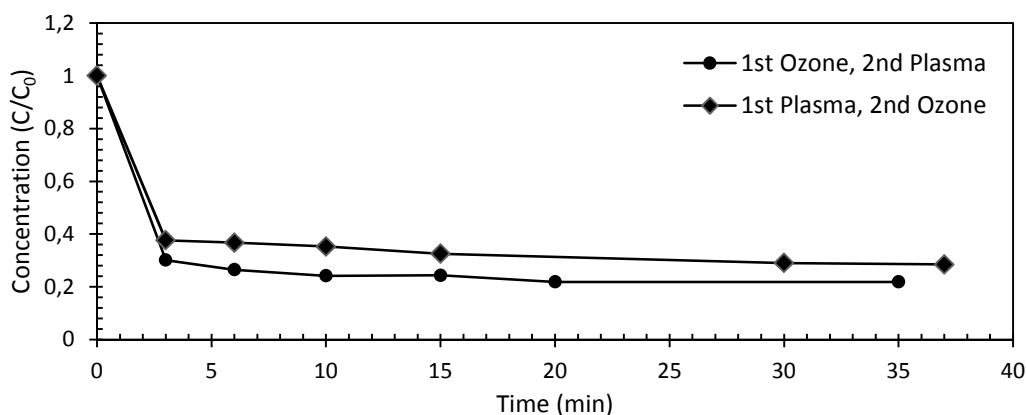


**Figure 8-9:** Degradation of pentachlorobenzene in function of time for a steady state configuration

These results were also present with methylene blue and can be explained in the same way. pH does not drop as fast in the ozone chamber, thus efficiency of ozone is less inhibited when this reactor is first in line. Another reason for the effectiveness of putting the ozone chamber first is eliminating the scavenger effects of  $N_xO_y$ . These plasma produced components will form oxidation reactions with active species and indirectly inhibit degradation of micropollutants.

## 8.5 Conclusion

As found in the last two figures (Figure 8-6 and Figure 8-7) the combination of an AOP such as plasma and an active carbon cloth deliver an ideal removal for the investigated components. Although the addition of plasma does not seem to have a lot of influence in the overall process, degradation of the micropollutants is more important.

In terms of efficiency, a lower power has the upper hand. With a duty cycle of 0.04 resulting in a cost effective use of the reactor, while maintaining a removal of at least 95% after 30 minutes of runtime.

In a continuous operation, it was found that it is more feasible to use the ozone reactor first. By doing so, pH in the ozone chamber is less affected by the plasma, resulting in an optimal functioning of the ozone in the gas phase.

## 9 Overall conclusion

---

In this research, degradation of organic compounds in water using plasma treatment was conducted. First a model compound such as methylene blue was used to check different parameters of the reactor. Subsequently, two micropollutants (PeCB and  $\alpha$ -HCH) were checked on their degradability with the same setup. It was found that both methylene blue and micropollutants have similar behavior when it comes to degradation.

There is little influence on degradation of MB and micropollutants when it comes to changing voltage settings. On the other hand, a duty cycle of 0.35 gives a significant degradation for all components. In terms of energy efficiency, a lower duty cycle of 0.04 gives the best result for both  $G_{50}$  and EEO. This means the higher removal by the higher duty cycle does not outweigh the lower energy consumption.

In this reactor different AOPs ( $O_3$ ,  $O_3/H_2O_2$ , etc. ) are combined due to plasma in contact with water. Because the addition of an activated carbon cloth adsorption and catalytic effects can help in the removal of both methylene blue and micropollutants.

The versatility of this plasma reactor, allows a single pass experiment can be conducted. This mimics a continuous flow of water through the system. There are 2 ways to configure this. First plasma, followed by the ozone reactor and one where the water passes first through the ozone chamber and then the plasma chamber. It was found that placing the ozone reactor first give the best results. A reason for that is that the pH is not affected, so ozone has more reaction potential to degrade the pollutants. Also scavenging effect by  $N_xO_y$  is reduced in this configuration.

## 10 Ideas for further research

---

The use of plasma technology, for the removal of micropollutants, has a promising future. Results show, it is clearly capable to degrading micropollutants to a high level. The costs for maintenance will be minimum, since all there is to the reactor is the power supply, the active carbon cloth and the pumps. Those components are easily swapped and require little skill. Besides that, the required input consists only out of dry air and electricity. These are way more basic, than for example  $H_2O_2$ , nanofilters and other components used for current micropollutant removal techniques.

## References

---

- Adams, C., Wang, Y., Loftin, K. and Meyer, M. (2002) Removal of antibiotics from surface and distilled water in conventional water treatment processes. *Journal of environmental engineering*, 128(3), pp. 253-260.
- Affam, A. C. and Chaudhuri, M. (2011) Activated Carbon/Hydrogen Peroxide (AC/H<sub>2</sub>O<sub>2</sub>) Treatment of Amoxicillin and Cloxacillin Antibiotics in Aqueous Solution.
- Andreozzi, R., Raffaele, M. and Nicklas, P. (2003) Pharmaceuticals in STP effluents and their solar photodegradation in aquatic environment. *Chemosphere*, 50(10), pp. 1319-1330.
- ATSDR (2005). Hexachlorocyclohexane: chemical and physical information [on line]. <http://www.atsdr.cdc.gov/toxprofiles/tp43-c4.pdf> (Date of consult: 6/12/2014).
- Bader, H. and Hoigné, J. (1981) Determination of ozone in water by the indigo method. *Water Research*, 15(4), pp. 449-456.
- Ballard, B. D. and MacKay, A. A. (2005) Estimating the removal of anthropogenic organic chemicals from raw drinking water by coagulation flocculation. *Journal of environmental engineering*, 131(1), pp. 108-118.
- Bergqvist, P.-A., Strandberg, B., Ekelund, R., Rappe, C. and Granmo, Å. (1998) Temporal monitoring of organochlorine compounds in seawater by semipermeable membranes following a flooding episode in Western Europe. *Environmental Science & Technology*, 32(24), pp. 3887-3892.
- Brisset, J.-L., Benstaali, B., Moussa, D., Fanmoe, J. and Njoyim-Tamungang, E. (2011) Acidity control of plasma-chemical oxidation: applications to dye removal, urban waste abatement and microbial inactivation. *Plasma Sources Science and Technology*, 20(3), pp. 034021.
- Bruggeman, P. and Leys, C. (2009) Non-thermal plasmas in and in contact with liquids. *Journal of Physics D: Applied Physics*, 42(5), pp. 053001.
- Cater, S. R., Stefan, M. I., Bolton, J. R. and Safarzadeh-Amiri, A. (2000) UV/H<sub>2</sub>O<sub>2</sub> treatment of methyl tert-butyl ether in contaminated waters. *Environmental Science & Technology*, 34(4), pp. 659-662.
- Cenens, J. and Schoonheydt, R. (1988) Visible spectroscopy of methylene blue on hectorite, laponite B, and barasym in aqueous suspension. *Clays and Clay Minerals*, 36(3), pp. 214-224.
- CEPA (2007). Pentachlorobenzene [on line]. <http://www.hc-sc.gc.ca/ewh-semt/pubs/contaminants/psl1-lsp1/pentachlorobenzene/index-eng.php> (Date of consult: 27/11/2014).
- Chang, J. (2009) Thermal plasma solid waste and water treatments: A critical review. *Int. J. Plasma Environ. Sci. Technol*, 3(2), pp. 67-84.

- Chu, P. K. and Lu, X. P. (2013) *Low Temperature Plasma Technology: Methods and Applications*, Taylor & Francis.
- Contineanu, M., Bercu, C., Contineanu, I. and Neacșu, A. (2009) A CHEMICAL AND PHOTOCHEMICAL STUDY OF RADICALIC SPECIES FORMED IN METHYLENE BLUE ACIDIC AND BASIC AQUEOUS SOLUTIONS. *Analele Universitatii Bucuresti: Chimie*, 18(2).
- Daneshvar, N., Aleboyeh, A. and Khataee, A. (2005) The evaluation of electrical energy per order (E Eo) for photooxidative decolorization of four textile dye solutions by the kinetic model. *Chemosphere*, 59(6), pp. 761-767.
- Dobrin, D., Magureanu, M., Bradu, C., Mandache, N., Ionita, P. and Parvulescu, V. (2014) Degradation of methylparaben in water by corona plasma coupled with ozonation. *Environmental Science and Pollution Research*, pp. 1-8.
- Echigo, S., Yamada, H., Matsui, S., Kawanishi, S. and Shishida, K. (1996) Comparison between O<sub>3</sub>/VUV, O<sub>3</sub>/H<sub>2</sub>O<sub>2</sub>, VUV and O<sub>3</sub> processes for the decomposition of organophosphoric acid triesters. *Water Science and Technology*, 34(9), pp. 81-88.
- Ecobichon, D. J. (1998) *Occupational Hazards Of Pesticide Exposure: Sampling, Monitoring, Measuring*, Taylor & Francis.
- EFSA (2006). Opinion of the scientific panel on contaminants in the food chain on the request from the commission related to hexachlorobenzene as undesirable substance in animal feed. The EFSA Journal 402, pp. 1-49.
- EPA (1987). Pentachlorobenzene; CASRN 608-93-5 [on line]. <http://www.epa.gov/iris/subst/0085.htm> (Date of consult: 30/11/2014).
- EPA (2000). Hexachlorobenzene [on line]. <http://www.epa.gov/ttnatw01/hlthef/hexa-ben.html> (Date of consult: 27/11/2014).
- EPA (2014). Basic information about hexachlorobenzene in drinking water [on line]. <http://water.epa.gov/drink/contaminants/basicinformation/hexachlorobenzene.cfm> (Date of consult: 6/12/2014).
- Esplugas, S., Bila, D. M., Krause, L. G. T. and Dezotti, M. (2007) Ozonation and advanced oxidation technologies to remove endocrine disrupting chemicals (EDCs) and pharmaceuticals and personal care products (PPCPs) in water effluents. *Journal of Hazardous Materials*, 149(3), pp. 631-642.
- Faria, P. C., Órfão, J. J. and Pereira, M. F. R. (2006) Ozone decomposition in water catalyzed by activated carbon: influence of chemical and textural properties. *Industrial & engineering chemistry research*, 45(8), pp. 2715-2721.
- Galbán-Malagón, C., Cabrerizo, A., Caballero, G. and Dachs, J. (2013) Atmospheric occurrence and deposition of hexachlorobenzene and hexachlorocyclohexanes in the Southern Ocean and Antarctic peninsula. *Atmospheric Environment*, 80, pp. 41-49.

- Galbán-Malagón, C. J., Berrojalbiz, N., Gioia, R. and Dachs, J. (2013) The “degradative” and “biological” pumps controls on the atmospheric deposition and sequestration of hexachlorocyclohexanes and hexachlorobenzene in the North Atlantic and Arctic Oceans. *Environmental Science & Technology*, 47(13), pp. 7195-7203.
- GSI (2013). Pentachlorobenzene [on line]. <http://www.gsi-net.com/en/publications/gsi-chemical-database/single/426.html> (Date of consult: 6/12/2014).
- Hart, E. J., Sehested, K. and Holoman, J. (1983) Molar absorptivities of ultraviolet and visible bands of ozone in aqueous solutions. *Analytical Chemistry*, 55(1), pp. 46-49.
- Haynes, W. M. (2013) *CRC handbook of chemistry and physics*, CRC press.
- Houas, A., Lachheb, H., Ksibi, M., Elaloui, E., Guillard, C. and Herrmann, J.-M. (2001) Photocatalytic degradation pathway of methylene blue in water. *Applied Catalysis B: Environmental*, 31(2), pp. 145-157.
- Huang, F., Chen, L., Wang, H. and Yan, Z. (2010) Analysis of the degradation mechanism of methylene blue by atmospheric pressure dielectric barrier discharge plasma. *Chemical Engineering Journal*, 162(1), pp. 250-256.
- Jarusutthirak, C., Amy, G. and Croué, J.-P. (2002) Fouling characteristics of wastewater effluent organic matter (EfOM) isolates on NF and UF membranes. *Desalination*, 145(1), pp. 247-255.
- Jiang, B., Zheng, J., Qiu, S., Wu, M., Zhang, Q., Yan, Z. and Xue, Q. (2014) Review on electrical discharge plasma technology for wastewater remediation. *Chemical Engineering Journal*, 236, pp. 348-368.
- Karimi, B., Ehrampoush, M. H., Ebrahimi, A., Mokhtari, M. and Amin, M. M. (2012) Catalytic oxidation of hydrogen peroxide and the adsorption combinatory process in leachate waste pretreatment from composting factory. *International Journal of Environmental Health Engineering*, 1(1), pp. 15.
- Kogelschatz, U., Eliasson, B. and Hirth, M. (1988) Ozone generation from oxygen and air: discharge physics and reaction mechanisms.
- Kuiper-Goodman, T., Grant, D., Moodie, C., Korsrud, G. and Munro, I. (1977) Subacute toxicity of hexachlorobenzene in the rat. *Toxicology and applied pharmacology*, 40(3), pp. 529-549.
- Lachheb, H., Puzenat, E., Houas, A., Ksibi, M., Elaloui, E., Guillard, C. and Herrmann, J.-M. (2002) Photocatalytic degradation of various types of dyes (Alizarin S, Crocein Orange G, Methyl Red, Congo Red, Methylene Blue) in water by UV-irradiated titania. *Applied Catalysis B: Environmental*, 39(1), pp. 75-90.
- Li, X., Hai, F. I. and Nghiem, L. D. (2011) Simultaneous activated carbon adsorption within a membrane bioreactor for an enhanced micropollutant removal. *Bioresource Technology*, 102(9), pp. 5319-5324.

- Li, Y. (1999) Global technical hexachlorocyclohexane usage and its contamination consequences in the environment: from 1948 to 1997. *Science of the Total Environment*, 232(3), pp. 121-158.
- Linder, R., Scotti, T., Goldstein, J., McElroy, K. and Walsh, D. (1980) Acute and subchronic toxicity of pentachlorobenzene. *Journal of environmental pathology and toxicology*, 4(5-6), pp. 183-196.
- Liu, B., Wen, L., Nakata, K., Zhao, X., Liu, S., Ochiai, T., Murakami, T. and Fujishima, A. (2012) Polymeric Adsorption of Methylene Blue in TiO<sub>2</sub> Colloids—Highly Sensitive Thermochromism and Selective Photocatalysis. *Chemistry – A European Journal*, 18(40), pp. 12705-12711.
- Locke, B., Sato, M., Sunka, P., Hoffmann, M. and Chang, J.-S. (2006) Electrohydraulic discharge and nonthermal plasma for water treatment. *Industrial & engineering chemistry research*, 45(3), pp. 882-905.
- Locke, B. R. and Shih, K.-Y. (2011) Review of the methods to form hydrogen peroxide in electrical discharge plasma with liquid water. *Plasma Sources Science and Technology*, 20(3), pp. 034006.
- Lukes, P., Dolezalova, E., Sisrova, I. and Clupek, M. (2014) Aqueous-phase chemistry and bactericidal effects from an air discharge plasma in contact with water: evidence for the formation of peroxyxynitrite through a pseudo-second-order post-discharge reaction of H<sub>2</sub>O<sub>2</sub> and HNO<sub>2</sub>. *Plasma Sources Science and Technology*, 23(1), pp. 015019.
- Luo, Y., Guo, W., Ngo, H. H., Nghiem, L. D., Hai, F. I., Zhang, J., Liang, S. and Wang, X. C. (2014) A review on the occurrence of micropollutants in the aquatic environment and their fate and removal during wastewater treatment. *Science of the Total Environment*, 473, pp. 619-641.
- Machala, Z., Tarabova, B., Hensel, K., Spetlikova, E., Sikurova, L. and Lukes, P. (2013) Formation of ROS and RNS in Water Electro - Sprayed through Transient Spark Discharge in Air and their Bactericidal Effects. *Plasma Processes and Polymers*, 10(7), pp. 649-659.
- Maehara, T., Miyamoto, I., Kurokawa, K., Hashimoto, Y., Iwamae, A., Kuramoto, M., Yamashita, H., Mukasa, S., Toyota, H. and Nomura, S. (2008) Degradation of methylene blue by RF plasma in water. *Plasma Chemistry and Plasma Processing*, 28(4), pp. 467-482.
- Malik, M. (2010) Water Purification by Plasmas: Which Reactors are Most Energy Efficient? *Plasma Chemistry and Plasma Processing*, 30(1), pp. 21-31.
- Malik, M. A. (2010) Water purification by plasmas: which reactors are most energy efficient? *Plasma Chemistry and Plasma Processing*, 30(1), pp. 21-31.
- Malik, M. A., Ghaffar, A. and Ahmed, K. (2002) Synergistic effect of pulsed corona discharges and ozonation on decolourization of methylene blue in water. *Plasma Sources Science and Technology*, 11(3), pp. 236.

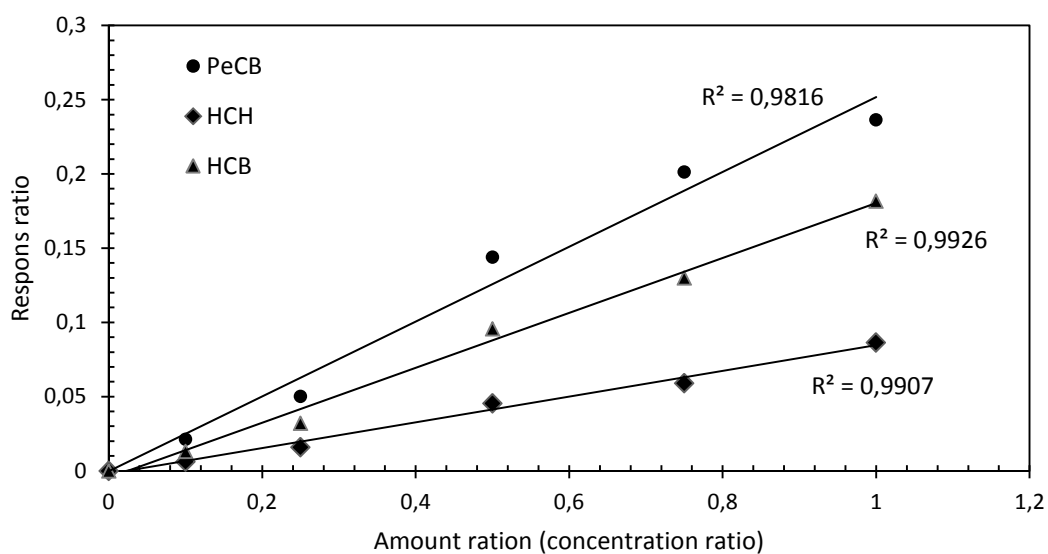
- Matamoros, V., Nguyen, L. X., Arias, C. A., Salvadó, V. and Brix, H. (2012) Evaluation of aquatic plants for removing polar microcontaminants: a microcosm experiment. *Chemosphere*, 88(10), pp. 1257-1264.
- Metcalf, R. L. (1955) Organic insecticides. *Organic insecticides*.
- Natarajan, K., Natarajan, T. S., Bajaj, H. and Tayade, R. J. (2011) Photocatalytic reactor based on UV-LED/TiO<sub>2</sub> coated quartz tube for degradation of dyes. *Chemical Engineering Journal*, 178, pp. 40-49.
- Nikolaou, A., Meric, S. and Fatta, D. (2007) Occurrence patterns of pharmaceuticals in water and wastewater environments. *Analytical and bioanalytical chemistry*, 387(4), pp. 1225-1234.
- Nogueira, R. F. P., Oliveira, M. C. and Paterlini, W. C. (2005) Simple and fast spectrophotometric determination of H<sub>2</sub>O<sub>2</sub> in photo-Fenton reactions using metavanadate. *Talanta*, 66(1), pp. 86-91.
- Paternina, E., M Arias, J. and Barragán, D. (2009) Kinetic study of the catalyzed decomposition of hydrogen peroxide on activated carbon. *Química Nova*, 32(4), pp. 934-938.
- Pekárek, S. (2003) Non-thermal plasma ozone generation. *Acta Polytechnica*, 43(6).
- Pekárek, S. (2014) Ozone production of hollow-needle-to-mesh negative corona discharge enhanced by dielectric tube on the needle electrode. *Plasma Sources Science and Technology*, 23(6), pp. 062001.
- Plasma Universe (2014). Electric discharge regimes [on line]. [http://www.plasma-universe.com/images/thumb/f/f2/Glow\\_D.jpg/600px-Glow\\_D.jpg](http://www.plasma-universe.com/images/thumb/f/f2/Glow_D.jpg/600px-Glow_D.jpg) (Date of consult: 17/12/2014).
- Quinlivan, P. A., Li, L. and Knappe, D. R. (2005) Effects of activated carbon characteristics on the simultaneous adsorption of aqueous organic micropollutants and natural organic matter. *Water Research*, 39(8), pp. 1663-1673.
- Robles-Molina, J., Gilbert-López, B., García-Reyes, J. F. and Molina-Díaz, A. (2014) Monitoring of selected priority and emerging contaminants in the Guadalquivir River and other related surface waters in the province of Jaén, South East Spain. *Science of the Total Environment*, 479, pp. 247-257.
- Saltechtips (2014). Electron Chain Reaction [on line]. <http://www.saltechtips.com/images/theory-fig1.gif> (Date of consult: 17/12/2014).
- Schutze, A., Jeong, J. Y., Babayan, S. E., Park, J., Selwyn, G. S. and Hicks, R. F. (1998) The atmospheric-pressure plasma jet: a review and comparison to other plasma sources. *Plasma Science, IEEE Transactions on*, 26(6), pp. 1685-1694.
- Shimadzu (2015). The Relationship Between UV-VIS Absorption and Structure of Organic Compounds [on line]. <http://www.shimadzu.com/an/uv/support/uv/ap/apl.html> (Date of consult: 6/04/2015).



- Stará, Z., Krčma, F., Nejezchleb, M. and Skalný, J. D. (2009) Organic dye decomposition by DC diaphragm discharge in water: Effect of solution properties on dye removal. *Desalination*, 239(1), pp. 283-294.
- Taube, H. and Bray, W. C. (1940) Chain reactions in aqueous solutions containing ozone, hydrogen peroxide and acid. *Journal of the American Chemical Society*, 62(12), pp. 3357-3373.
- Thevenet, F., Couble, J., Brandhorst, M., Dubois, J., Puzenat, E., Guillard, C. and Bianchi, D. (2010) Synthesis of hydrogen peroxide using dielectric barrier discharge associated with fibrous materials. *Plasma Chemistry and Plasma Processing*, 30(4), pp. 489-502.
- Thuy, P. T., Moons, K., Van Dijk, J., Viet Anh, N. and Van der Bruggen, B. (2008) To what extent are pesticides removed from surface water during coagulation–flocculation? *Water and Environment Journal*, 22(3), pp. 217-223.
- Vale, C., Damgaard, I., Suñol, C., Rodríguez - Farré, E. and Schousboe, A. (1998) Cytotoxic action of lindane in neocortical GABAergic neurons is primarily mediated by interaction with flunitrazepam - sensitive GABAA receptors. *Journal of neuroscience research*, 52(3), pp. 276-285.
- Van der Bruggen, B., Everaert, K., Wilms, D. and Vandecasteele, C. (2001) Application of nanofiltration for removal of pesticides, nitrate and hardness from ground water: rejection properties and economic evaluation. *Journal of Membrane Science*, 193(2), pp. 239-248.
- Van de Plassche, A. Schwegler, M. Rasenberg and G. Schouten (2002). Pentachlorobenzene. Pp 1-18
- Vasko, C., Liu, D., van Veldhuizen, E., Iza, F. and Bruggeman, P. (2014) Hydrogen Peroxide Production in an Atmospheric Pressure RF Glow Discharge: Comparison of Models and Experiments. *Plasma Chemistry and Plasma Processing*, pp. 1-19.
- Verliefde, A., Cornelissen, E., Amy, G., Van der Bruggen, B. and Van Dijk, H. (2007) Priority organic micropollutants in water sources in Flanders and the Netherlands and assessment of removal possibilities with nanofiltration. *Environmental pollution*, 146(1), pp. 281-289.
- VLAREM II (2014). Bijlage 2.3.1. Basismilieukwaliteitsnormen voor oppervlaktewater [online]. <http://navigator.emis.vito.be/milnav-consult/consultatieLink?wettekstId=10071&appLang=nl&wettekstLang=nl> (Date of consult: 28/11/2014).
- VMM (2013). Pesticiden in oppervlaktewater [on line]. <http://www.vmm.be/water/kwaliteit-oppervlaktewater/toestand-oppervlaktewater/fysisch-chemische-toestand/micropolluenten/pesticiden-in-oppervlaktewater> (Date of consult: 28/11/2014).
- Wang, L. K., Hung, Y. T. and Shamma, N. K. (2007) *Advanced Physicochemical Treatment Technologies*, Humana Press.
- Waterworld (2015). Survey Examines Wastewater Treatment [on line]. [Costshttp://www.waterworld.com/articles/iww/print/volume-11/issue-1/feature-editorial/survey-examines-wastewater-treatment-costs.html](http://www.waterworld.com/articles/iww/print/volume-11/issue-1/feature-editorial/survey-examines-wastewater-treatment-costs.html)(Date of consult: 8/05/2015).

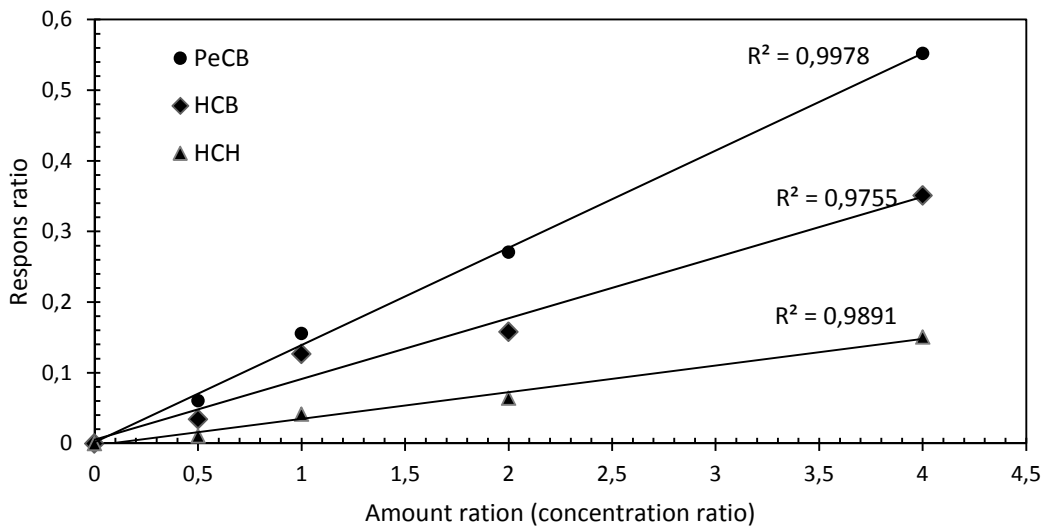
- Weiss, N. A. and Weiss, C. A. (2012) *Introductory statistics*, Pearson Education.
- Willett, K. L., Ulrich, E. M. and Hites, R. A. (1998) Differential toxicity and environmental fates of hexachlorocyclohexane isomers. *Environmental Science & Technology*, 32(15), pp. 2197-2207.
- Woodwell, G. M., Craig, P. P. and Johnson, H. A. (1975) DDT in the biosphere: where does it go? in *The Changing Global Environment*: Springer. pp. 295-309.
- Yrieix, C., Gonzalez, C., Deroux, J., Lacoste, C. and Leybros, J. (1996) Countercurrent liquid/liquid extraction for analysis of organic water pollutants by GC/MS. *Water Research*, 30(8), pp. 1791-1800.
- Yu, Y., Huang, Q., Wang, Z., Zhang, K., Tang, C., Cui, J., Feng, J. and Peng, X. (2011) Occurrence and behavior of pharmaceuticals, steroid hormones, and endocrine-disrupting personal care products in wastewater and the recipient river water of the Pearl River Delta, South China. *Journal of Environmental Monitoring*, 13(4), pp. 871-878.
- Zacharia, I. G. and Deen, W. M. (2005) Diffusivity and solubility of nitric oxide in water and saline. *Annals of biomedical engineering*, 33(2), pp. 214-222.
- Zhang, Q., Li, C. and Li, T. (2013) Rapid photocatalytic decolorization of methylene blue using high photon flux UV/TiO<sub>2</sub>/H<sub>2</sub>O<sub>2</sub> process. *Chemical Engineering Journal*, 217, pp. 407-413.
- Zhu, X.-M. and Pu, Y.-K. (2008) Using OES to determine electron temperature and density in low-pressure nitrogen and argon plasmas. *Plasma Sources Science and Technology*, 17(2), pp. 024002.

## Annex A: Calibration curves in Ethyl acetate



	Micropollutant	Intercept	Coëfficiënt	r <sup>2</sup>
Calibration with IS	PeCB	-0,0002804	0,25199	0,9816
	α-HCH	-0,002033	0,08673	0,9907
	HCB	-0,004726	0,18510	0,9926
Calibration without IS	PeCB	-830,5	71,34	0,9962
	α-HCH	-827,9	24,64	0,9895
	HCB	-1877,3	52,57	0,9908

## Annex B: Calibration curves after extraction with dichloromethane



	Micropollutant	Intercept	Coëfficiënt	r <sup>2</sup>
Calibration with IS	PeCB	-0,0011205	0,17545	0,9984
	HCH	0,001441	0,13770	0,9978
	HCB	-0,001281	0,15783	0,9948
Calibration without IS	PeCB	-830,5	71,34	0,9962
	HCH	-827,9	24,64	0,9895
	HCB	-1877,3	52,57	0,9908